

AD 745757

FEASIBILITY STUDIES OF  
MULTISPECTRAL MOSAIC IMAGE  
CONVERSION PANELS

FOR PERIOD 1 FEBRUARY 1971 TO 31 JANUARY 1972

D D C A  
RECORDED  
RELEASER  
AUG 1 1972  
C

OFFICE OF NAVAL RESEARCH

CONTRACT N00014-71-C-0188  
TASK NO. NR 215-165

APPROVED FOR PUBLIC RELEASE; DISTRIBUTION UNLIMITED  
REPRODUCTION IN WHOLE OR IN PART IS PERMITTED FOR  
ANY PURPOSE OF THE UNITED STATES GOVERNMENT

DR. D. E. ANDERSON, PRINCIPAL INVESTIGATOR

MR. R. L. SWISHER, CO-INVESTIGATOR

30 MARCH 1972

Reproduced by  
NATIONAL TECHNICAL  
INFORMATION SERVICE  
U.S. Department of Commerce  
Springfield, VA 22151

127

Unclassified

Security Classification

DOCUMENT CONTROL DATA - R & D

(Security classification of title, body of abstract and indexing annotation must be entered when the overall report is classified)

1. ORIGINATING ACTIVITY (Corporate author)		2a. REPORT SECURITY CLASSIFICATION	
G. T. Schjeldahl Company Northfield, Minnesota 55057 Attn: Advanced Programs Division		Unclassified	
3. REPORT TITLE		2b. GROUP	
Feasibility Studies of Multispectral Mosaic Image Conversion Panels			
4. DESCRIPTIVE NOTES (Type of report and inclusive dates) Final Technical Report for Period 1 February 1971 to 31 January 1972			
5. AUTHOR(S) (First name, middle initial, last name) Donald E. Anderson & Richard L. Swisher			
6. REPORT DATE 30 March 1972		7a. TOTAL NO. OF PAGES 120	7b. NO. OF REFS
8a. CONTRACT OR GRANT NO. N00014-71-C-0188		9a. ORIGINATOR'S REPORT NUMBER(S)	
b. PROJECT NO. Task No. NR 215-165		9b. OTHER REPORT NO(S) (Any other numbers that may be assigned this report)	
c.			
d.			
10. DISTRIBUTION STATEMENT Approved for public release; distribution unlimited.			
11. SUPPLEMENTARY NOTES Reproduction in whole or in part is permitted for any purpose of the United States Government.		12. SPONSORING MILITARY ACTIVITY Department of the Navy Office of Naval Research	
13. ABSTRACT A development program is described in which the feasibility of mosaic EL/PC image conversion panels sensitive to UV, near IR, X-rays, and visible light was studied. Thin Film photoconductors are electroded in a regular array with unit cells 0.020" on centers. These arrays are connected to opaque electrode arrays forming the back pads of an electroluminescent (EL) lamp array through the use of microglass spacer sheets. Both thick film EL and thin film (TFEL) lamp arrays were prepared and studied. Useful near IR response was obtained for inputs of $10^{-6}$ w/cm <sup>2</sup> . Useful visible light response was obtained for $5 \times 10^{-4}$ ft-cd input. Peak optical gains of 500 were achieved with thick film EL and optical gains of 3000 using TFEL output.			
The combinations of materials used were prepared in test sample form, electrically and optically parameterized, and then computer simulations were performed to determine the range of parameters needed for a successful assembly. The computer models simulate the transient or steady state optical stimulation of EL/PC cells with simple sinusoidal power applied or more complicated waveforms. All computer programs used are documented.			

DD FORM 1 NOV. 1973

H

Security Classification

Unclassified  
Security Classification

14. KEY WORDS	LINK A		LINK B		LINK C	
	ROLE	WT	ROLE	WT	ROLE	WT
Electroluminescence Photoconductors Mosaic Image Conversion Panels Electronic Assembly Simulation Infrared Image Conversion Displays UV Image Conversion						

II

Security Classification

FEASIBILITY STUDIES OF  
MULTISPECTRAL MOSAIC IMAGE  
CONVERSION PANELS

FOR PERIOD 1 FEBRUARY 1971 TO 31 JANUARY 1972

OFFICE OF NAVAL RESEARCH  
CONTRACT N00014-71-C-0188  
TASK NO. NR 215-165

APPROVED FOR PUBLIC RELEASE; DISTRIBUTION UNLIMITED  
REPRODUCTION IN WHOLE OR IN PART IS PERMITTED FOR  
ANY PURPOSE OF THE UNITED STATES GOVERNMENT

Details of illustrations in  
this document may be better  
studied on microfiche.

DR. D. E. ANDERSON, PRINCIPAL INVESTIGATOR

MR. R. L. SWISHER, CO-INVESTIGATOR

30 MARCH 1972

III

Reproduction in whole or in part is permitted for any purpose of the  
United States Government. This research was sponsored by the Office  
of Naval Research under ONR Contract Number N00014-71-C-0188, ONR  
Contract Authority Identification Number NR 215-165/10/30/70 (461).

IV

## N O T I C E

### Change of Address

Organizations receiving Reports on the initial distribution list should confirm correct address. This list is located at the end of the report. Any change of address or distribution should be conveyed to the Office of Naval Research, Code 461, Arlington, Virginia 22217.

### Disposition

When this report is no longer needed, it may be transmitted to other organizations. Do not return it to the originator or the monitoring office.

### Disclaimer

The findings in this report are not to be construed as an official Department of Defense or Military Department position unless so designated by other official documents.

V

## PREFACE

This document covers research as to the feasibility of multispectral mosaic image conversion panels carried out at the G. T. Schjeldahl Company, Inc. during the twelve months from 1 February 1971 to 31 January 1972.

The research was directed by Dr. Donald E. Anderson; co-investigator was Richard L. Swisher. The research staff during all or part of the period covered by this report included Robert Mracek, Eugene Hildreth, Lloyd Schultz and John Rooks.

VI

## ABSTRACT

A Development program is described in which the feasibility of mosaic EL/PC image conversion panels sensitive to UV, near IR, X-rays, and visible light was studied. Thin Film photoconductors are electroded in a regular array with unit cells 0.020" on centers. These arrays are connected to opaque electrode arrays forming the back pads of an electroluminescent (EL) lamp array through the use of microglass spacer sheets. Both thick film EL and thin film (TFEL) lamp arrays were prepared and studied. Useful near IR response was obtained for inputs of  $10^{-6}$  w/cm<sup>2</sup>. Useful visible light response was obtained for  $5 \times 10^{-4}$  ft-cd input. Peak optical gains of 500 were achieved with thick film EL and optical gains of 3000 using TFEL output.

The combinations of materials used were prepared in test sample form, electrically and optically parameterized, and then computer simulations were performed to determine the range of parameters needed for a successful assembly. The computer models simulate the transient or steady state optical stimulation of EL/PC cells with simple sinusoidal power applied or more complicated waveforms. All computer programs used are documented.

## TABLE OF CONTENTS

<u>SECTION</u>	<u>PAGE</u>
1.0 GENERAL INTRODUCTION	1
1.1 General Description of Construction and Operation of EL/PC Image Conversion Panels	1
1.2 Philosophy of This Program	7
2.0 THIN FILM EL FABRICATION AND TESTING	7
2.1 Introduction	7
2.2 TFEL Fabrication Techniques and Results	8
2.3 Interesting Anomalies of TFEL	18
3.0 UV-TO-VISIBLE IMAGE CONVERSION PANELS	21
3.1 Introduction	21
3.2 Results	21
4.0 X-RAY TO VISIBLE IMAGE CONVERSION PANELS	22
4.1 Introduction	22
4.2 Results	22
4.3 Recommendations	22
5.0 VISIBLE-TO-VISIBLE IMAGE CONVERSION PANELS	25
5.1 Introduction	25
5.2 Sensitive Light Amplifiers	25
5.3 Assembly Techniques	26
5.4 Assembly Test Results	29
5.5 Feasibility of Stacking Visible-to-Visible Image Conversion Panels Onto Other Panels	32
6.0 IR-TO-VISIBLE IMAGE CONVERSION PANELS	40
6.1 Introduction	40
6.2 Results	40
7.0 GENERAL CONCLUSIONS AND RECOMMENDATIONS	44

LIST OF ILLUSTRATIONS

<u>FIGURE NO.</u>		<u>PAGE</u>
1	Photomicrograph of PC Layer	2
2	Interface Layer of Mosaic EL/PC Device	3
3	Self-Illuminated Photomicrograph of EL Output Mosaic	5
4	Simple 3D Geometry of Image Conversion Panel	6
5	Extremely Simplified Schematic of Operation of EL/PC Image Conversion Panel	7
6	Co-Planar TFEL Electrodes	9
7	"Moated" Drive Electrodes for TFEL Output Cell	10
8	Thin Film EL Lamp	12
9	Diagram of ZnS, CdSe, PbS, PbSe Deposition Fixture	13
10	Trends in B vs V for Different TFEL Construction Parameters	15
11	Brightness vs Voltage of Laboratory Sample Lamp Compared with Available TFEL Lamps	16
12	TFEL Lamp with CdS Layer Included	19
13	Low Voltage TFEL Output Brightness	20
14	Heterojunction Configuration for Carrier Injection Transverse to E Field	23
15	Typical Conductivity of PC Cells Vs Green Light Stimulation	27
16	Cross Section of EL/PC Image Conversion Panel Using Thick Film EL	28
17	Interconnection Technique for TFEL/PC Structure	30
18	TFEL Visible-to-Visible Image Conversion Panel	31
19	Performance of Thick Film EL Visible-to-Visible Image Conversion Panel	33
20	Calculated Overall IR/Visible Performance of Two-Stage Cascaded Image Converter	34

LIST OF ILLUSTRATIONS Cont.

<u>FIGURE NO.</u>		<u>PAGE</u>
21	Simulation of EL/PC Panel Operation at 70 V rms	35
22	Simulation of EL/PC Panel Operation at 100 V rms	36
23	Simulated Operation of CdSe 494-95-8 With Thick Film EL Using 3 Frequency Drive	38
24	Simulated Operation of CdSe 494-95-8 With TFEL 494-79-2, 5A Using 3 Frequency Drive	39
25	Thick Film EL/PC IR Image Converters Present and Previous	42
26	TFEL IR-to-Visible Image Converter	43

## 1.0 General Introduction

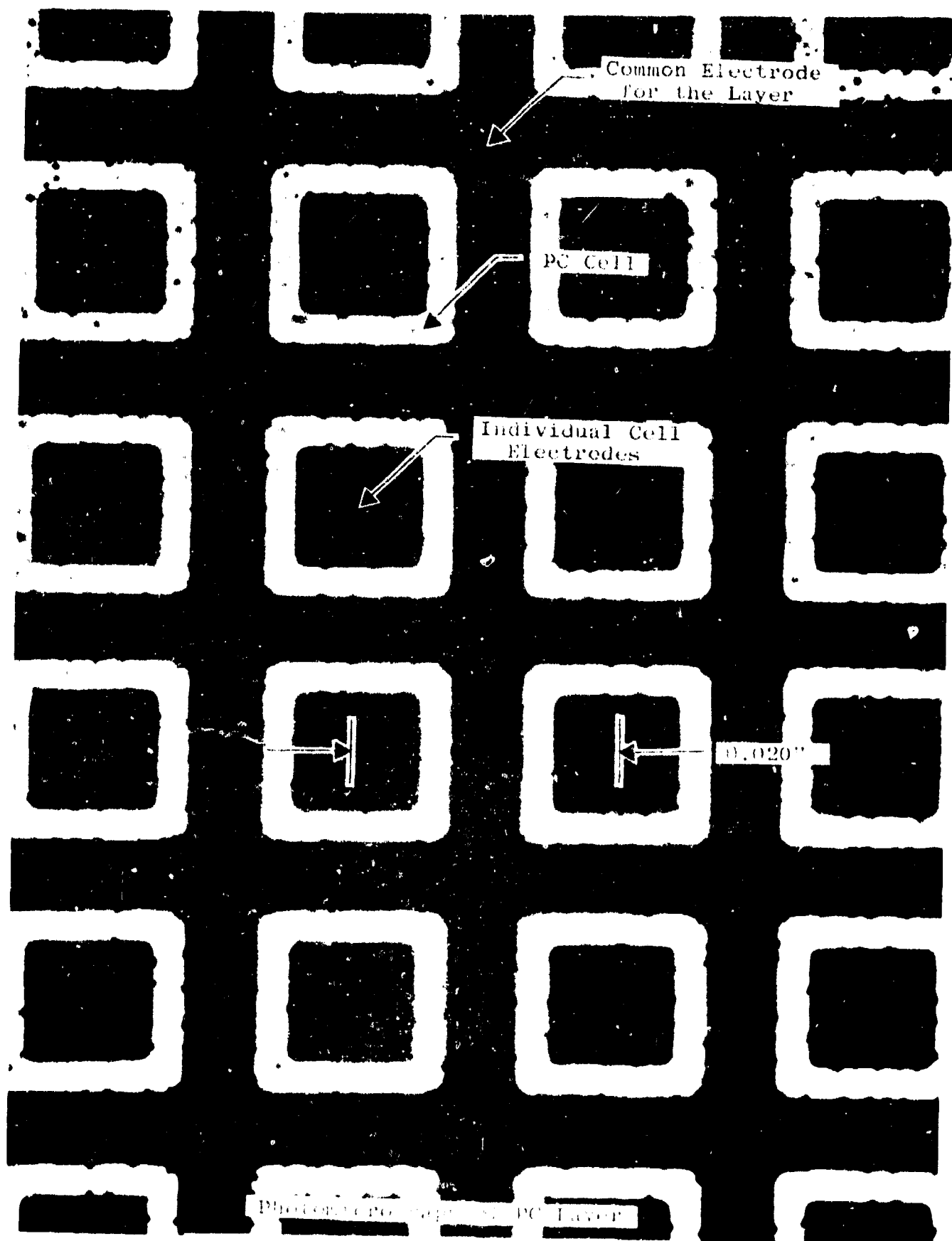
### 1.1 General Description of Construction and Operation of EL/PC Image Conversion Panels

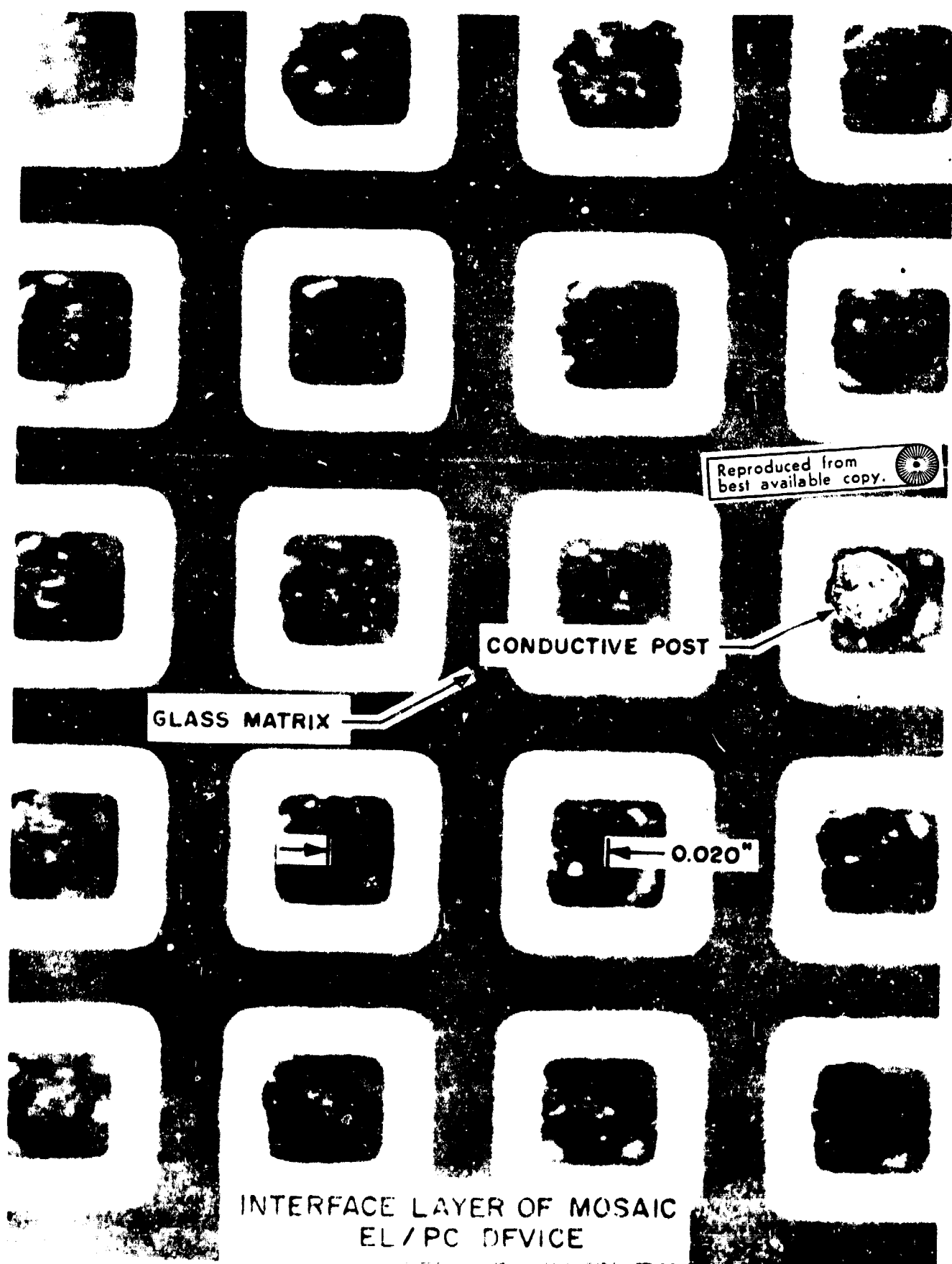
A solid state electroluminescent-photoconductor (EL/PC) image converter is a device which responds to radiation of a certain intensity and wavelength distribution by emitting radiation of higher intensity and/or different spectral distribution. Our studies have concentrated on image conversion panels having a structural geometry consisting of layers of mosaic patterned cells. All photoconductors studied were deposited as thin films with mosaics of patterned electrodes. Input radiation is incident normal to the PC film and photocurrent flow is in the plane of the PC film. Figure 1 is a back-lighted photomicrograph of a mosaic electroded PC layer fabricated in our laboratory. The opaque material is the molybdenum electrodes.

To connect the small square electrodes of the PC layer in Figure 1 to individual EL lamps in a layer above the PC layer, we need an interface layer. One type of successful interface layer that we have previously developed is shown in Figure 2. In this photomicrograph, the round dots are "posts" of solder alloy. Each of these posts are bonded to one of the small square electrodes of the PC layer in Figure 1. The light colored matrix is 0.003" thick glass. This is used for dimensional stability of the sheet.

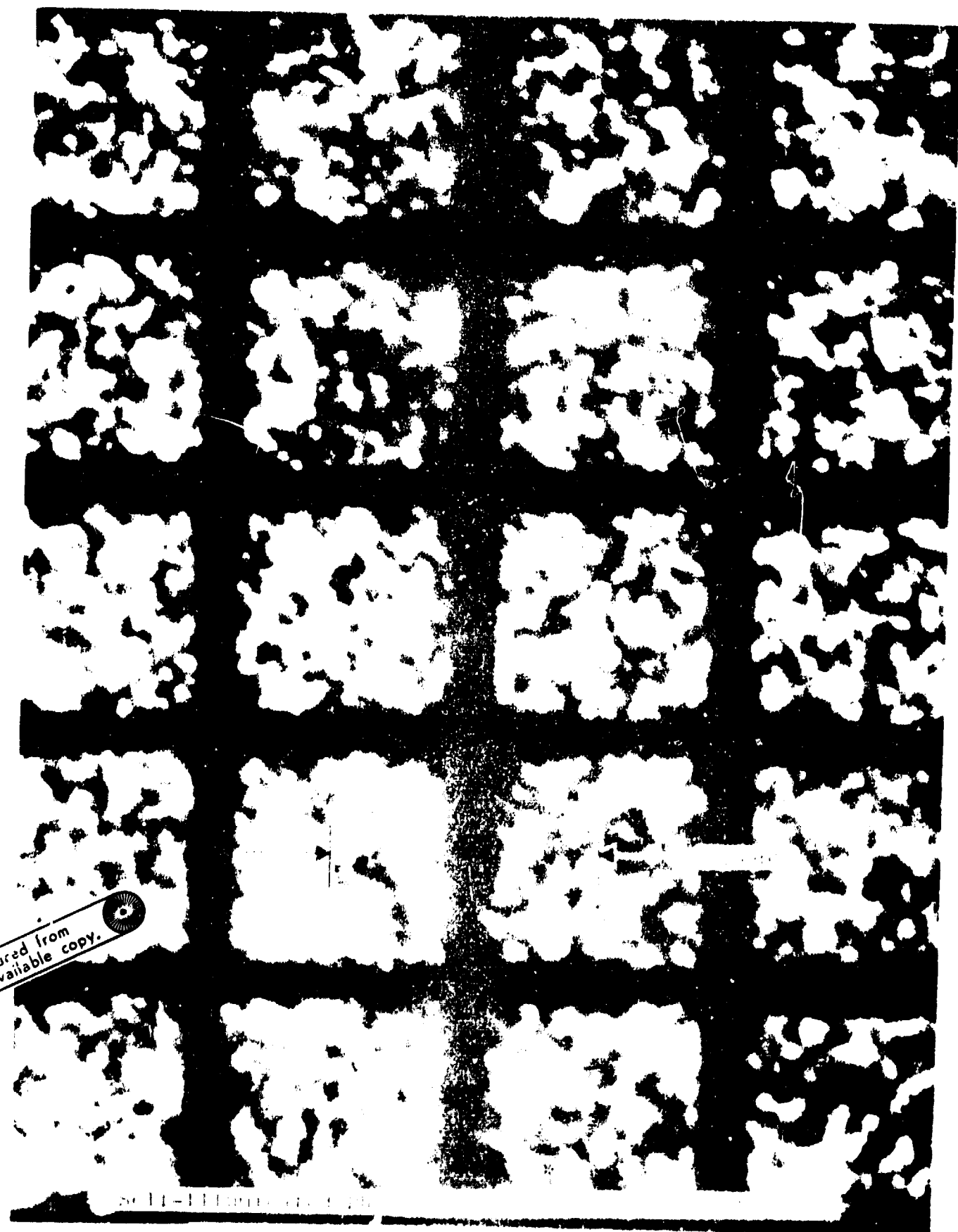
The forward or "upper" ends of the conductive posts are connected to an array of rear electrode pads for the EL output layer. If thick film EL is used, it is sprayed onto the electroded interface layer and a continuous semi-transparent front electrode is applied. Figure 3 is a photomicrograph of the light emitted by an array of thick film EL lamps fabricated in this manner. An opaque dielectric layer is usually applied behind the output EL layer to prevent light feedback to the PC layer. If thin film EL (TFEL) is used as an output media, then it must be prepared on a separate substrate and electroded and then bonded to the interface layer.

Figure 4 is a vertically exaggerated drawing of a section of an EL/PC image conversion panel using thick film EL. The operation can be visualized by tracing the flow of electrical power from the conductive lattice across and modulated by a stimulated PC cell, up a conductive post, and by means of capacitance, through the EL layer to the continuous front electrode. Figure 5 is a schematic of how one EL/PC cell operates. As radiation impinges upon the PC, its resistance decreases. This switches an increasing fraction of the applied voltage onto the EL capacitor. In response to this voltage, the EL material emits light. The image conversion panel can be thought of as an array of photoresistive voltage dividers.



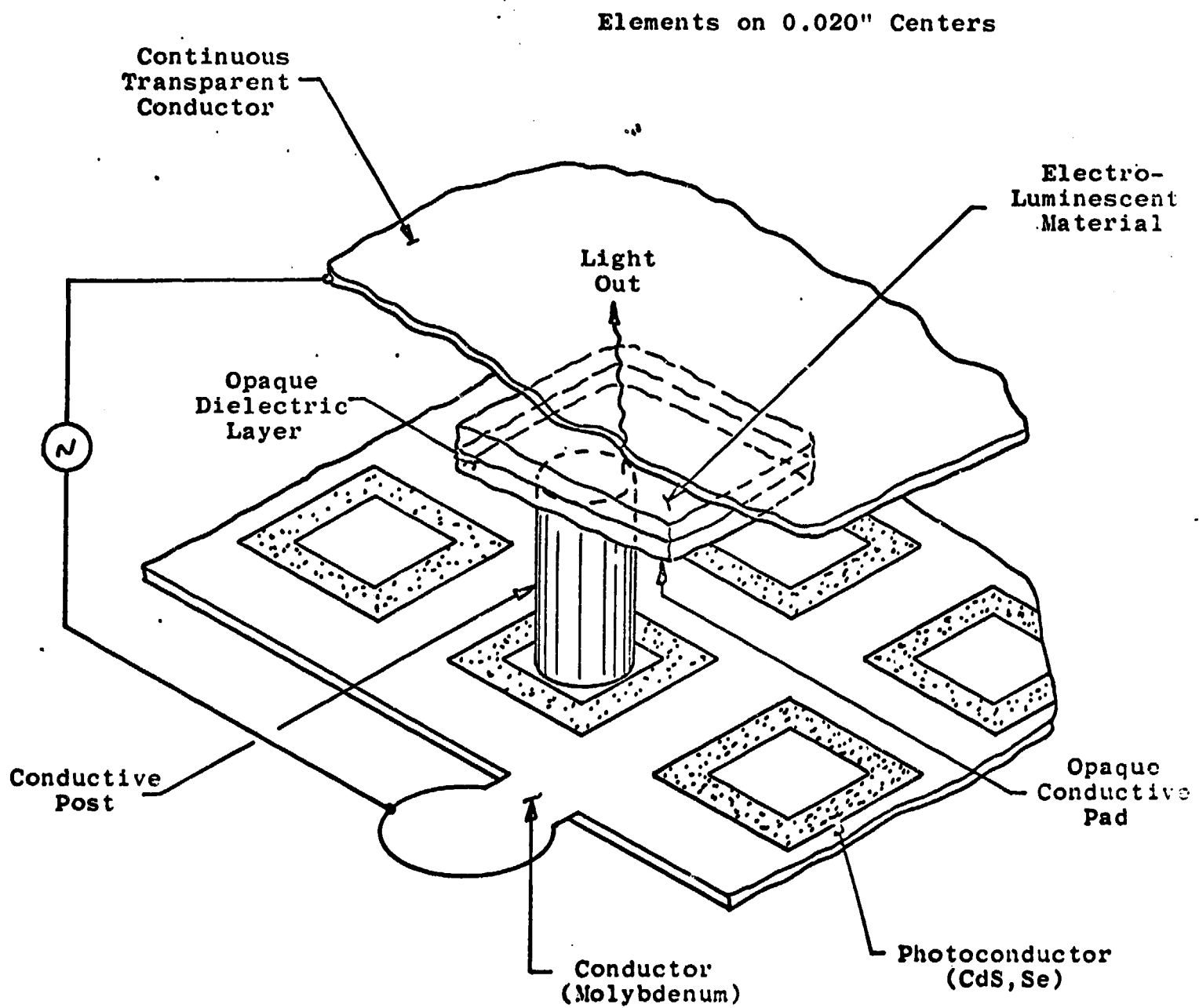


Reproduced from  
best available copy.



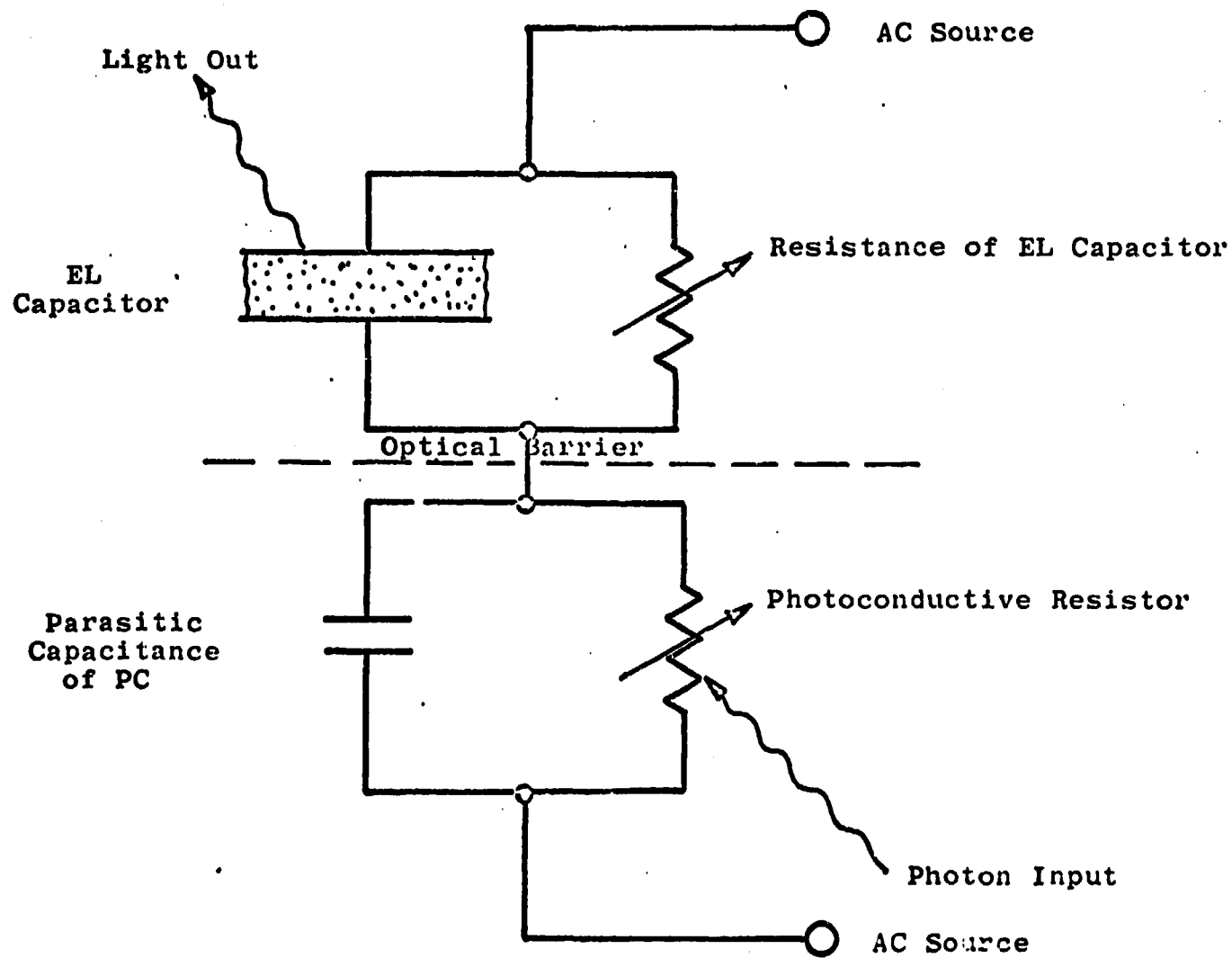
 **Schjeldahl Company**  
NORTHFIELD, MINNESOTA 55057

Figure 3



Simple 3D Geometry of Image Conversion Panel

FIGURE 4



Extremely Simplified Schematic of Operation  
of  
EL/PC Image Conversion Panel

FIGURE 5

## 1.2 Philosophy of This Program

Under a previous contract (N00017-70-C-0213), it was shown that mosaic EL/PC infrared image converters could be simulated by computer modeling and the operating characteristics of a completed test assembly agreed with the predictions. This type of simulation makes possible many economies in the search for useful combinations of photoconductors and electroluminescent materials.

In this program, we were to continue studies of infrared (IR) photoconductors used with thick film EL and to extend this work to photoconductors sensitive to ultra-violet, visible, and X-ray radiation. Also, we were to further investigate the possibility of using thin film EL(TFEL) in image conversion panels. If the computer simulations indicated that a combination of materials could function properly, then test assemblies were to be fabricated, if possible, and compared with the simulations. In addition, we were to investigate the possibility of placing a visible-to-visible image conversion panel on top of any other type of image conversion panel to boost the conversion gain of the pair.

The work and this report was divided into five tasks:

- Develop Thin Film EL lamp arrays compatible with possible assembly techniques
- Investigate UV sensitive photoconductors to find possible candidates for use in test assemblies
- Investigate X-ray sensitive photoconductors to find possible candidates for use in test assemblies
- Investigate PbS-TFEL combinations and improve the CdSe device fabricated under previous contract.
- Improve CdS,Se visible-to-visible image conversion panels and investigate possibility of cascading with similar panels or any of the image conversion panels above.

## 2.0 Thin Film EL Fabrication and Testing

### 2.1 Introduction

Thin film EL (TFEL) has these advantages over thick film EL:

- Higher brightness
- Better brightness maintenance characteristics
- More uniform appearance. It is microscopically uniform in brightness within a cell.

TFEL has these major disadvantages:

- It is much more difficult to fabricate consistent lamps from sample to sample. Many vacuum deposition processes are involved. The heat treatments necessary to form a good lamp limit the possible assembly procedures of an EL/PC device.
- Its brightness is a very steep function of applied voltage which results in very little gray scale range in an EL/PC image conversion panel.
- Its capacitance per unit area is much larger than thick film EL and hence, its impedance per unit area is lower. This requires that PC cells be fabricated with a lower range of impedances than those necessary for thick film EL.

Despite the above shortcomings and difficulties, TFEL is still a desirable light output media because of its high brightness and excellent life if made properly. These characteristics are especially important for aircraft displays.

During this program, we improved upon the performance obtained from TFEL fabricated under the previous contract.

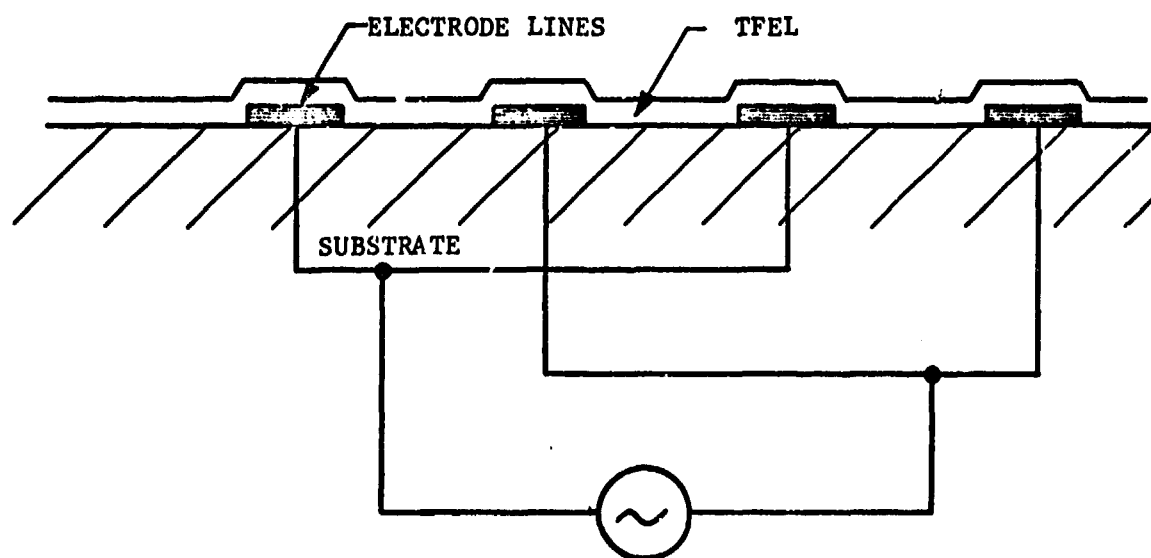
## 2.2 TFEL Fabrication Techniques and Results

### 2.2.1 Co-Planar Electrodes

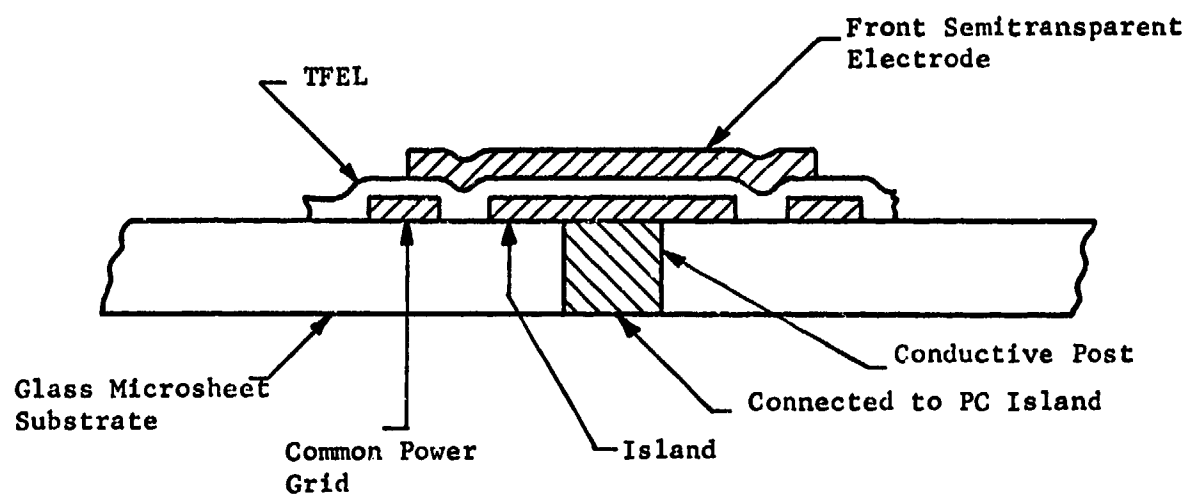
It was originally planned that we try to increase the impedance of the TFEL cells by using a co-planar electroding scheme as shown in Figure 6. Experimental trials indicated that such a configuration held little promise for success because of extreme demands on electrode edge smoothness and electrode spacing of less than 0.001". This electrode spacing is impractical for large area panels.

### 2.2.2 Series TFEL Lamps

Another impedance raising approach was then tried. This electroding technique is shown in Figure 7. The technique used a "moated" rear electrode for the TFEL cell and a "floating" semitransparent front electrode. If the area of the region common to the power grid and floating electrode and the area common to the "island" and the floating electrode are equal, then the impedance of the TFEL lamp is quadrupled over a simple sandwich electrode structure. The total operating voltage of the TFEL lamp is doubled but the electric fields in the material remain the same as for a simple sandwich cell. We abandoned this approach because the lamp could



CO-PLANAR TFEL ELECTRODES  
FIGURE 6



"MOATED" DRIVE ELECTRODES  
FOR  
TFEL OUTPUT CELL

FIGURE 7

not be fabricated as in Figure 7. Because the TFEL needs high temperature baking, the front semitransparent electrode has to be  $\text{SnO}_2$  or  $\text{InO}_2$  deposited on a substrate first. The coated rear electrode had to be deposited last and we could not find an etching technique for the metals used (Au, Ni, or Al) that didn't damage the lamps in some unknown way. All lamp samples suffered from voltage breakdown problems.

At this time we decided to concentrate on the simple sandwich cell of TFEL and try harder to adjust the impedance range of the photoconductors.

### 2.2.3 Sandwich Style TFEL Cells

Concurrent with the unsuccessful attempts at using novel TFEL cell geometries, we were attempting to improve the performance of "simple" sandwich style TFEL cells. Figure 8 is a cross-section through such a cell. The transparent substrates we used were typically boro-silicate glass. We tried two types of semitransparent front electrodes:  $\text{SnO}_2$  and  $\text{InO}_2$ . The phosphor was ZnS doped with manganese. The dielectric is  $\text{GeO}_2$ . The rear electrode is typically Au.

At the beginning of the program, we performed an abbreviated matrix study using:

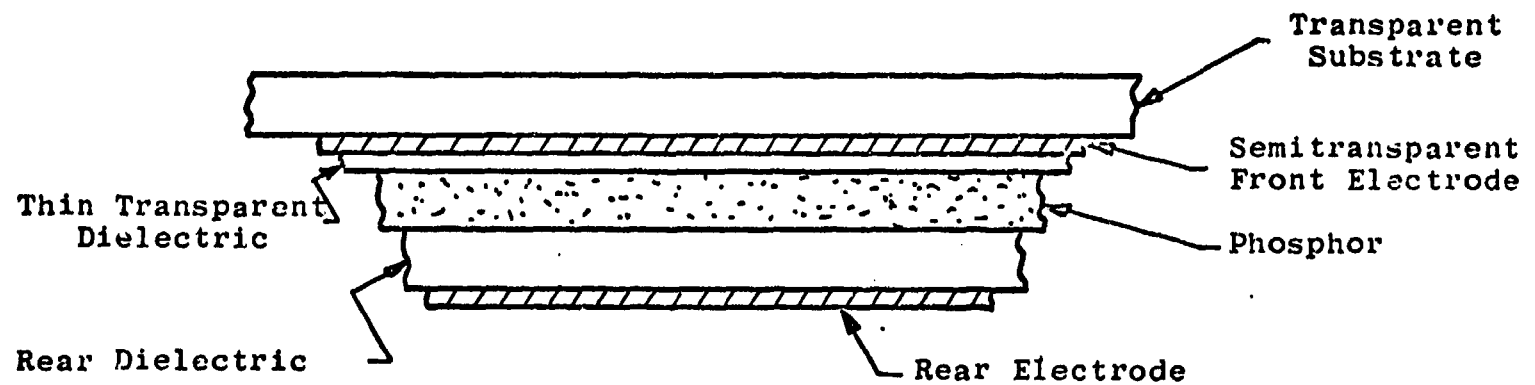
- a) Three types of  $\text{SnO}_2$  coated substrates.
- b) Three types of  $\text{GeO}_2$  evaporation sources.
- c) Two types of ZnS:Mn phosphor evaporation sources.

The plan was to abbreviate the matrix by building lamps using all types of processes in (a) above with a standard set of processes from (b) and (c) above. The best (a) process was then used with all types of (b) processes and the same (c) standard. This optimization was carried through each successive layer of the lamp structure. The types of substrates included commercially obtained substrates and  $\text{SnO}_2$  and  $\text{InO}_2$  coated substrates prepared in our laboratory.

All ZnS:Mn depositions were made in a bell jar vacuum system using an internal chimney deposition system as shown in Figure 9.

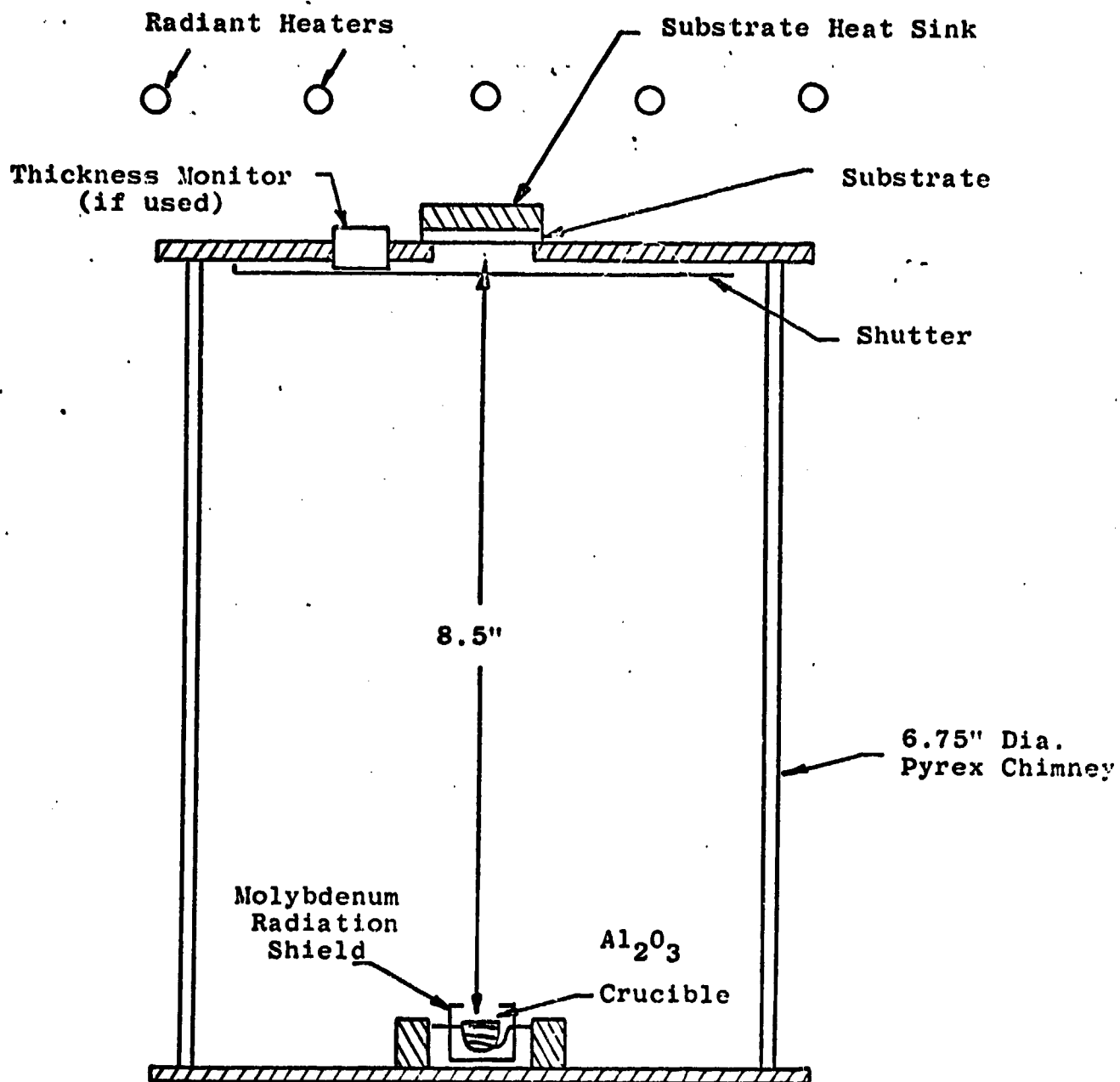
The best lamp obtained by this matrix of permutations was fabricated of:

1. Commercially obtained  $\text{SnO}_2$  coated glass substrate.
2.  $250\text{\AA}$  of  $\text{GeO}_2$ ; vacuum baked 2 hrs. at  $500^\circ\text{C}$ .
3.  $18,000\text{\AA}$  of ZnS (shot from charge containing 20% MnS); vacuum baked 2 hrs. at  $500^\circ\text{C}$ .



Thin Film EL Lamp

FIGURE 8



The  $\text{Al}_2\text{O}_3$  Crucible is Heated by a Tungsten Coil. A Close Fitting Plug of  $\sim \frac{1}{4}$ " thick Quartz Wool is Placed Over the Deposition Charge and Held in Place by a Simple Refractory Metal Split Ring.

Diagram of ZnS, CdSe, PbS, PbSe  
Deposition Fixture

FIGURE 9

4. 9,000Å of  $\text{GeO}_2$ .
5. Karma<sup>TM</sup> rear electrode.

This lamp would emit 1,000 ft-L when driven at 260 V rms and 5KHz. Lifetimes of this type of lamp were only ~50 hrs. at which time voltage breakdown at small spots would begin to destroy the test cells. Decay was very slight before failure. The voltage breakdown problem plagued us throughout the program.

Figure 10 is a representative sample of the brightness vs. voltage characteristics of the TFEL lamps fabricated in this matrix study. The results are typically that:

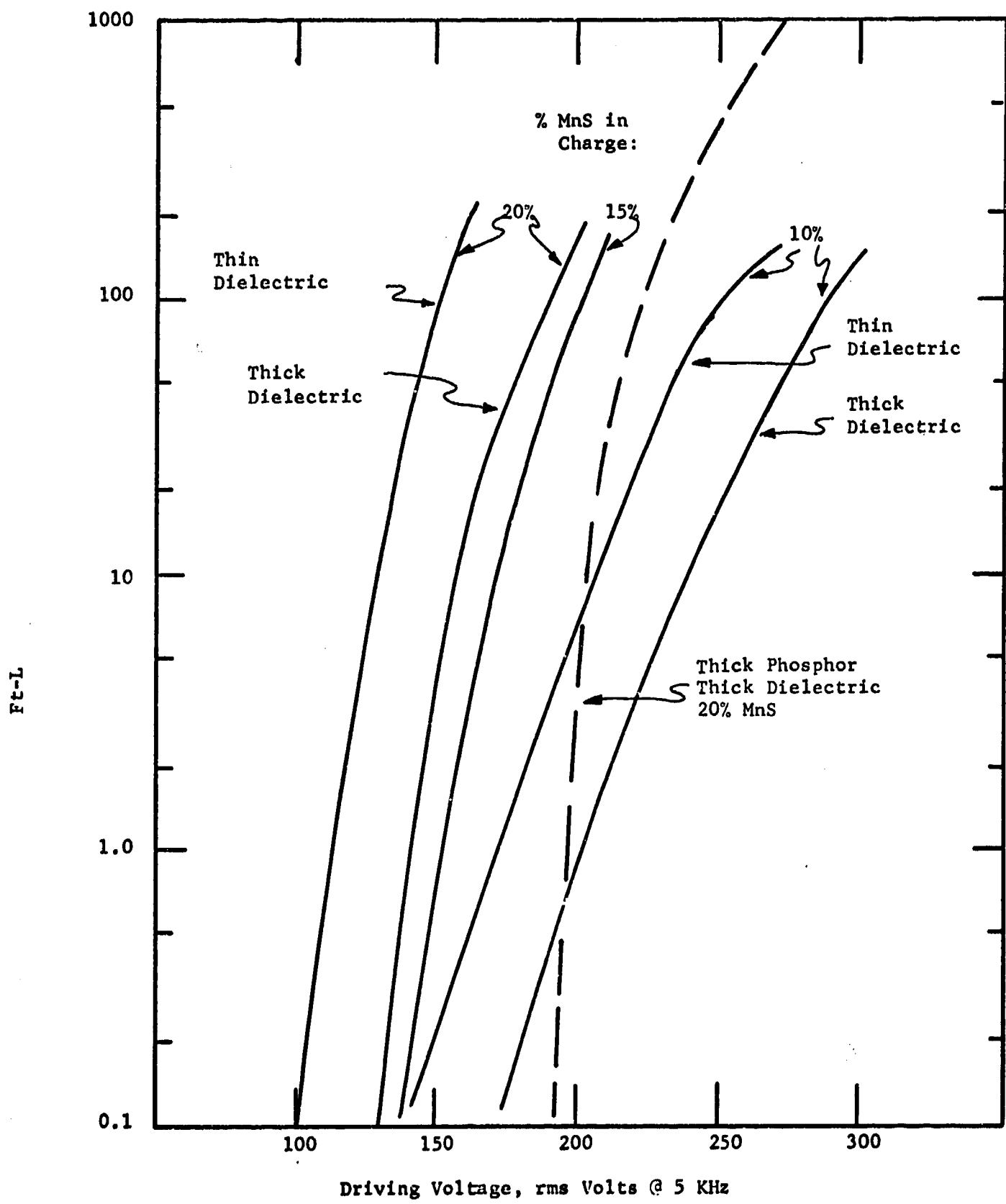
1. Increasing thickness of  $\text{GeO}_2$  layer shifts the curves to increased operating voltage.
2. Increasing Mn concentration in the phosphor layer (No.3 above) shifts the curve to lower operating voltage and steepens the slope of the curve.
3. Post deposition vacuum baking of the phosphor layer is very important for maximum phosphor brightness and lifetime.

Figure 11 is a comparison of a lamp fabricated in the matrix study with a commercially available TFEL lamp (Sigmatron, Inc., Goleta, California). Our lamp was fabricated as follows:

1. Commercial  $\text{SnO}_2$  coated glass substrate
2. 250Å  $\text{GeO}_2$ , unbaked
3. 15,000Å  $\text{ZnS}$  phosphor, shot from charge containing 20%  $\text{MnS}$ , vacuum baked 2 hrs. at 500°C.
4. 9,000Å  $\text{GeO}_2$ ,
5. Au rear electrode

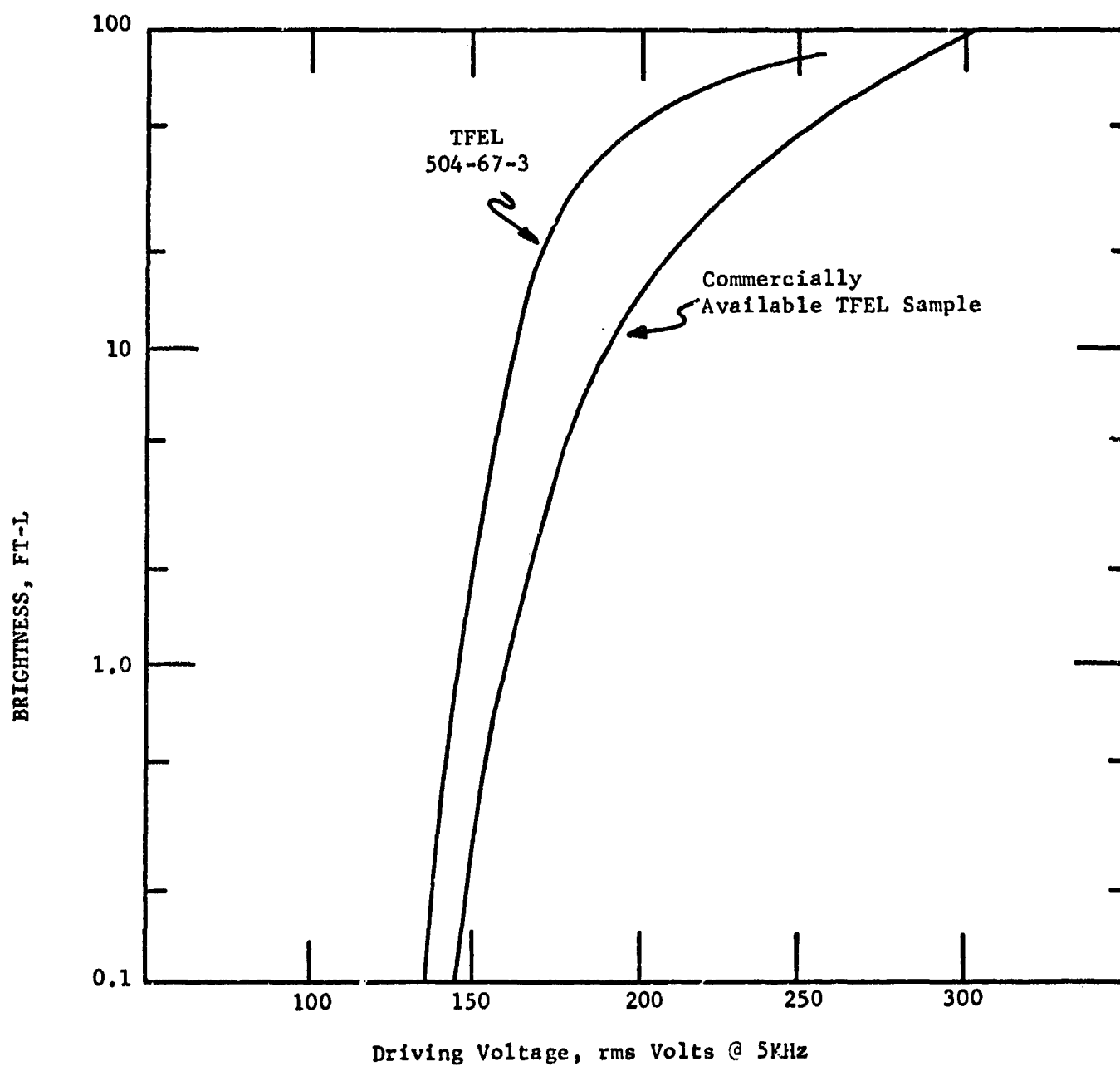
All dielectric and phosphor depositions were made with a substrate temperature of 200°C. The  $\text{ZnS}$  evaporation crucible has a quartz "wool" plug placed on top of the charge. A thermocouple encapsulated in quartz is used to monitor the temperature of the quartz "wool" plug. For this lamp, the temperature was 1150°C. The lamp operated for 240 hours at near 50 ft-L before voltage breakdown occurred.

The operating frequency was 5 KHz and the voltage was 209 V rms. The voltage was gradually increased to 218 V to compensate for aging. All good lamps exhibited excellent brightness maintenance. But at some time after approximately one hundred hours, they suffered a catastrophic breakdown which obliterated the entire cell.



TRENDS IN B vs V FOR DIFFERENT TFEL CONSTRUCTION PARAMETERS

FIGURE 10



BRIGHTNESS VS. VOLTAGE OF LABORATORY SAMPLE LAMP COMPARED WITH AVAILABLE  
TFEL LAMPS

FIGURE 11

This catastrophic failure mode of the TFEL lamps which plagued us was traced to almost sub-microscopic pinholes in the phosphor layer. Very small defects in the surface of the finished lamps were observed to be the center of destruction of macroscopic areas that broke down in operation. We were already using a quartz "wool" plug in our phosphor deposition boat. If we increased the thickness of this plug or used a less porous plug, we expected deposition times to become very lengthy. Consequently, we began experimenting with thicker nucleating layers under the phosphor layer. Previously, if a  $GeO_2$  nucleating layer of greater than  $\sim 250\text{\AA}$  was used, the lamp surface crazed during vacuum baking. We changed the  $GeO_2$  evaporation source from an  $Al_2O_3$  crucible to a Pt resistance heated source of simple folded ribbon geometry. Much better adhesion of  $GeO_2$  to the front electrode was then observed.

The catastrophic failure mode of the TFEL lamps was reduced. The deposition source for the  $GeO_2$  layers and the increased thickness of the phosphor nucleating layer helped.

The best lamp fabricated since using a thicker nucleating layer was manufactured in cross grid matrix style with 0.016" wide  $InO_2$  lines on 0.020" centers for the semitransparent electrode.

The lamp was fabricated of:

1.  $InO_2$  coated substrate (etched into lines).
2.  $500\text{\AA}$   $GeO_2$  unbaked, deposited from Pt boat. Charge is fused before opening shutter.
3.  $20,000\text{\AA}$  of  $ZnS$ , shot from a charge containing 20%  $MnS$ , vacuum baked two hours at  $500^\circ C$ . Source diffuser plug temperature is  $1150^\circ C$ .
4.  $6,000\text{\AA}$  of  $GeO_2$  deposited from Pt boat. Charge is fused before opening shutter.
5. Al rear electrode (deposited as lines).

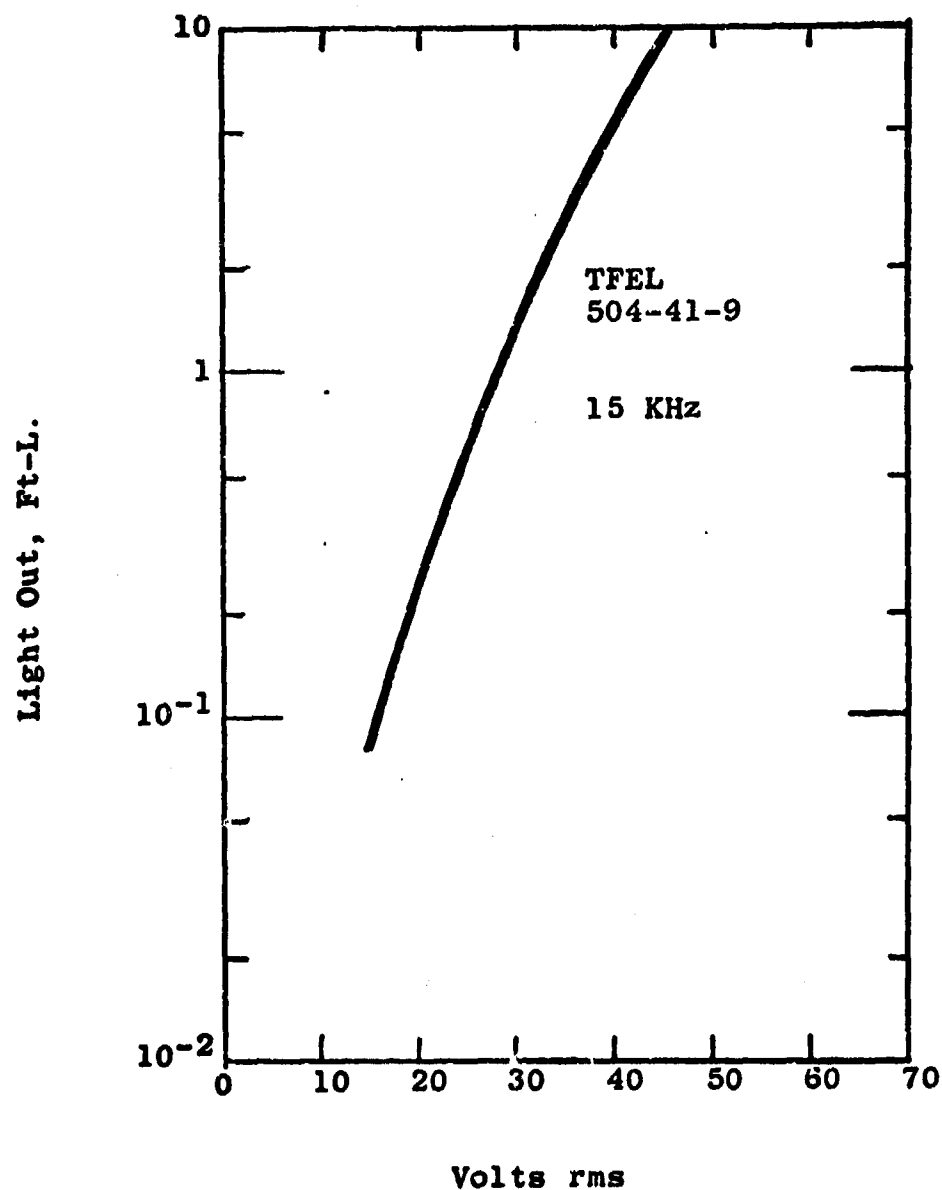
This lamp was operated in a constant brightness mode. It exhibited a fast decay mode after initial turn-on. Its beginning operating parameters were 185 V rms at 5 KHz to emit 50 ft-L. Its "first" half life was  $\sim 10$  hrs. At this time, the voltage was raised to 192 V rms. Its projected half life at this voltage was  $\sim 1125$  hrs. After 800 hrs. running time, the lamp required 200 V to emit 50 ft-L. Small portions of the lamp did suffer catastrophic failures; final failure occurred at approximately 1200 hours. We feel that this particular phosphor fabrication technique does yield a useful phosphor layer but our substrate preparation procedures need further refining. At this stage of development, the TFEL effort was then directed toward methods of integrating TFEL cells into EL/PC test assemblies.

### 2.3 Interesting Anomalies of TFEL

While fabricating a test EL/PC assembly, a small portion of the assembly was coated with the following layers:

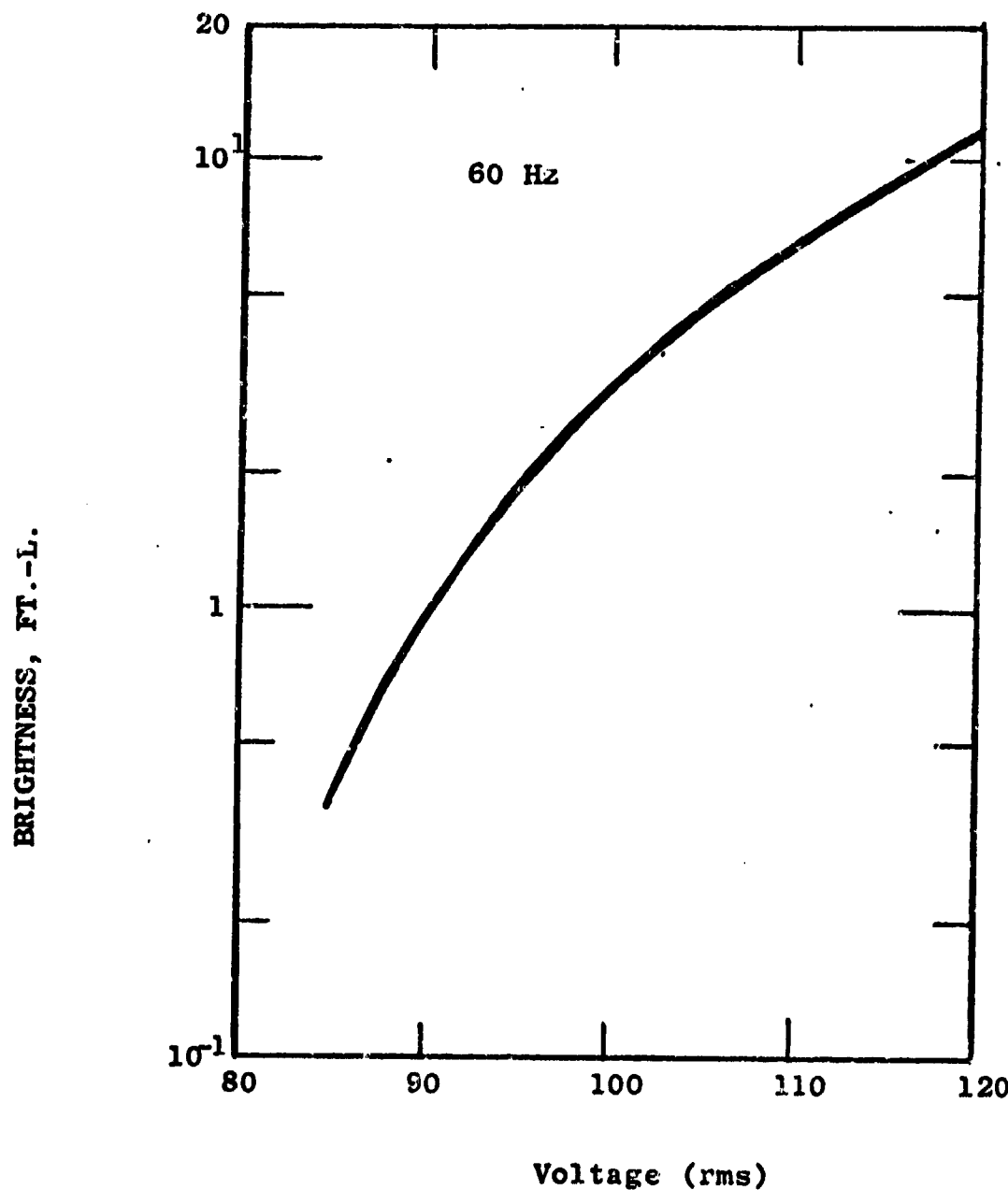
1. Glass substrate
2. Molybdenum base electrode
3. ~ 10,000Å of CdS, Se:Cl
4. 3,000Å GeO<sub>2</sub>
5. 16,000Å of ZnS:Mn (shot from a charge containing 15% MnS)
6. 3,000Å GeO<sub>2</sub>
7. Semitransparent (~ 40%) Karma<sup>TM</sup> electrode

This combination of materials produced a very low-voltage TFEL lamp. The operating characteristics of the lamp are shown in Figure 12. The lamp would not emit light under direct current stimulation. As circumstances permitted, we used scrap samples of TFEL lamps to try to determine what caused this behavior. Our best guess as a result of several loosely controlled experiments is that Cl doping from the CdS, Se layer caused the phenomena. As a check, we ran a ZnS:Mn TFEL layer through a photoconductor Cl doping cycle. After depositing the dielectric layer, we obtained a TFEL lamp having operating characteristics as shown in Figure 13. This was the lowest voltage lamp we fabricated (when operated at low frequencies). The lifetime of the lamp was only a few hours.



TFEL Lamp with CdS Layer Included

FIGURE 12



LOW VOLTAGE TFEL OUTPUT BRIGHTNESS

FIGURE 13

### 3.0 UV-to-Visible Image Conversion Panels

#### 3.1 Introduction

We originally proposed that ultra violet-to-visible mosaic image converters might be feasible if large band gap photoconductor materials, those greater than 3 ev, exist which are compatible with current EL/PC construction techniques and exhibit fast photocurrent rise and decay times. Such a candidate material is ZnO (band gap ~ 3.2 ev). The literature shows it to have a slow photocurrent rise and decay time. However, these reports do not clearly indicate its behavior in thin film form under the large signal voltage biases necessary for mosaic EL/PC image conversion. Thus, materials such as  $Al_2S_3$ , ZnO, ZnS,  $In_2O_3$ ,  $SnO_2$ ,  $Sb_2O_3$ ,  $Bi_2O_3$ , and/or others, as indicated by brief literature search, were to be prepared in thin film form and doped according to the best information available. Photocurrent under near UV stimulation was to be measured while ac voltages of 50 to 250 volts rms at 400 to 4,000 Hz were applied. These measurements of photocurrent when used in the computer simulation of EL/PC devices would help determine the feasibility of a UV-to-visible image converter.

#### 3.2 Results

The literature search turned up deposition techniques only for ZnO and of course, ZnS. ZnS has a very low conductivity. The few samples of pure ZnS that we prepared with 0.002" electrode spacings and thicknesses of  $6,000\text{\AA}$  to  $20,000\text{\AA}$  had resistance values  $> 10^9 \Omega$ . We could not detect any photoconductivity when stimulated with intense  $.336\mu$  radiation.

We then turned to ZnO as it is somewhat better documented as a photoconductor. It seems that most techniques for producing ZnO as a photoconductor are held as proprietary and little has been published on the subject. We first attempted to deposit ZnO by reactive sputtering in a partial atmosphere of  $O_2$ . All attempts had very poor adhesion to the substrates. Next we used r-f sputtering and obtained clear, well adhering films. In thicknesses of  $6,000\text{\AA}$  to  $18,000\text{\AA}$  the films had a cell resistance (.002" electrode spacing, see Figure 1) of  $1.5 \times 10^5 \Omega$  to  $10^3 \Omega$ . However, we could detect no photoconductivity under intense UV stimulation. We attempted to Cu dope the films by imbedding the substrates in doped powder and baking the container at  $400^\circ C$  for various lengths of time. The only result was cloudy, peeling films. Again, no photoconductivity was observed but the results are not conclusive since the films were very crazed and cracked.

As one last experiment we checked to see if the ZnS:Mn TFEL lamps would emit light at less than their normal voltage under UV stimulation. No effect other than simple fluorescence was observed.

As a consequence of the above negative results and lacking information as to proper ways to proceed in post deposition treatment of ZnO films, we discontinued effort on this task.

#### 4.0 X-Ray to Visible Image Conversion Panels

##### 4.1 Introduction

Past work on EL/PC mosaic structures showed that uncooled PbS photoconductive cells appeared to not have a useful dynamic range of resistance for use in a PC-EL infrared image converter. Very little has been done to investigate its use as an X-ray sensitive photoconductor, and it is judged that carrier lifetime is probably too short for this application.

However, a heterojunction device of PbS and CdS or PbSe and CdSe shown in Figure 14 was proposed as a possible X-ray sensitive photoconductor combination.

A sound theoretical justification for expecting useful performance from such a device couldn't be presented. The photoconductivity mechanisms for PbS are not well understood. However, work performed on a proprietary X-ray dosimeter utilizing thin films of Pb as X-ray to electron converters indicated that such a heterojunction device should be investigated.

##### 4.2 Results

The first problem encountered with the structure of Figure 14 is that we could not prepare PbS with small enough dark conductivity to adequately turn off an EL cell.

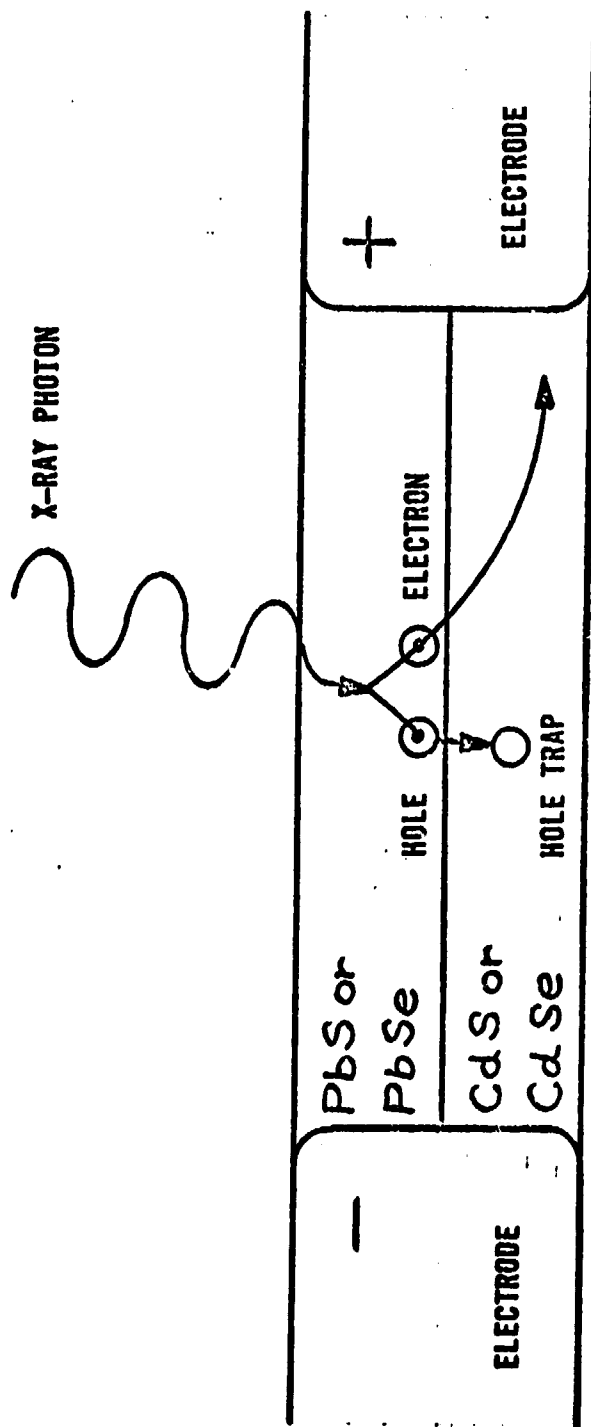
The PbS layer would effectively short out the CdS layer. The only way we could decrease the conductivity of the PbS layer was to decrease the thickness to  $\sim 1000\text{-}2000\text{\AA}$  and sinter it in an  $\text{O}_2$  atmosphere for several hours. However, films that were this thin were obviously too thin to absorb enough X-ray photons to be useful. The only other thing we could try was to see what happened if the PbS layer was patterned so that it did not contact the electrodes. If a high resistance layer formed at the PbS-CdS junction, the CdS film could retain a smooth enough electric field across its electrode gap to function as a photoconductor. Experimental trials indicated that the opposite effect occurred. It appeared that the PbS-CdS interface became a very conductive region compared to either material. As an increasing voltage was applied to the electrodes, the CdS layer would begin to break down near the electrodes. It acted as if the PbS-CdS interface was a current shunt.

At this point in the program, it was decided to cease effort on this task as proposed.

We checked to see if the operating voltage of a TFEL lamp was reduced by X-ray stimulation. There was no observable effect.

##### 4.3 Recommendations

Using thin film photoconductors to convert X-ray photons into photocurrents of a magnitude suitable for controlling the emission of electroluminescent lamps is most probably not practical.



HETEROJUNCTION CONFIGURATION FOR  
CARRIER INJECTION TRANSVERSE TO E FIELD

FIGURE 14

As long ago as eighteen years, moderately successful X-ray-to-visible conversion panels were fabricated of thick film EL and thick film CdS layers. These devices were never practical due to construction problems. Thick film CdS is very difficult to prepare in uniform layers of the necessary ~ 0.010" thickness for adequate X-ray absorption. Also, if the devices are prepared in a "sandwich" structure, which was the only practical process in the past, the shunting capacitance across the PC limits the useful range of the device. However, if TFEL instead of thick film EL could be used, the effective shunting capacitance across the CdS would be reduced significantly. If further work with direct conversion of X-rays is to be pursued, the TFEL and thick film CdS or CdSe sandwich structure should be investigated.

It should be noted that indirect conversion, using a conventional Patterson CB-2 phosphor screen to convert X-rays to visible light and then a visible-to-visible image intensifier panel to amplify the image, has been successfully developed under another contract\*. In this way, reductions in radiation levels have been achieved which are quite significant. Optical gains in excess of 100 were achieved on 10" x 10" panels with 0.020" center-to-center cell spacing; image saturation can be obtained with less than 20 mR exposure to 70 KeV X-rays. This then constitutes a performance "yardstick" against which any direct conversion approach must be measured.

---

\*U.S. Army Electronics Command, Fort Monmouth,  
Contract No. DAAB07-71-C-0267.

## 5.0 Visible-to-Visible Image Conversion Panels

### 5.1 Introduction

Under this part of the program, we were to develop, if possible, two basic types of visible light amplifier panels. The first type was to be a very sensitive panel. This type was to be sensitive to as small an input light level as possible. The second type was to have as large an output brightness as possible with its sensitivity threshold possibly no better than  $10^{-2}$  to  $10^{-1}$  ft-cd. The high brightness panel was to be considered mostly for use as the second stage of an image conversion system. The first stage of such a system could be whatever type of image converter we developed (IR, UV, X-ray, or Visible Light sensitive). This high brightness second stage would be used as a "brightener" to overcome ambient light problems in viewing an image on the first stage panel by itself. To build such a high brightness panel, a TFEL output is virtually required if we were to have a chance of achieving many tens of ft-Lamberts output brightness.

The first type or sensitive panel would probably have to be one using thick film EL for output. Based on previous experience, thick film EL cells are a much better impedance match for sensitive CdS type photoconductors than are TFEL cells. Also, TFEL cells had not been successfully integrated into an assembly.

As was mentioned in Section 4.3 above, concurrent with this contract we were also working on a contract from Fort Monmouth (DAAB07-71-C-0267) to develop our existing light amplifier technology into the capability for fabricating 10" x 10" image conversion panels using 0.020" EL/PC cells. This excellent research mix involving an assembly technique development program greatly benefited both programs. We used the PC doping results of this program in fabricating 10" x 10" light amplifier panels for the Army and we used the improved assembly techniques in fabricating thick film EL devices in this program.

### 5.2 Sensitive Light Amplifiers

#### 5.2.1 PC Materials Study

We began with three types of PC deposition material. The first type was CdS. In all doping experiments with Cu and Cl as dopants, the resulting films were sensitive to light levels of  $5 \times 10^{-3}$  ft-cd or greater but response times were very sluggish. Response time for a CdS:Cu, Cl cell to reach 90% of its final conductivity was typically minutes for a stimulation of  $5 \times 10^{-3}$  ft-cd. Also, this material was very history-sensitive. After an hour of light stimulation for testing, the PC cells typically had to be kept in the dark overnight to be able to duplicate the results of the testing.

We also tried using a mixture of 80% CdS and 20% CdSe as a deposition material. When doped with Cu and Cl, films of this material exhibit no long-term "history" effects. However, it was difficult to include enough Cu in the films. The only way we could Cu dope with any success was to imbed the films in a crucible filled with an overdoped ( $Cu_2S$ ) CdS powder and fire the covered crucible in a  $N_2$  atmosphere at  $4000^\circ C$  for times of 15 minutes to 2 hrs. This method would increase the resistivity and sensitivity of the films. But the films are cloudy and have poor uniformity. Subsequent doping with HCl gas further reduced the uniformity but sensitivity was generally increased.

With the poor results of the previous two types of PC, we returned to the material we have used for several years. This is an 80% CdS, 20% CdSe finely divided powder already doped with Cu and Cl and quite photoconductive. Before depositing this material, it must be baked in vacuum at  $600^\circ C$  for at least sixty minutes to drive out the chlorides. The PC films will not adhere to the substrates if this is not done. By using this doped powder, the PC film received adequate Cu doping during formation. Prior to this contract, we had attempted to Cu dope the PC films by evaporating minute amounts of Cu during PC film deposition but the results were always erratic.

Figure 15 is a plot of the PC cell conductivities of a 2" x 2" PC array made with the pre-doped CdS,Se powder. The bars represent the ranges of conductivity observed by measuring 25 cells spaced uniformly about the substrate. The straight line drawn through the plot is the least squares fit to the data used in the simulation programs discussed in the Appendices.

This type of photoconductor can have its impedance values at a stimulation level of  $10^{-1}$  ft-cd varied by almost two orders of magnitude by varying the amount of Cl doping. This feature allowed us to use this same type of photoconductor in assemblies having TFEL output layers.

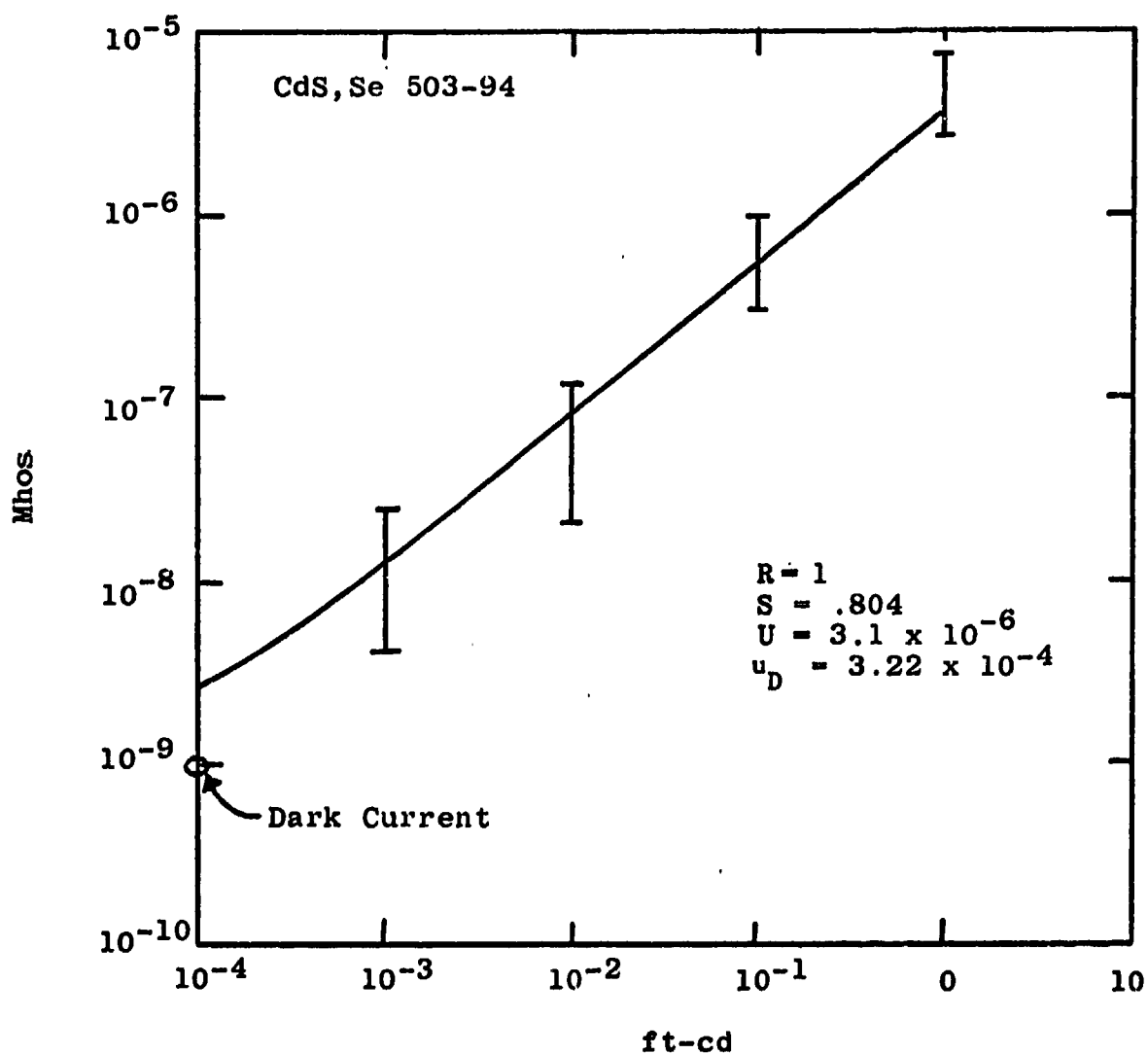
### **5.3 Assembly Techniques**

#### **5.3.1 Thick Film EL Assemblies**

Figure 16 shows a cross-sectional view of the structure we use for thick film EL assemblies. This structure is basically the same as we have successfully used for some time. The device is assembled from the PC layer forward. The thick film EL layer is simply sprayed on.

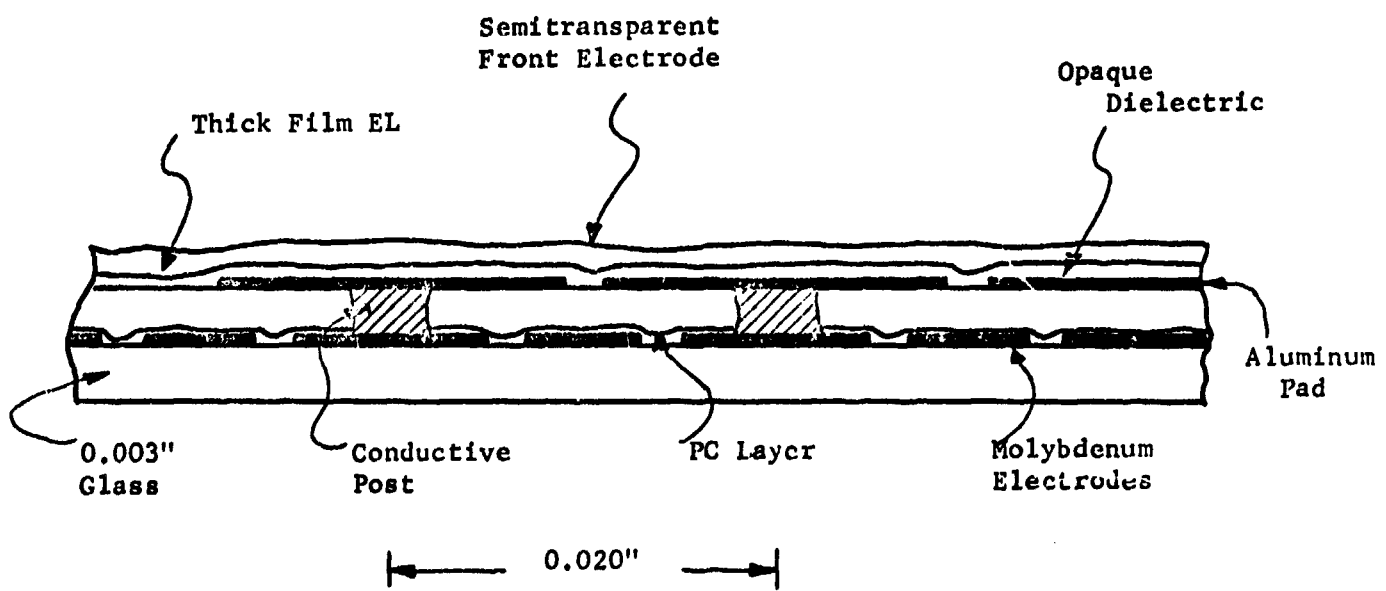
#### **5.3.2 TFEL Assemblies**

This proved to be a very difficult task. We were able to dope arrays of CdS,Se photoconductive cells to give us impedance ranges compatible with simple "sandwich" electroded TFEL lamps. We had great difficulty in successfully attaching our standard interconnect layer to the TFEL lamp array. The interconnect layer is a glass-epoxy composite



TYPICAL CONDUCTIVITY OF PC CELLS VS GREEN LIGHT STIMULATION

FIGURE 15



CROSS SECTION OF EL/PC IMAGE CONVERSION PANEL USING THICK FILM EL

FIGURE 16

layer 0.003" thick which contains solid conductive posts on 0.020" center-to-center spacing to connect the center electrode of each PC cell to the rear electrode of each TFEL cell. Our fundamental problem seemed to be that in the initial turn-on of the TFEL lamp array, there are always a number of pinhole defects that must blow out and clear the short circuits at those points. Some of these defects occur in the interface between the TFEL lamp and the conductive post. It appears that these defects enlarge to destroy the entire post-TFEL interface and then the entire TFEL cell breaks down and the effects propagate (probably because of trapped gases and heat) to neighboring cells. Eventually, most of the TFEL lamp array is destroyed.

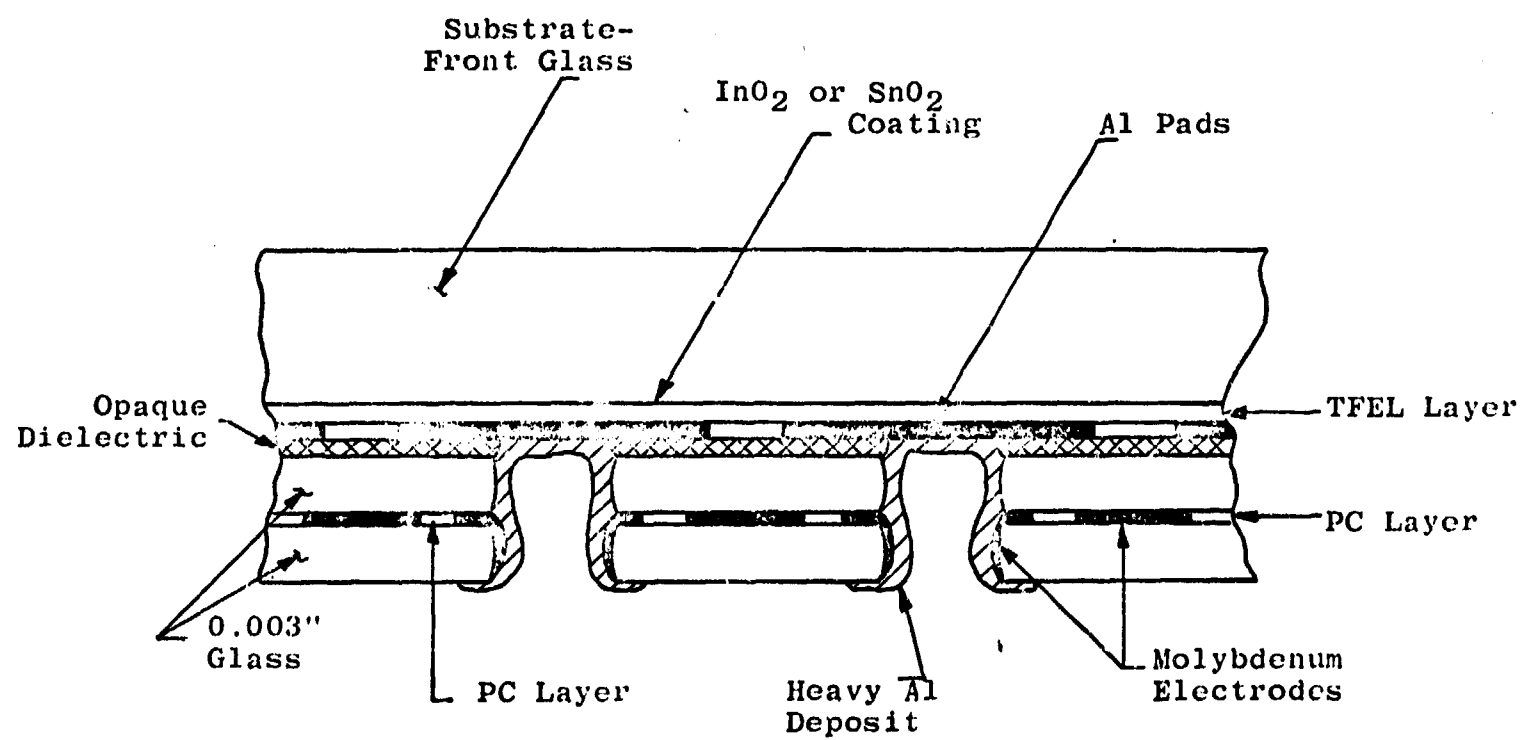
Our next approach to the problem was to omit the interconnect layer. We fabricated the PC cells on a sheet of 0.003" glass which had holes etched through the glass in the center of each center electrode of the PC cell. We bonded this PC substrate to the rear of the TFEL lamp array with the PC itself facing away from the TFEL. The PC substrate then became the interconnect layer. Then thin film through-hole interconnect techniques were used to connect the PC cell electrodes to the TFEL lamp electrodes.

This technique showed promise. For this technique to work, an opaque dielectric layer must be included at the rear of the TFEL layer to prevent light feedback from reaching the PC layer. The best thin film opaque dielectric layer that we made was made of Ge co-deposited with  $GeO_2$ . We have achieved 0.1% transparency (in the green) with a film  $\sim 5,000\text{\AA}$  thick. The film has a resistivity of greater than  $10^9$  ohms per square. The film contained  $\sim 15\%$  excess Ge. We experienced problems in achieving uniformity of resistivity of the films. The basic technique seems to be that the  $GeO_2$  evaporation must begin first with the Ge evaporation phased in slowly until the desired ratio of rates is achieved. The usual results were that high resistance films peeled off in baking and low resistance films adhered nicely. The problem seems to be in finding the best evaporation rate schedule for getting both adhesion and high resistivity. We could not complete this task before the program was finished. So we fabricated a TFEL light amplifier using a thick film opaque dielectric. This structure is shown in Figure 17. This structure is cumbersome but it verified that the  $CdS,Se:CuCl$  photoconductor in thin film form can successfully control TFEL sandwich cells.

#### 5.4 Assembly Test Results

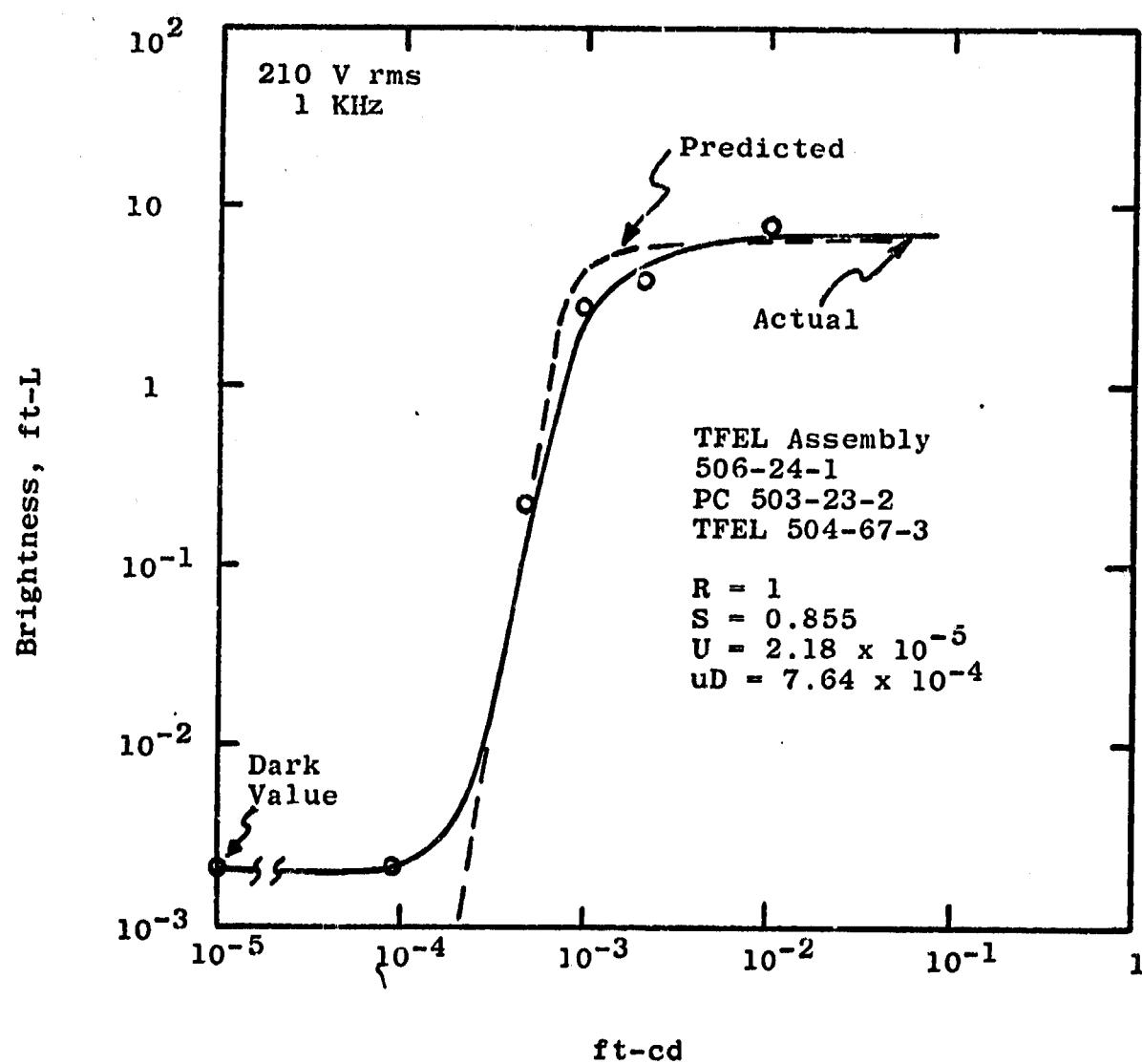
##### 5.4.1 TFEL Assembly

A TFEL assembly built as in Figure 17 had response characteristics as shown in Figure 18. The points plotted are the averaged output of the assembly. Because of the sharp "turn-on threshold" of the device, small variations in TFEL characteristics or PC characteristics cause the vertical portion of the curve to vary over two-thirds of decade of input values. We plotted the prediction vs. the average of several cells since the prediction is an average of PC characteristics measured before assembly. The discrepancy in the dark output for the assembly is most probably due to halation from nearby shorted cells.



INTERCONNECTION TECHNIQUE FOR TFEL/PC STRUCTURE

FIGURE 17



TFEL Visible-to-Visible Image Conversion Panel

FIGURE 18

#### 5.4.2 Thick Film EL Assembly

A thick film EL assembly built as in Figure 16 had response characteristics as shown in Figure 19. This assembly did not fit the computer simulation. Investigating the discrepancy, we discovered that the opaque dielectric layer in the thick film EL layer had been inadvertently sprayed on too thick. This decreased the response of the EL layer and consequently diminished the gain we had expected. This points up the necessity for further development of thin film opaque dielectric layers. The opaque layer should be minimized in thickness as much as possible so that as much as possible of the voltage applied to the EL cell can be across the EL material and not be wasted in the opaque layer.

#### 5.5 Feasibility of Stacking Visible-to-Visible Image Conversion Panels onto Other Panels

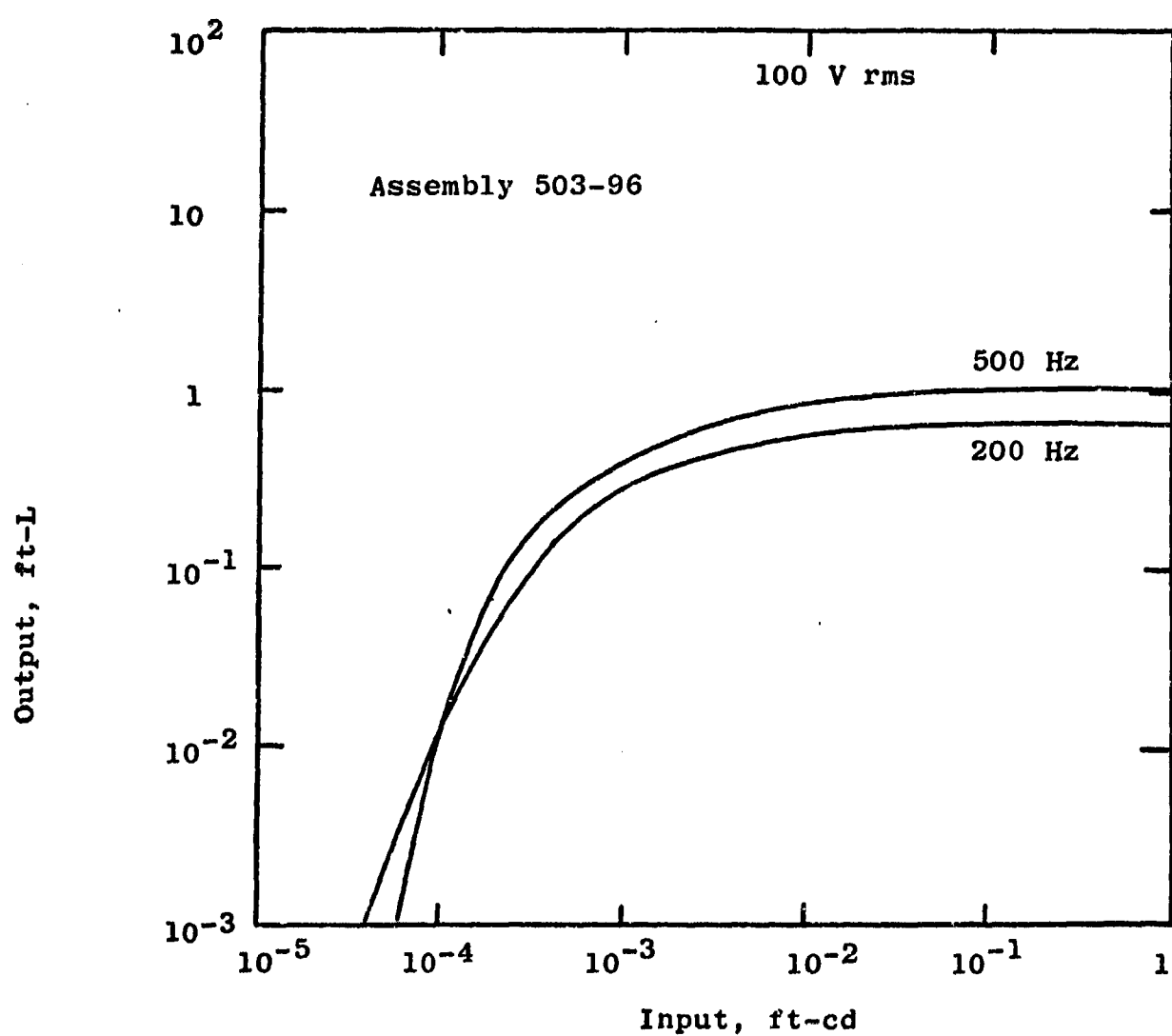
The final assemblies of TFEL and thick film EL image conversion panels were not finished in a form compatible with actual stacking of one onto another because of electroding problems.

Preliminary simulations have been performed using our best CdSe - thick film EL combination from the previous contract and data we have from previous visible-to-visible image converters. The resultant combination would have an output of less than  $10^{-3}$  ft-L for an input of  $\sim 8 \times 10^{-6}$  w/cm<sup>2</sup> and an output of  $\sim 1$  ft-L for an input of  $\sim 2 \times 10^{-5}$  w/cm<sup>2</sup>. The usable contrast range is very narrow which makes the device almost a saturating threshold type image converter. This type of performance is due to the fact that both CdSe and CdS PC/EL image converters have a ratio of output/input that increases rapidly to saturation as a function of input. When two of these ratios are multiplied together in a "stacked" device, the resultant ratio yields an input-output curve that resembles a step function. Figure 20 is a plot of the IR input vs. output of a simulated device.

There are two methods to overcome this lack of gray scale range. The first technique is to develop photoconductors which have smaller conductivity change per unit increase in input radiation than the present photoconductors used. Past evidence indicates that some improvement can be made in this area.

The other technique is to make use of the variation in input-output properties of the EL/PC devices as frequency of voltage is changed. Figures 21 and 22 illustrate how the input-output curves shift with voltage and frequency variation.

We are attempting to determine whether the easily implementable techniques of amplitude modulating and/or frequency modulating the driving voltage of the image converters will effectively expand the gray scale range. The basic idea is to time share the different input-output curves within the limits of the integration time of the eye so that for a fixed input level a non-flickering image is perceived.



PERFORMANCE OF THICK FILM EL VISIBLE-TO-VISIBLE IMAGE CONVERSION  
PANEL

FIGURE 19

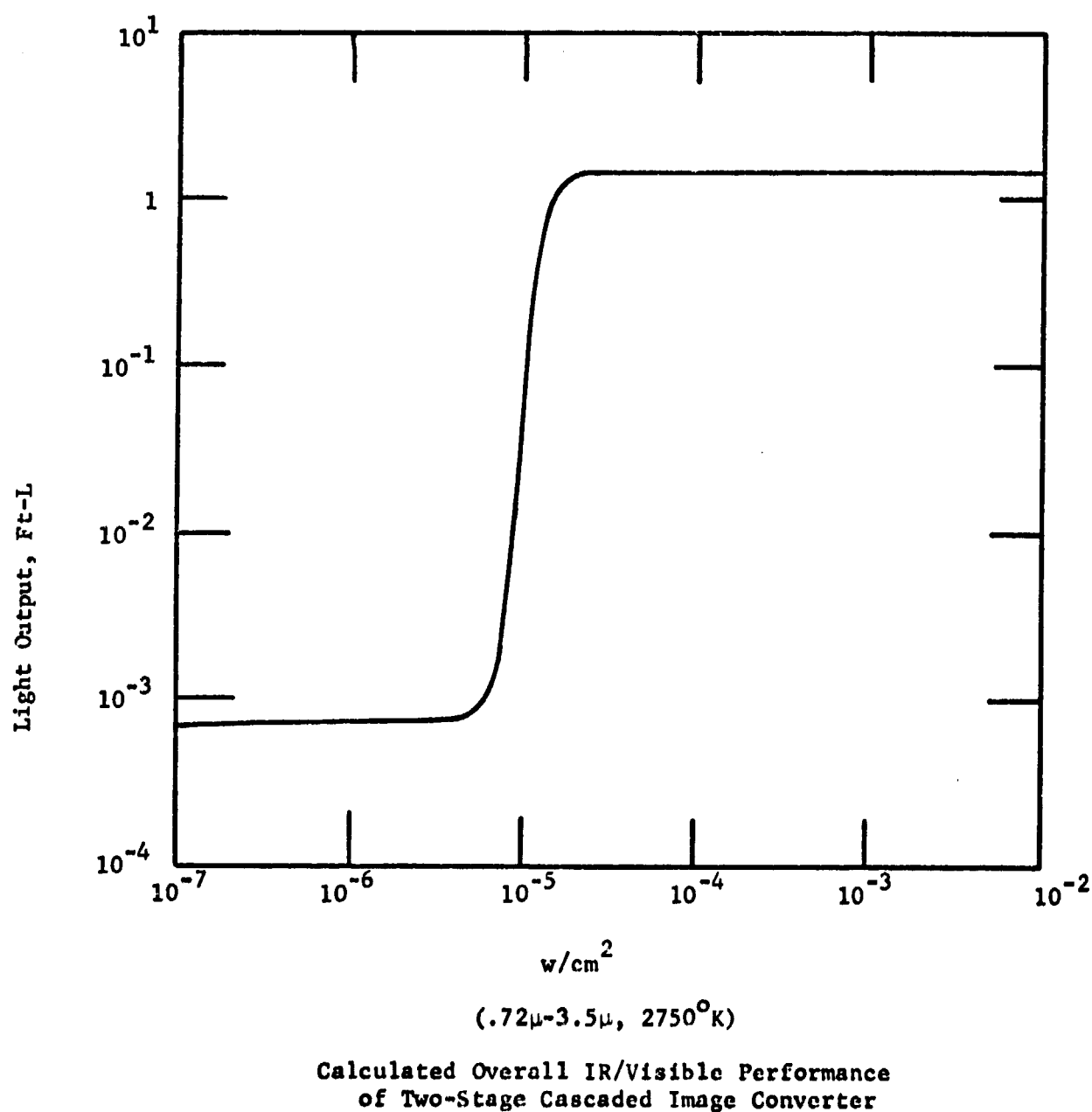
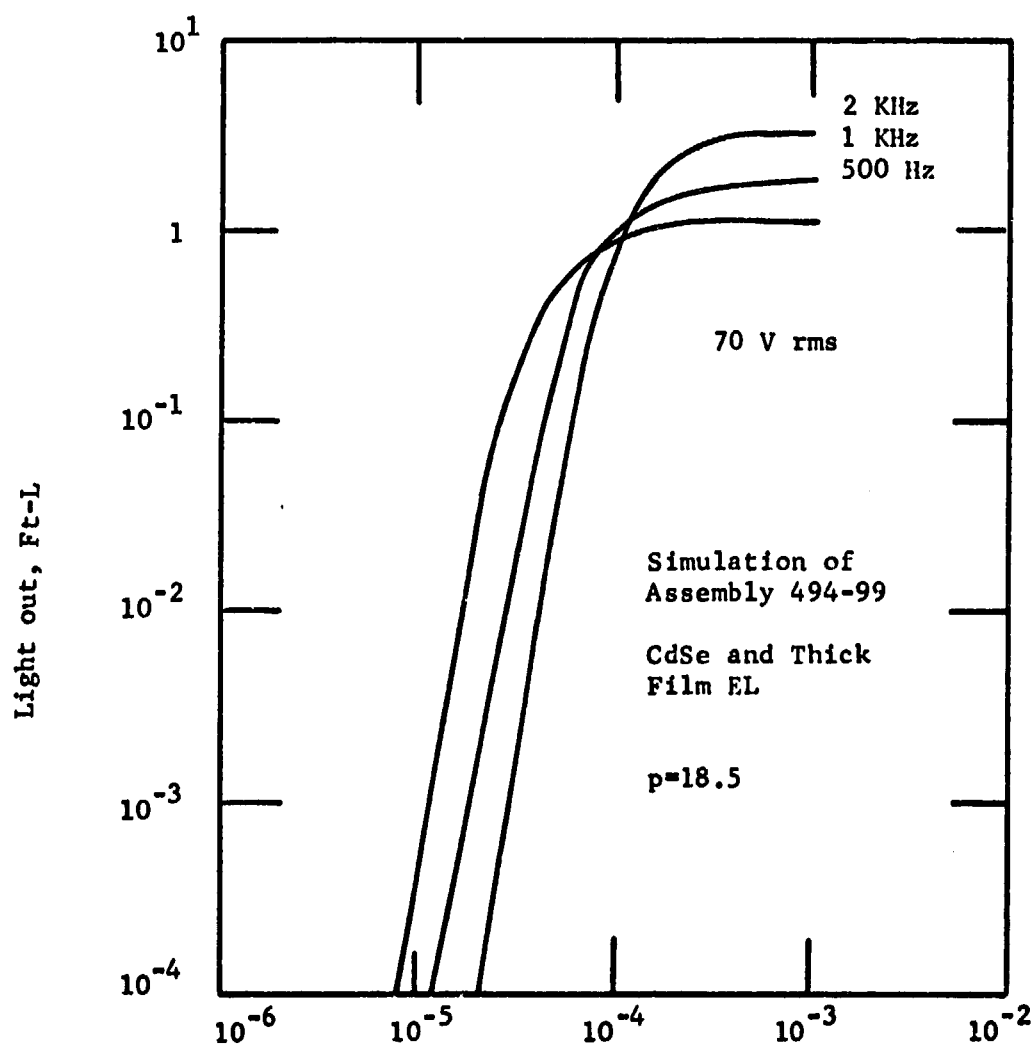


FIGURE 20

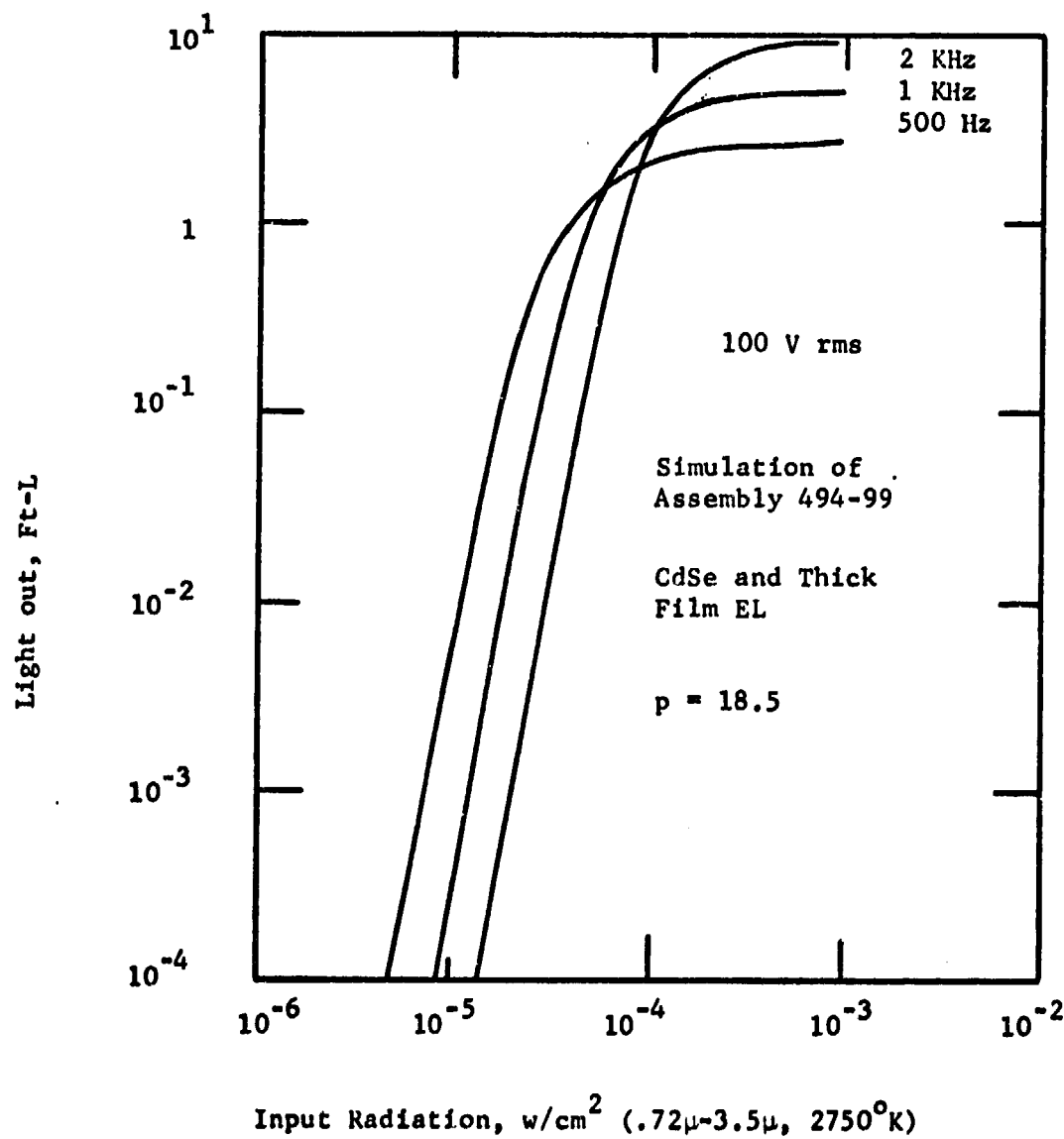


Input Radiation,  $w/cm^2$  (.72 $\mu$ -3.5 $\mu$ , 2750 $^{\circ}$ K)

(P is the ratio of El capacitance to shunt capacitance across the photoconductor)

Simulation of EL/PC Panel Operation at 70 V rms

FIGURE 21



(P is the ratio of EL capacitance to shunt capacitance across the photoconductor)

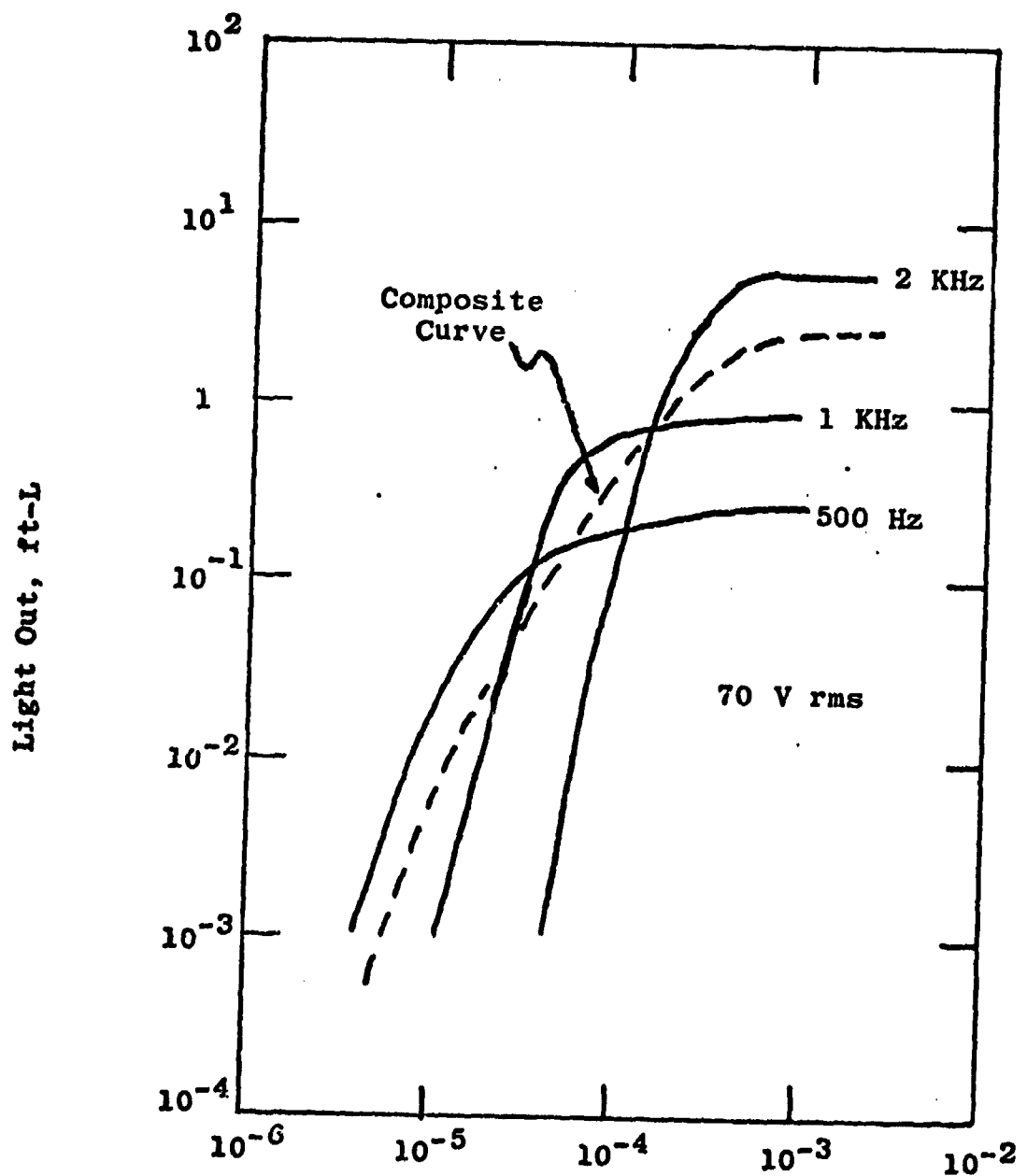
Simulation of EL/PC Panel Operation at 100 V rms

FIGURE 22

Toward this end, the computer simulations developed under the previous contract were "streamlined" and expanded to assist in easier reduction of greater quantities of data. The multi-frequency driving techniques being studied under a concurrent ONR contract have been simulated for an equal mixture of three frequencies and is plotted as the dashed curve in Figure 23. This driving technique has been experimentally verified.

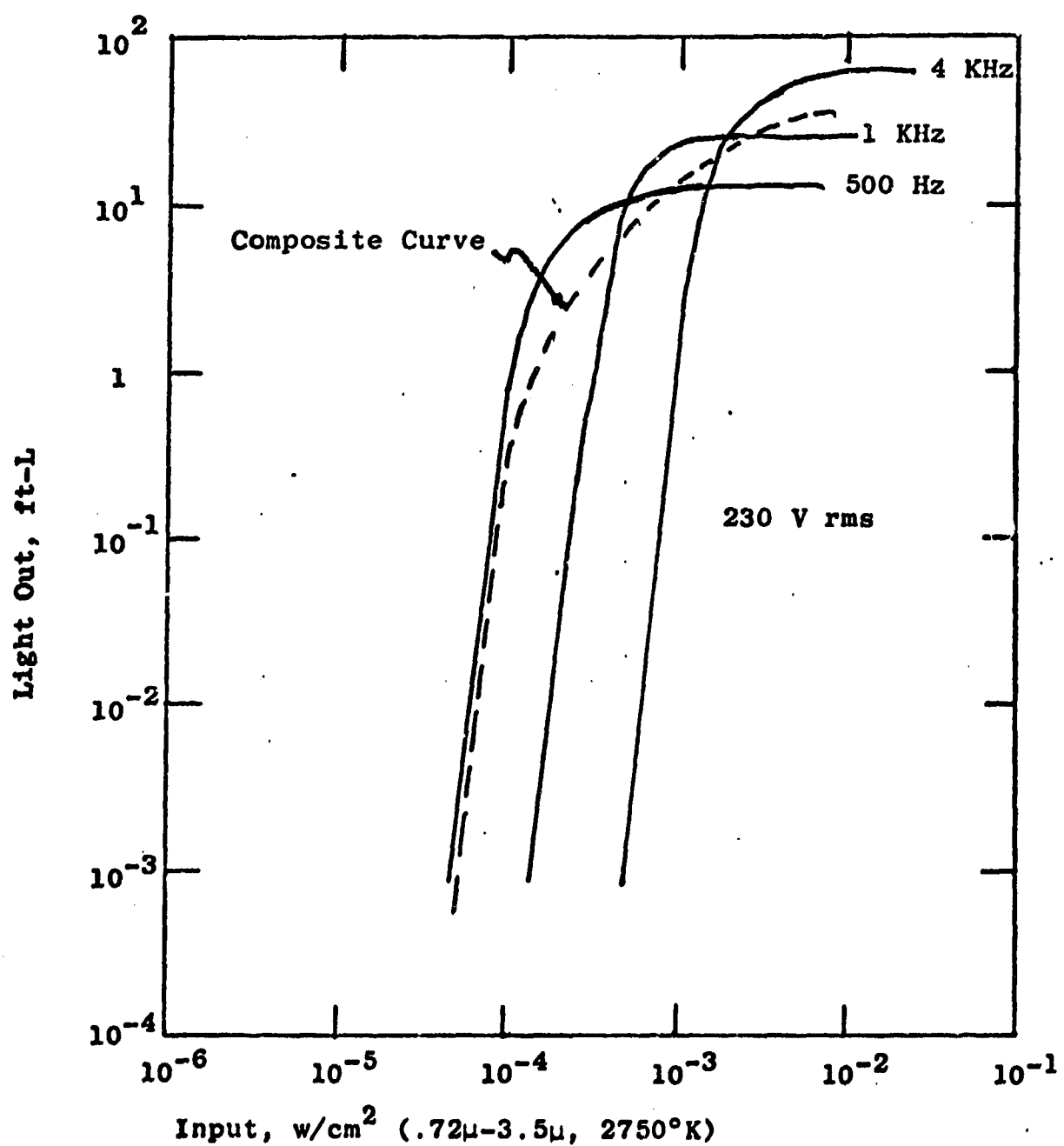
Figure 24 is the same driving technique used with a simulation of the same CdSe as Figure 23 only using TFEL for the output lamps. Again the three frequencies shown were mixed in equal proportions in the composite simulation.

It appears that if the output of the final image conversion panel is to be viewed and analyzed by the human eye, then the slope of the light-in vs. light-out curve of the final panel can be effectively made unity. This will avoid shrinking the response range of a cascaded pair of image conversion panels.



Simulated Operation of CdSe 494-95-8  
With Thick Film EL Using 3 Frequency Drive

Figure 23



Simulated Operation of CdSe 494-95-8  
With TFEL 494-79-2, 5A Using 3 Frequency Drive

Figure 24

## 6.0 IR-to-Visible Image Conversion Panels

### 6.1 Introduction

Under this task we were to continue development of the IR sensitive CdSe-thick film EL panels we worked on under the previous contract (N00014-70-C-0213). We were to also extend the work to using TFEL as an output media. Also, we were to investigate the feasibility of placing a visible-to-visible light amplifier panel on top of an IR-to-visible image conversion panel. In this way, rather large conversion gains might be realized for the cascaded pair of panels.

### 6.2 Results

We finished the last program by using a CdSe PC cell array which was made by depositing pure CdSe onto an etched molybdenum electrode array (see Figure 1) on a substrate of 0.003" thick glass. The CdSe was doped with HCl gas at 400°C for 18 minutes.

Our first attempts at improving upon this technique was to dope the CdSe powder with CuCl<sub>2</sub> solution, sinter in vacuum, regrind the powder, and use this powder as deposition material. The Cl would mostly escape during sintering so the deposited films were doped with HCl gas as before. We were never able to get reproducible or uniform films with this process. Small regions of some of the films were extremely sensitive but uniformity was very poor. Vacuum annealing of the CdSe films before Cl doping didn't improve the results.

Next we tried depositing pure CdSe, ~ 10,000Å thick, and then depositing approximately 10Å of Cu on the CdSe films. The 10Å of Cu was deposited by an extrapolation method. First ribbons of Molybdenum with a known thickness of Cu were used as flash evaporation sources and the thickness of the resulting deposit was measured. This measurement gave us a source film to substrate film ratio per unit area of the source ribbon. From this data, we prepared ribbon sources to give us a 10Å Cu deposit on the CdSe. The CdSe films were then baked in vacuum at 400°C for 1 hour to diffuse in the Cu.

Again, the resulting films exhibited very poor uniformity.

Next, we attempted to improve upon a procedure that was first tried under the previous contract. This procedure was to imbed the CdSe coated substrate in a finely ground powder consisting of 98% CdSe, 1% CuCl<sub>2</sub>, and 1% NaCl as a flux. This combination of imbedding powder and substrate was then placed in a closed crucible and baked at temperatures equal to or greater than 350°C for various periods of time. All attempts produced films with very non-uniform response. We substituted Cu<sub>2</sub>S for the CuCl<sub>2</sub>, and used various amounts of NaCl and many combinations of baking times and temperatures. No improvement in uniformity was noted. The

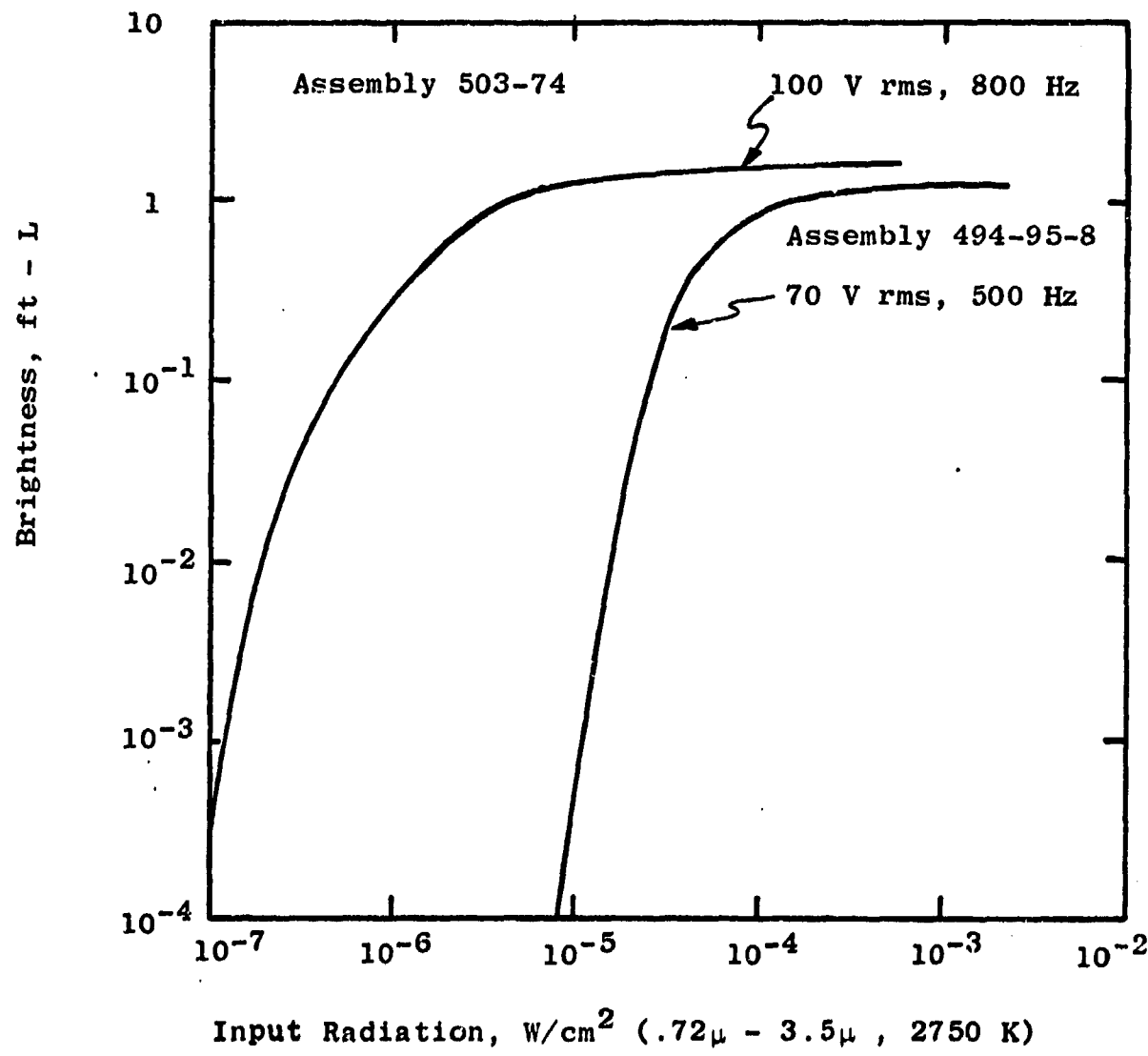
literature had many excellent descriptions of techniques similar to this being used with good results. However most experimenters reported a large class of different types of recrystallization phenomena seen when using this imbedding technique. We deduced that most previous experimenters had used rather macroscopic electrode sizes and spacings when measuring the response of their resultant films. We have found that we can only use electrode gaps of ~ .0015 to ~ 0.004" in the simple square "moated" electrode pattern (see Figure 1) and achieve proper ranges of cell impedance. The best conclusion we can draw from all the unsuccessful doping-by-imbedding experiments is that this technique is unsatisfactory when using small electrode spacings and buried electrodes.

We then returned to trying by other means to get a CdSe film properly doped with Cu and with Cl as a co-activator. Knowing that using a pre-doped powder for film deposition yielded good results for visible light photoconductors of 80% CdS and 20% CdSe, we again attempted to duplicate this technique using only CdSe doped with Cu and Cl. Initial results from using the pre-doped powder were disappointing. As a point of reference, though, it took more than six man-months of dogged effort to develop a reliable technique for depositing the pre-doped CdS,Se film. The first few pre-doped CdSe films exhibited poor adhesion in patterns very reminiscent of the ones seen in early attempts with the CdS, Se films. However, we did not have 6 man-months of effort left in the program at this time.

At this time, we decided to see just how IR sensitive our green-sensitive CdS, Se films were. A good green-sensitive thick film EL with CdS,Se:CuCl assembly was tested on the IR source and we received a pleasant surprise. It was as sensitive as was predicted for the best cells of CdSe:CuCl that we had occasionally found on some substrates. We had never thought to measure the IR response of the PC for this assembly. Figure 25 shows the response of this assembly to near IR and for comparison, the best assembly that we fabricated under the previous contract.

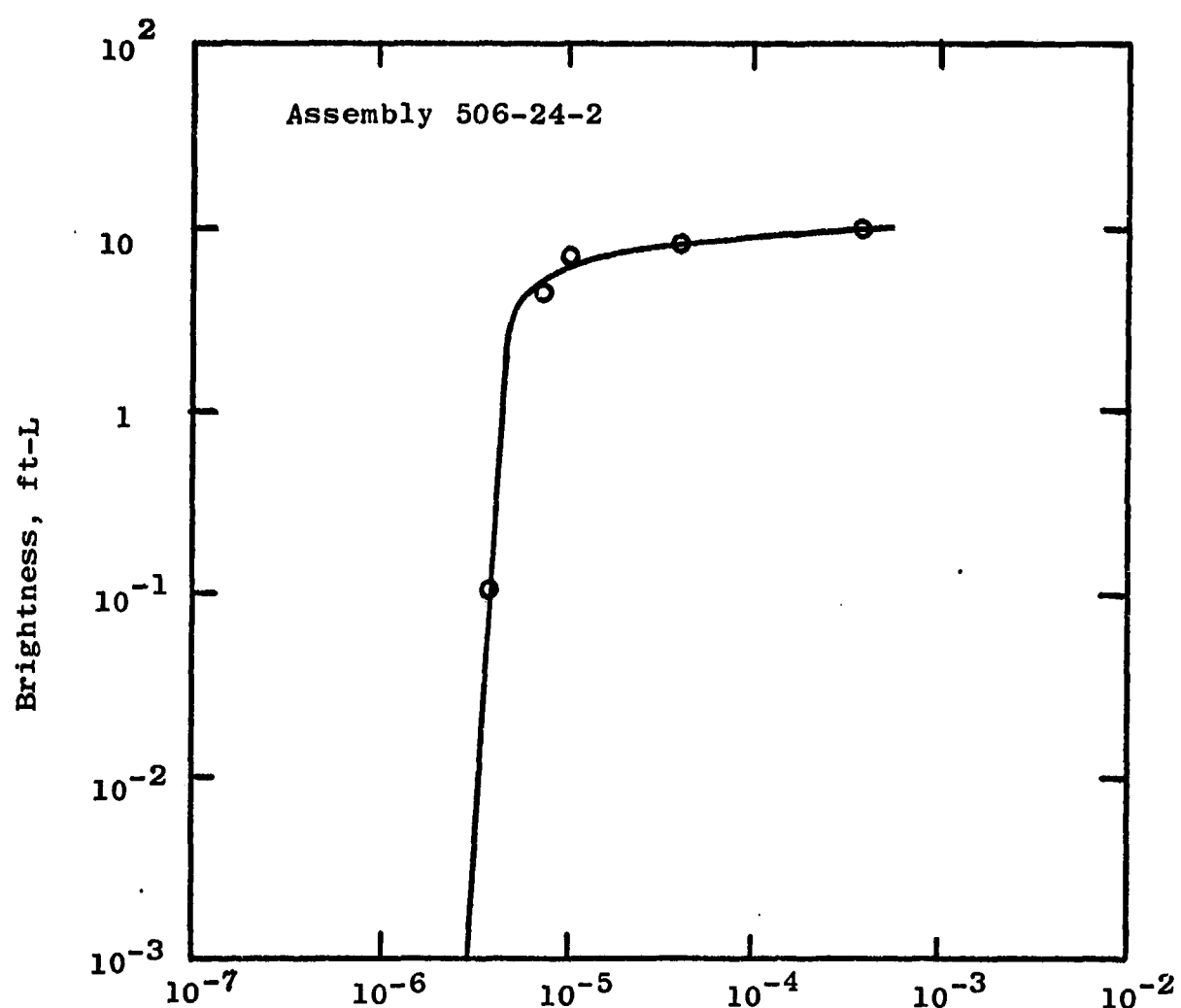
Following this lucky turn of events, we then tested a TFEL green-sensitive test assembly on the IR source. The results are shown in Figure 26. Again the PC used in this assembly had not been characterized with IR stimulation.

It now appears that the shortest development route to the best IR-to-visible image converter is to modify our CdS, Se:CuCl deposition powder by changing the ratio of CdS to CdSe in small increments until the best IR response is found.



THICK FILM EL/PC IR IMAGE CONVERTERS  
PRESENT AND PREVIOUS

FIGURE 25



TFEL IR-TO-VISIBLE IMAGE CONVERTER

FIGURE 26

## 7.0 General Results, Conclusions, and Recommendations

- 1) We expanded modeling techniques to facilitate parameterization of materials, to investigate more complex forms of excitation waveforms, and to simulate the cascaded operation of various potential PC/EL candidate systems.
- 2) TFEL developed to point where can fabricate in useful brightnesses ( $> 50$  F-L) for useful lifetimes ( $\sim 1200$  hours); test assemblies have been successfully integrated with photoconductors using these films in mosaic form.
- 3) Visible: P/C has been developed which, with useful uniformity over large areas, is capable of controlling output for input values around  $5 \times 10^{-4}$  foot-candles. Peak optical gains of the order of 500 have been achieved using thick film EL outputs (Figure 17), and of the order of 3,000 using thin film EL outputs (Figure 18).
- 4) IR (Figure 25): Response curve moved down 2 orders of magnitude with useful response now available at  $10^{-6}$  w/cm<sup>2</sup>.
- 5) UV: Unsuccessful in obtaining photoconductors with useful characteristics, in terms of impedance and voltage levels required to control series EL mosaic cells, with measurable sensitivity in the UV spectrum.

### Recommendations:

Further studies of electroding and interconnecting TFEL would be required before mosaic arrays with the brightness and contrast required for high-ambient displays, such as avionic systems, can be realized with practical geometries and useful yields.

State of the art, in simulation, analysis, design, and fabrication, has developed to the point at which specific applications in IR and visible image amplifiers, image conversion panels, and opto-electronic logic can be evaluated using simulation techniques. In those cases where a simulation shows predicted useful performance, fabrication techniques have been perfected to the point where we can predict the feasibility of realizing a useful structure.

APPENDIX A  
IR PROGRAM AND PLOT SUBROUTINE

**A1. Introduction**

The IR Program is written in FORTRAN IV and is used on a time sharing computer network with a remote teletypewriter terminal. The input files and keyboard inputs and the styles of data output have all been programmed with ease of data handling for the designer in mind. The details of the equations used in the circuit analysis are given in Section A2 below and a detailed description of the program itself is also given. In addition, tables of all the input parameters and a form of useful data sheets for these input parameters are given.

**A2. Circuit Analysis and Solution Procedure**

Figure A1 shows the form of circuit that this program solves. It is only a series parallel combination of resistors; however, the resistors vary nonlinearly. We treat this circuit as an almost linear circuit. The voltage across the EL cell is given in rms form by the equation:

$$V_2 = V_o \left| \frac{Z_2}{Z_1 + Z_2} \right| \quad \text{Equation A1}$$

where  $V_o$  is the rms applied voltage,  $Z_1$  is the complex impedance of the photoconductor, and  $Z_2$  is the complex impedance of the EL cell. For simplification:

$$\text{let } S_1 = \omega C_1 \text{ and } S_2 = \omega C_2$$

$$\text{then } Z_1 = \frac{1}{G_1 + jS_1} = \frac{G_1 - jS_1}{G_1^2 + S_1^2} = \text{PC Impedance}$$

$$Z_2 = \frac{1}{G_2 + jS_2} = \frac{G_2 - jS_2}{G_2^2 + S_2^2} = \text{EL Impedance}$$

Equation A2

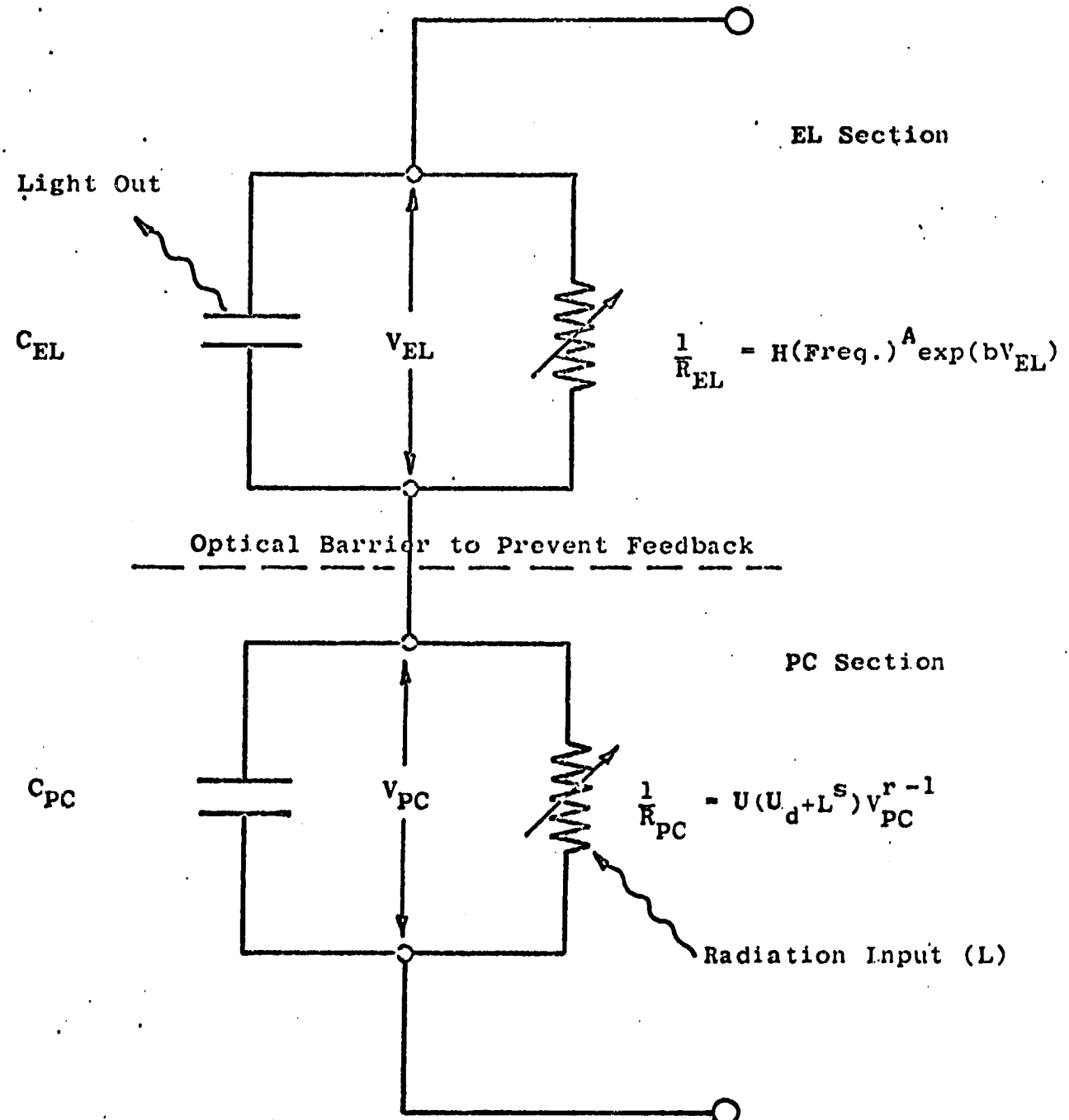
Taking the absolute values, we have:

$$|Z_1|^2 = (G_1^2 + S_1^2)^{-1}$$

$$|Z_2|^2 = (G_2^2 + S_2^2)^{-1}$$

$$|Z_1 + Z_2|^2 = \frac{(G_1 + G_2)^2 + (S_1 + S_2)^2}{(G_1^2 + S_1^2)(G_2^2 + S_2^2)}$$

Equation A3



Circuit Used in Steady State EL/PC Image Converter Simulation

FIGURE A 1

Putting these values in Equation A1, we have:

$$v_2 = v_o \sqrt{\frac{G_1^2 + S_1^2}{(G_1 + G_2)^2 + (S_1 + S_2)^2}} \quad \text{Equation A4}$$

To help in simplification in terms later on:

$$\text{let } p = \frac{C_2}{C_1} = \frac{S_2}{S_1}, \text{ note } \frac{pG_1}{\omega C_2} = \frac{G_1}{\omega C_1} \quad \text{Equation A5}$$

Using this simplification, Equation A1 becomes:

$$v_2 = v_o \sqrt{\frac{\left(\frac{pG_1}{\omega C_2}\right)^2 + 1}{\frac{p(G_1 + G_2)^2}{\omega C_2} + (1+p)^2}} \quad \text{Equation A6}$$

Solving similarly for  $v_1$  we have:

$$v_1 = v_o \sqrt{\frac{\left(\frac{pG_2}{\omega C_2}\right)^2 + p^2}{\frac{p(G_1 + G_2)^2}{\omega C_2} + (1 + p)^2}} \quad \text{Equation A7}$$

Also, for the ratio of voltages of the EL to the PC element, we have:

$$\frac{v_2}{v_1} = \sqrt{\frac{\left(\frac{pG_1}{\omega C_2}\right)^2 + 1}{\left(\frac{pG_2}{\omega C_2}\right)^2 + p^2}} \quad \text{Equation A8}$$

The photoconductor conductivity  $G_1$  is usually described by an equation of the form:

$$G_1 = U(U_d + L^s) V_1^{r-1} \quad \text{Equation A9}$$

Where  $U$  is a dimensional constant,  $U_d$  is a dark conductivity term,  $L$  is the input radiation, and  $s$  and  $r$  are constants. For completeness, the leakage conductivity of the EL is usually found to be best fit by an equation of the form:

$$G_2 = H \omega^A \exp(b(V_2)) \quad \text{Equation A10}$$

Where  $H$  is a dimensional constant, and  $A$  and  $b$  are constants. Usually  $b$  is very small so in the computations that follow, we neglect the voltage dependence of  $G_2$ . Strictly speaking, if one were to have a large  $b$  value one should modify the derivation that follows to include this voltage dependence in  $G_2$ . The final thing to be calculated is the brightness of the EL. This brightness usually has a functional dependence as given by:

$$B = D F^\alpha \exp\left(-\sqrt{\frac{A}{V_2}}\right) \quad \text{Equation A11}$$

Where  $D$  is a dimensional constant,  $F$  is the driving frequency,  $\alpha$  and  $A$  are constants. Taking Equations A9 and A10 and substituting in equation  $V_1$ , we have:

$$G_1 = U(U_d + L^s)(f(G_1))^{r-1} \quad \text{Equation A12}$$

Where  $f(G_1)$  represents the right hand side of Equation A7. In solving this implicit equation, we now need the services of the computer. Equation A11 is of the form:

$$G_1 = f(G_1) \quad \text{Equation A13}$$

This equation can be solved by Newton's iteration method.

Basically, this method finds the zeros of a function of the type:

$$y = f(x) \quad \text{Equation A14}$$

By repeatedly doing an iteration of the form:

$$x_{n+1} = x_n - (y_n/y'_n) \quad \text{Equation A15}$$

To get faster convergence, we used the second order form of this iteration equation as given below:

$$x_{n+1} = x_n - \frac{y(x_n)}{y'(x_n)} \left[ 1 + \frac{y(x_n) y''(x_n)}{(2 y'(x_n))^2} \right] \quad \text{Equation A16}$$

After the iteration is complete, the value of  $G_1$  is used in Equation A6 to get the rms voltage applied to the EL cell. The actual equations used in the second order iteration are very long and are contained in the iteration calculation section of the IR Program.

### A3. Description of IR Program and Plot Subroutine

IR is written in FORTRAN IV and is used on a time-sharing computer system through a standard teletype terminal. Figure A2 contains a listing of IR. Figure A3 contains a listing of PLOT. The time sharing system it has been used on has excellent file editing capabilities if the file contains line numbers. The first field of numbers on a line are the line numbers. The second field of numbers is the FORTRAN statement number field. The "\*" are for comment lines. The program is liberally laced with comments as to the function of flags and switches and the purpose of a group of statements. In the program, the values of input radiation are referred to as "steps". Unless problems with the PC conductivity iteration are encountered, the input radiation as incremented as integers times powers of ten i.e.,  $1 \times 10^{-6}$ ,  $2 \times 10^{-6}$ ,  $3 \times 10^{-6}$ , ...,  $1 \times 10^{-5}$ , .... If, for example, iteration convergence is not obtained for an input step of  $9 \times 10^{-4}$ , then the input radiation value is "backed up" to  $8.1 \times 10^{-4}$  ( $8.0 \times 10^{-4}$  would have been successfully used). If iteration convergence is still not achieved, the input radiation is "backed up" to  $8.01 \times 10^{-4}$ . If convergence is then achieved, the input steps are then  $8.02 \times 10^{-4}$ , ...,  $8.09 \times 10^{-4}$ ,  $8.1 \times 10^{-4}$ , ...,  $8.9 \times 10^{-4}$ ,  $9 \times 10^{-4}$ . When the program is working in one of these modes, the terms "back up" or "small step" appear in the comment lines.

A feature which might be overlooked upon first glance at the program or the block diagram is that whatever form of data output is chosen, the program computes a value of light output for zero radiation input for every voltage and frequency. This computation is done at the beginning of every input light loop.

The linearized circuit equations discussed in the previous section are utilized in the program under the comment "iteration calculations" and at line 1260 and line 1300.

Table AI lists all the parameters for the data files, the file numbers, and gives a brief description of the parameters.

If desired, the resultant data may be written into a data file defined at program execution time.

Figure A4 is a block diagram of the IR program. This is not a flow chart. It is meant to be used as a guide to finding one's way through the program in addition to providing a brief overview of the operation of the program.

Figure A5 is a data sheet that has been useful to the computer operator when using the program and it contains the format specifications used in the files.

The subroutine PLOT plots logarithmically the light output versus the radiation input. The abscissa is not internally scaled and accepts only the fifty-five "normal step" values generated in IR. The ordinate scale is controlled by the variable LP which allows a vertical scale on the teletypewriter of six orders of magnitude. After the plot, 3 lines of data identification will be printed if they were included in the data files. This subroutine is used with several other programs that are described later.

## IR PROGRAM

```

20    * IMAGE INTENSIFIER, G=U*(UD+T**S)*(V1***(R-1.0))
40    * CHOOSE TYPE OF OUTPUT; KKK=1, DATA TABLE
60    * KKK=2, PLOT ONLY
80    * KKK=3, DATA TABLE AND PLOT
100   DIMENSION P(5),V(5),FR(5)
120   DIMENSION TT(19,5),BB(19,5)
130   COMMON TS,BB,LP
140   DIMENSION GVOL(55)
160   DIMENSION DV(3),AV(3),VEA(3),ALF(3)
180   CALL DEFINE(1,3HEL, )
200   CALL DEFINE(2,3HPC, )
220   CALL DEFINE(3,6HKNBBS, )
240   CALL DEFINE(4,6HBRITE )
260   KILLD=0
280   KKK=2
320   READ (2,1) R, S, U, UD
340   IF(IEUF(2).NE.1) READ (2,552)
360   552 FORMAT('
380   READ(1,2) C
400   READ(1,901) AALF, DD, AA
420   IF(IEUF(1).NE.1) READ(1,551)
440   551 FORMAT('
460   READ(3,4) (V(J), J=1,5)
480   READ(3,4) (FR(K), K=1,5)
500   READ(4,106) (VEA(I), I=1,3)
520   READ(4,106) (DV(I), I=1,3)
540   READ(4,106) (AV(I), I=1,3)
560   READ(4,106) (ALF(I), I=1,3)
580   IF(IEUF(4).NE.1) READ(4,550)
600   550 FORMAT('
620   WRITE(9,811)
640   811 FORMAT(/'CREATE A DATA FILE? 0=NO, 1=YES'/)
660   READ(9,812) KD
680   812 FORMAT(I1)
700   IF(KD.EQ.1) WRITE(9,813)
720   813 FORMAT(/'SUPPRESS OTHER OUTPUT? 0=NO, 1=YES'/)
740   IF(KD.EQ.1) READ(9,812) KILLD
760   IF(KILLD.EQ.1) GU TO 701
780   WRITE(9,107)
800   READ(9,999) KKK
880   705 FORMAT(I10)
900   701 WRITE(9,997)
920   READ(9,996) CSHUNT
940   CSHUNT=CSHUNT*1.0E-12
960   WRITE(9,5)
980   READ(9,996) TBEGIN
990   LP=ALUG10(TBEGIN)
991   IF(KD.EQ.1) WRITE(5,792) LP
992   792 FORMAT(I2)
1000  WRITE(9,101) R,S,U,UD
1020  WRITE(9,102) C
1040  WRITE(9,902) AALF, DD, AA
1060  P(1)=C/CSHUNT
1080  WRITE(9,3) P(1)
1100  WRITE(9,104) V
1120  WRITE(9,105) FR

```

Figure A2  
Page 1 of IR Program

## IR PROGRAM

```

1140      WRITE(9,517) DV
1160      WRITE(9,518) AV
1180      WRITE(9,519) VEA
1200      WRITE(9,520) ALF
1220      * NVT=2 PUT G VALUES INTO GVOL(L) ARRAY
1240      * NVT=1 USE GVOL(L) ARRAY FOR G IN IMPEDANCE CALC.
1260      IF(ABS(R-1.0).LE..1) NVT=2
1280      * 'NCK' SAVES LAST 'L' INDEX OF INPUT LIGHT
1300      * LOOP IN CASE OF SATURATION BREAKOUT
1320      NCK=0
1340      * 'NVTCK' USED AS SWITCH TO STATEMENT 581 IN CASE
1360      * OF ITERATION BLOWUP WHEN COMPUTING GVOL(L) VALUES
1380      * USING OTHER THAN FIRST FREQ. VALUE
1400      NVTCK=1
1420      * SET 'IVE' TO FIRST SECTION OF B VS V EL. CURVE
1440      IVE=1
1460      I=1
1480      * VOLTAGE VALUES DO LOOP
1500      DO 88 J=1,5
1520      IF (V(J)-0.0) 99, 99, 10
1540 10 CONTINUE
1560      * PUT NON-ZERO VALUES IN INPUT,OUTPUT LIGHT MATRICES
1580      DO 516 LM=1,19
1600      DO 515 LLM=1,5
1620      TT(LM,LLM)=1.E-7
1640      S15 DB(LM,LLM)=1.E-7
1660      516 CONTINUE
1680      * FREQUENCY VALUES DO LOOP
1700      DO 77 K=1,5
1720      * SET LIGHT LOOP TERMINAL PARAMETER
1740      IDK=1
1760      IF(FR(K)-0.0)89,89,6
1780      6 CONTINUE
1800      IF(KILLD.EQ.1) GO TO 815
1820      WRITE (9,7) P(I), V(J), FR(K)
1840 815 CONTINUE
1860 301 CONTINUE
1880      * PRINT COLUMN HEADINGS
1900      IF(KILLD.EQ.1) GO TO 922
1920      IF(IDK.EQ.1) GO TO 921
1940      GO TO (921,922,921), KKK
1960 921 WRITE(9,12)
1980 922 CONTINUE
2000      * SET FIRST LIGHT VALUE
2020      T=TBEGIN
2040      IF(IDK.EQ.1) T=0.
2060      * SET VALUES FOR LOG. INPUT LIGHT VALUE GENERATOR
2080      LT=ALUG10(TBEGIN*.99)
2100      ILT=0
2120      * SET MAIN PRINT COUNTER
2140      N=0
2160      * SET VPC AND VI FOR ENTERING LIGHT LOOP
2180      VPC=V(J)/4.0
2200      V1=V(J)-VPC
2220      * SET SUBSCRIPTS FOR FIRST INPUT,OUTPUT MATRIX VALUES
2240      II=0

```

Figure A2  
Page 2 of IR Program

## IR PROGRAM

```

2260      KK=0
2280  * INPUT LIGHT LOOP
2300      D0 IS L=1, IDK
2320  * INPUT LIGHT LOG STEP GENERATOR
2340      ILT=ILT+1
2360      GO TO (53, 53, 53, 53, 53, 53, 53, 53, 53, 52), ILT
2380  52 LT=LT+1
2400      ILT=1
2420  53 CONTINUE
2440      *
2460  * SET ITERATION BLOWUP COUNTER
2480      MM=1
2500  * ADVANCE NORMAL LARGE LIGHT STEP PRINT COUNTER
2520      N=N+1
2540  * SET SMALL STEP PRINT COUNTER
2560      MMM=1
2580  * REENTER FROM SUCCESSFUL SMALL STEP CALC.
2600  51 CONTINUE
2620  * SET ITERATION COUNTER
2640      M=0
2660  * ENTER ITERATION LOOP ON SMALL LIGHT STEP
2680  87 CONTINUE
2700      IF (L-1) 23, 23, 22
2720  22 VPC=V(J)-VE
2740      V1=VE
2760  23 CONTINUE
2780  * CHECK VOLTAGE DEPENDENCE OF CONDUCTIVITY
2800  IF(ABS(R-1.0).GT..1) GO TO 863
2820      GO TO (867, 863), NVT
2840  867 IF(L.GT.NCK) GO TO 863
2860      G=GVOL(L)
2880      GO TO 864
2900  863 G=U*(UD+T**S)*(VPC***(R-1.0))
2920  864 CONTINUE
2940  * NORMAL ITERATION REENTRY
2960  8 CONTINUE
2980  * COMPUTE IMPEDANCE OF PC
3000  Y1=P(I)*G/(6.28*FR(K)*C)
3020  * ADVANCE ITERATION COUNTER
3040      M=M+1
3060  * COMPUTE 1/R OF EL
3080  Y2G=DD*(FR(K)**AQLF)*EXP(AA*(V(J)-V1))
3100  * COMPUTE POWER FACTOR
3120  PF=1./SQRT(((6.28*FR(K)*C)/Y2G)**2+1.)
3140  *
3160  * ITERATION CALCULATIONS
3180  Y2=P(I)+PF/SQRT(1.-PF*PF)
3200  Y=Y1+Y2
3220  Z=(1.+P(I))*(1.+P(I))
3240  V1=V(J)*SQRT((Y2+Y2+P(I)*P(I))/(Y*Y+Z))
3260  G1=U*(UD+T**S)*(V1***(R-1.0))
3280  DIFG=(R-1.0)*P(I)*G1/(6.28*FR(K)*C*(Y*Y+Z))
3300  DDIFG=((DIFG+P(I)/6.28*FR(K)*C*Y)+(2.0*(-DIFG)*P(I)*Y*
3320  + (DIFG))/(6.28*FR(K)*C*(Y*Y+Z)))/(1.0+(DIFG/G1))
3340  GD=(G1-G)/(-DIFG-1.0)
3360  G2=G-(GD)*(1.0+((GD)+DDIFG)/(2.0*(-DIFG-1.0)))

```

Figure A2  
Page 3 of IR Program

## IR PROGRAM

```

3380 * CONVERGENCE TEST
3400 ESC=ABS((G2-G)/G2)
3420 G0 T0 (511,512,513), MM
3440 511 IF(ESC-0.01) 20, 20, 13
3460 512 IF(ESC-0.02) 20, 20, 13
3480 513 IF(ESC-0.05) 20, 20, 13
3500 * VALUE FOR NEXT ITERATION
3520 13 G=G2
3540 IF (M-500) 66, 66, 44
3560 66 G0 T0 8
3580 * END OF ITERATION, NO CONVERGENCE
3600 * TRY ADVANCING LIGHT INPUT BY 1/10 PREVIOUS STEP
3620 44 G0 T0 (43,131,132),MM
3640 * FIRST BACKUP, MM=1
3660 43 T=T-((10.0**LT)*0.9)
3680 M=0
3700 MM=2
3720 MMM=2
3740 NVT=2
3760 G0 T0 87
3780 * SECOND BACKUP, MM=2
3800 131 T=T-((10.0**LT)*0.09)
3820 M=0
3840 MM=3
3860 NNN=MMM
3880 MMM=2
3900 G0 T0 37
3920 * ITERATION HAS CONVERGED
3940 20 CONTINUE
3960 * COMPUTE OUTPUT VARIABLES
3980 Y3=P(I)*G2/(6.28*FR(K)*C)
4000 VE=V(J)*SORT((Y3*Y3+1.0)/((Y3+Y2)*(Y3+Y2)+Z))
4010 D0 181 IT=1,3
4020 IF(VE-VEAC(IT) > 182,181,181
4030 182 IVE=IT
4035 G0 T0 183
4040 181 CONTINUE
4050 183 CONTINUE
4060 400 DVLOG=ALOG(DV(IVE))
4080 FLUG=ALF(IVE)*(ALOG(FR(K)))
4100 ELUG=SORT(AV(IVE)/VE)
4120 BLUG=DVLOG+FLUG-ELUG
4130 IF(ELUG.LT.-23.026) BLUG=-23.026
4140 B=EXP(BLUG)
4180 * SMALL STEP PRINT CHECK
4200 G0 T0 (393,396,395,396,395,396,395,396,395,394), MMM
4220 396 WRITE(9,11) T, B, VE, G2
4240 395 CONTINUE
4260 G0 T0 (393,397,398), MM
4280 398 T=T+((10.0**LT)*0.01)
4300 G0 T0 399
4320 397 T=T+((10.0**LT)*0.1)
4340 399 MMM=MMM+1
4360 M=0
4380 G0 T0 87
4400 394 G0 T0 (571,572,573),MM

```

Figure A2  
Page 4 of IR Program

## IR PROGRAM

```

4420 573 T=T+((10.**LT)*.01)
4440     MMM=NNN
4460     MM=2
4480     G0 T0 571
4500 572 T=T+((10.**LT)*.1)
4520     MMM=1
4540     MM=1
4560     G0 T0 (571,581),NVTCK
4580 581 NVT=1
4600 571 G0 T0 51
4620 * END OF SMALL STEP CALC.
4640 * MAIN STEP PRINT CHECK
4660 393 CONTINUE
4680     IF(IDK.EQ.1)G0 T0 951
4700     IF(ABS(R-1.0).GT..1) G0 T0 862
4720     G0 T0 (866,869),NVT
4740 866 IF(L.LE.NCK) G0 T0 862
4760 869 GVOL(L)=G2
4780 862 G0 T0 (96,96,15,15,96,15,15,15,98),N
4800 96 CONTINUE
4820     G0 T0 (693,930,930), KKK
4840 930 CONTINUE
4860     II=II+1
4880     JJ=K
4900     KK=KK+1
4920     LL=K
4940     TT(II,JJ)=T
4960     BB(KK,LL)=B
4980     IF(KD.EQ.1) WRITE(5,810) B,T,V(J),FR(K)
5000 810 F0RMA1(4E12.4)
5020     IF(II-19) 693,692,692
5040     692 II=0
5060     KK=0
5080 693 CONTINUE
5100     G0 T0 (951,950,951), KKK
5120 951 CONTINUE
5140     IF(KILLD.EQ.1) G0 T0 814
5160     WRITE(9,11) T, B, VE, G2
5180 814 CONTINUE
5200     IF(IDK.EQ.1) G0 T0 300
5220 950 CONTINUE
5240 * BREAKOUT OF LIGHT LOOP IF OUTPUT IS SATURATED
5260     IF (L-1) 232, 232, 231
5280 231 IF ((VE/V(J))-0.995) 232, 111, 111
5300 232 CONTINUE
5320 98 IF (N-9) 612, 611, 611
5340 611 N=0
5360 612 CONTINUE
5380 * END OF LIGHT STEP LOOP
5400 15 T=T+(10.0**LT)
5420     IDK=1
5440     NCK=55
5460     G0 T0 111
5480 * CHANGE LIGHT LOOP TO FULL RANGE
5500 300 IDK=55
5520     G0 T0 301

```

FIGURE A2  
Page 5 of IR Program

## IR PROGRAM

```

5540 * ESCAPE FROM LIGHT LOOP ( SATURATED OUTPUT )
5560 111 CONTINUE
5580   NVT=1
5600   NVICK=2
5620   IF(NCK.EQ.55) GO TO 63
5640   NCK=L
5660 63 CONTINUE
5680   GO TO 77
5700 * NO ITERATION CONVERGENCE FOR THIS FREQ., VOLTAGE
5720 132 WRITE(9,33) ESC
5740 * END OF FREQ DO LOOP
5760 77 CONTINUE
5780 89 CONTINUE
5800   GO TO (940,941,941), KKK
5820 941 CONTINUE
5840 * CALL PLOTTING SUBR.
5860   IF(KILLD.EQ.1) GO TO 940
5880   CALL L9GPL
5900   WRITE(9,552)
5920   WRITE(9,551)
5940   WRITE(9,550)
5960 940 CONTINUE
5980   NVT=2
6000   NCK=0
6020   NVICK=1
6040 * END OF VOLT DO LOOP
6060 88 CONTINUE
6080 99 CONTINUE
6100 *
6120 * FORMAT STATEMENTS
6140 517 FORMAT('DV = ',3(1PE8.2,2X))
6160 12 FORMAT('WATTS/CM2',2X,'LIGHT OUT',4X,'V EL',6X,'PCOND')
6180 11 FORMAT(1P4E10.2)
6200 1 FORMAT(4E15.2)
6220 101 FORMAT(//4H R=,1PE10.2,4H S=,E10.2,4H U=,1PE10.2,
6240   + 4H UD=,1PE10.2)
6260 2 FORMAT(E15.6)
6280 102 FORMAT(' C=',1PE10.2)
6300 901 FORMAT(3E15.6)
6320 902 FORMAT(5HAA,1PE9.2,4H DD=,1PE10.2,4H AA=,E10.2)
6340 3 FORMAT('CAP RATIO= ',1PE8.2)
6360 518 FORMAT('AV = ',3(1PE8.2,2X))
6380 4 FORMAT(SF10.1)
6400 104 FORMAT(10H V APPL= ,SF10.1)
6420 5 FORMAT('BEGINNING INPUT RAD. //')
6440 105 FORMAT(10H FREQ= ,SF10.1)
6460 7 FORMAT(10H CAP RATIO= ,F6.1,10H V APPL= ,F6.1,
6480   + 8H FREQ= ,F7.1)
6500 33 FORMAT(3HESC,1PE20.8)
6520 106 FORMAT(3E16.2)
6540 107 FORMAT('TYPE "2" IF PLOT IS DESIRED//'
6560   + 'TYPE "1" IF ONLY DATA IS DESIRED//'
6580   + 'TYPE "3" IF BOTH DATA AND PLOT ARE DESIRED//')
6600 997 FORMAT('TYPE PC SHUNT CAPACITANCE IN PF//')
6620 996 FORMAT(E16.2)
6640 999 FORMAT(1)

```

FIGURE A2  
Page 6 of IR Program

PAGE 7

IR PROGRAM

```
6660 519 F0RMA7C 'VEA = ',3(1PE8.2,2X))  
6680 520 F0RMA7C 'ALF= ',3(1PE8.2,2X))  
6780      STOP  
6800      END
```

FIGURE A2  
Page 7 of IR Program

## PLOT SUBROUTINE

```

20      SUBROUTINE LOGPL
40      INTEGER X, PLOT, BLANK, DOT
60      DIMENSION LINE(61), XX(19,5), YY(19,5), PLOT(5)
80      COMMON XX, YY, LP
100 * CHOOSE PLOTTING SYMBOLS
120      DATA BLANK/1H /, DOT/1H*/, X/1H/
140      DATA PLOT/1H1,1H2,1H3,1H4,1H5/
160 * LABEL THE PLOT
180      WRITE (9,201)
200 201 FORMAT(///20H  LIGHT OUT, FT L  )
220 207 WRITE(9,600)
240 600 FORMAT('10-4',5X, '10-3',6X, '10-2',6X, '10-1',7X,
260      + '1',5X, '10+1',6X, '10+2')
280 * PRINT LEFT BORDER
300 99 CONTINUE
320      DO 101 N=1,61
340      LINE(N)=DOT
360 101 CONTINUE
380 602 DO 605 I=1,7
400      LIN=1+10*(I-1)
420      LINE(LIN)=X
440 605 CONTINUE
460 603 WRITE(9,102) LINE, LP
480 102 FORMAT (61A1, '1.0E', 12)
500 * BLANK THE LINE
520      DO 103 I=1,61
540      LINE(I)=BLANK
560 103 CONTINUE
580 * WE ONLY PLOT 1,2,5,10, ETC ON X-AXIS; 2=2, 5=4, 10=6
600 * COMPUTE YY POINTS
620      DO 105 K=1,19
640      DO 104 L=1,5
660      IF(YY(K,L).LT.1.E-7) YY(K,L)=1.E-7
680      Y(L)=ALOG10(YY(K,L))
700 222 YY(K,L)=Y(L)*10.+41.
720 104 CONTINUE
740 105 CONTINUE
760 * X AXIS STEP LOOP
780      DO 107 I=1,19
800 * MAKE SURE LINE(N) IS BLANK
820      DO 120 NN=1,61
840      LINE(NN)=BLANK
860 120 CONTINUE
880 * LOAD IN PLOTTING SYMBOLS IN CORRECT POSITION
900      ICHECK=0
920      DO 106 J=1,5
940      N=YY(1,J)
960      IF (N>0) 106, 106, 103
980 103 IF (N<0) 109, 109, 106
1000 109 LINE(N)=PLOT(J)
1020      ICHECK=ICHECK+1
1040 106 CONTINUE
1060      LINE(1)=DOT
1080 * SELECT HORIZ. POSITION
1100      GO TO (107,111,112,114,111,112,114,111,112,114,111,112,
1120      + 114,111,112,114,111,112,114), 1

```

FIGURE A3  
PAGE 1 of PLOT PROGRAM

## PLOT SUBROUTINE

```

1140 * PLOT 2
1160 111 IF(ICHECK-0) 400, 400, 411
1180 400 WRITE(9,402) LINE(1)
1200 402 FORMAT(1H./1A1)
1220      GO TO 107
1240 411 IC=61
1260      DO 70 IV=1,61
1280      IF(LINE(IC).NE.BLANK) GO TO 80
1300      IC=IC-1
1320 70 CONTINUE
1340 80 CONTINUE
1360 503 WRITE(9,403) (LINE(NNN), NNN=1,IC)
1380      GO TO 107
1400 403 FORMAT(1H./61A1)
1420 * PLOT 5
1440 112 IF(ICHECK-0) 400, 400, 412
1460 412 IC=61
1480      DO 82 IV=1,61
1500      IF(LINE(IC).NE.BLANK) GO TO 84
1520      IC=IC-1
1540 82 CONTINUE      "
1560 84 CONTINUE
1580      WRITE(9,404) (LINE(NNN),NNN=1,IC)
1600 404 FORMAT(1H./61A1)
1620      GO TO 107
1640 * PLOT 1, 10, ETC.
1660 114 LINE(1)=X
1680      LINE(61)=X
1690      LP=LP+1
1700      IF (I-19) 443, 445, 445
1720 443 CONTINUE
1740      IF(ICHECK-0) 400, 400, 444
1760 * RIGHT BORDER DECADE MARKERS
1780 445 DO 714 IDUM=1,7
1800      LIN=1+10*(IDUM-1)
1820      LINE(LIN)=X
1840 714 CONTINUE
1860 713 WRITE(9,301) LINE,LP
1880 301 FORMAT(1H./61A1,'1.0E',I2)
1890      GO TO 107
1900 444 CONTINUE
1920 511 WRITE (9,405) LINE,LP
1940 405 FORMAT(1H./61A1,'1.0E',I2)
1960 107 CONTINUE
1970      LP=LP-6
1980      RETURN
2000      END

```

FIGURE A3  
PAGE 2 OF PLOT PROGRAM

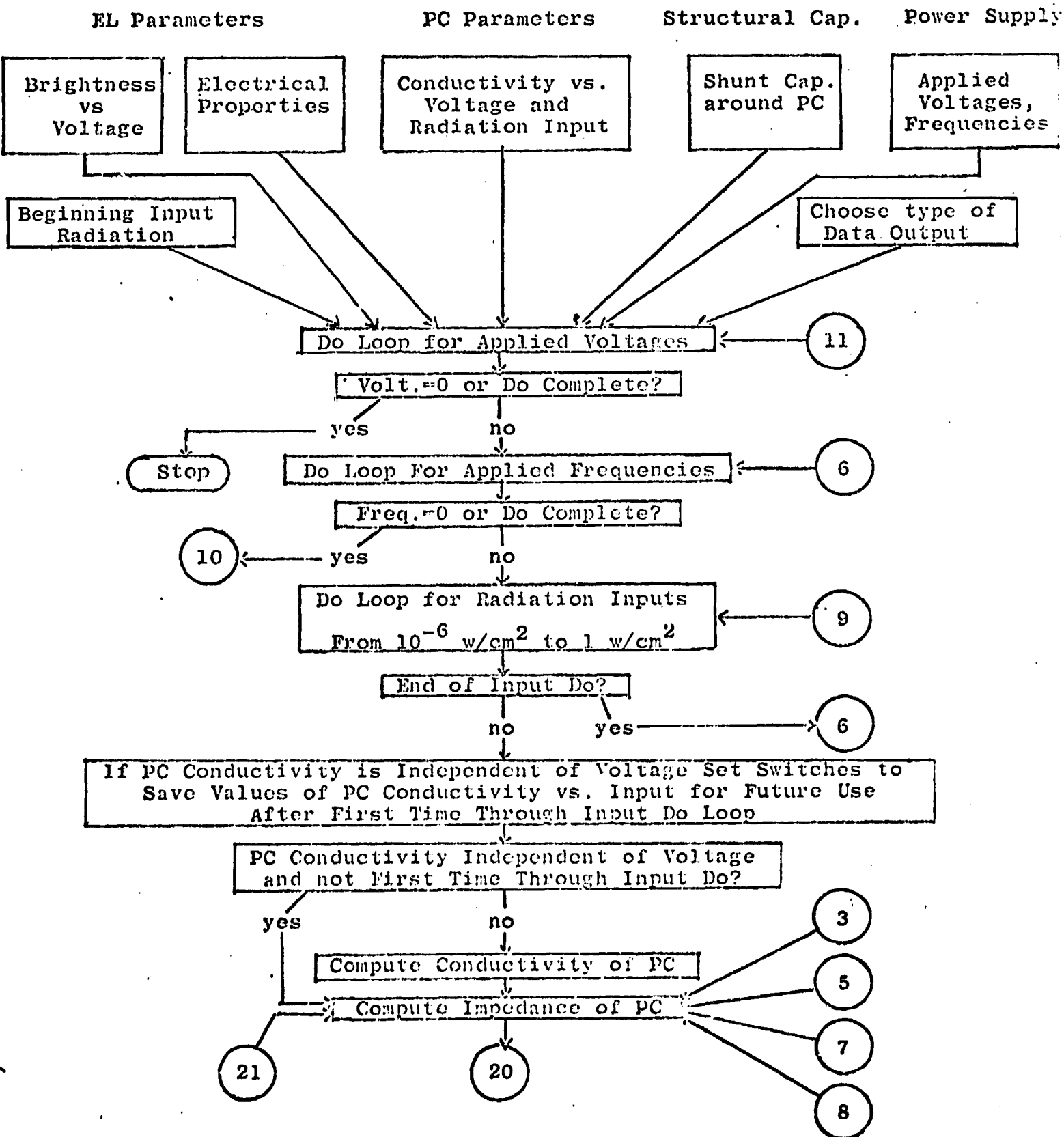
TABLE AI  
Input Parameters for IR Program

<u>File Name</u>	<u>Input Device</u>	<u>Variable</u>	<u>Comments</u>
EL	1	C	Capacitance of EL/cell
		AALF	Frequency dependence of EL leakage conductivity. $G_{EL} \propto$ (Freq.) AALF
		DD	Dimensional constant (H) for EL leakage conductivity (EL conductivity is in mhos)
		AA	Coefficient (b) of voltage dependence of EL leakage conductivity. $G_{EL} \propto$ Exp(AA*(Voltage))
PC	2	(Optional)	30 character line for data identification
		R	Exponent of voltage dependence of PC conductivity. $G_{PC} \propto$ (Volt) <sup>R-1</sup>
		S	Exponent of input energy dependence of PC conductivity. $G_{PC} \propto$ (L) <sup>S</sup>
		U	Dimensional constant for PC conductivity (PC conductivity in mhos)
		UD	Dark current constant ( $U_d$ ) for PC conductivity
KNOBS	3	(Optional)	30 character line for data identification
		V(I)	Array of up to 5 r.m.s. applied voltages [in Volts]
		FR(I)	Array of up to 5 applied frequencies [in Hz]

TABLE AI  
Input Parameters for IR Program (cont.)

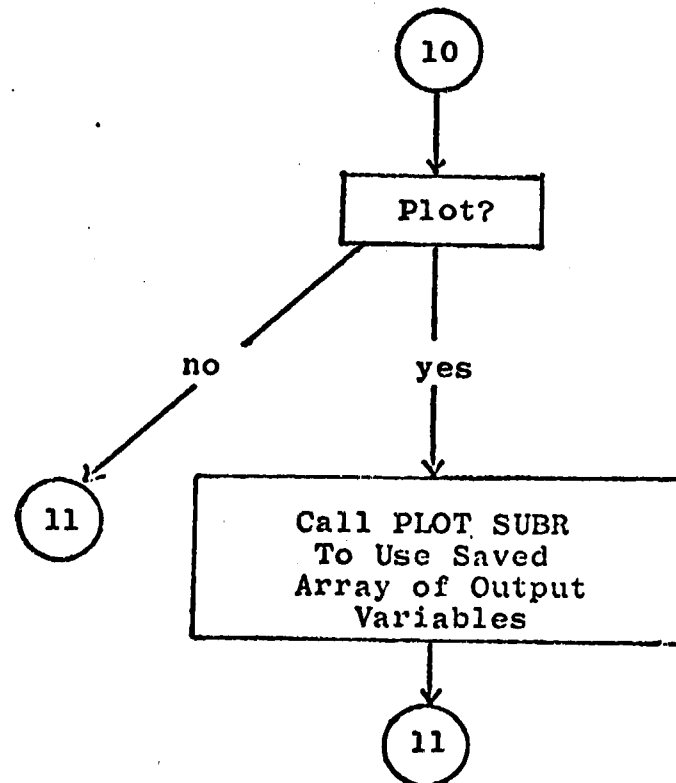
<u>File Name</u>	<u>Input Device</u>	<u>Variable</u>	<u>Comments</u>
BRITE	4	VEA(I)	If brightness of EL vs. voltage fits the equation $B \propto \exp(-\sqrt{\frac{A}{VOLT}})$ only over limited ranges one can fit this equation to the experimental curve over 3 ranges of voltage. VEA(I) are the upper voltage limits of each approximation.
		DV(I)	Array of up to 3 dimensional constants to fit an EL brightness vs. voltage curve (Brightness in Ft-L).
		AV(I)	Array of up to 3 exponential constants to fit the equation, $B \propto \exp(-\sqrt{\frac{AV(I)}{VOLT}})$ to an EL brightness vs. voltage plot over the full range of possible applied voltages.
		ALF(I)	Array of up to 3 exponential constants of EL brightness. $B \propto (\text{Freq.})^{ALF(I)}$ derived from fitting of an EL brightness vs. voltage curve.
		(Optional)	30 character line for data identification.
Keyboard Inputs		CSHUNT	Shunting capacitance around the PC due to structure of device [in pf]. (E16.2)
		TBEGIN	Smallest input radiation value for the simulation. (E16.2)

Inputs:



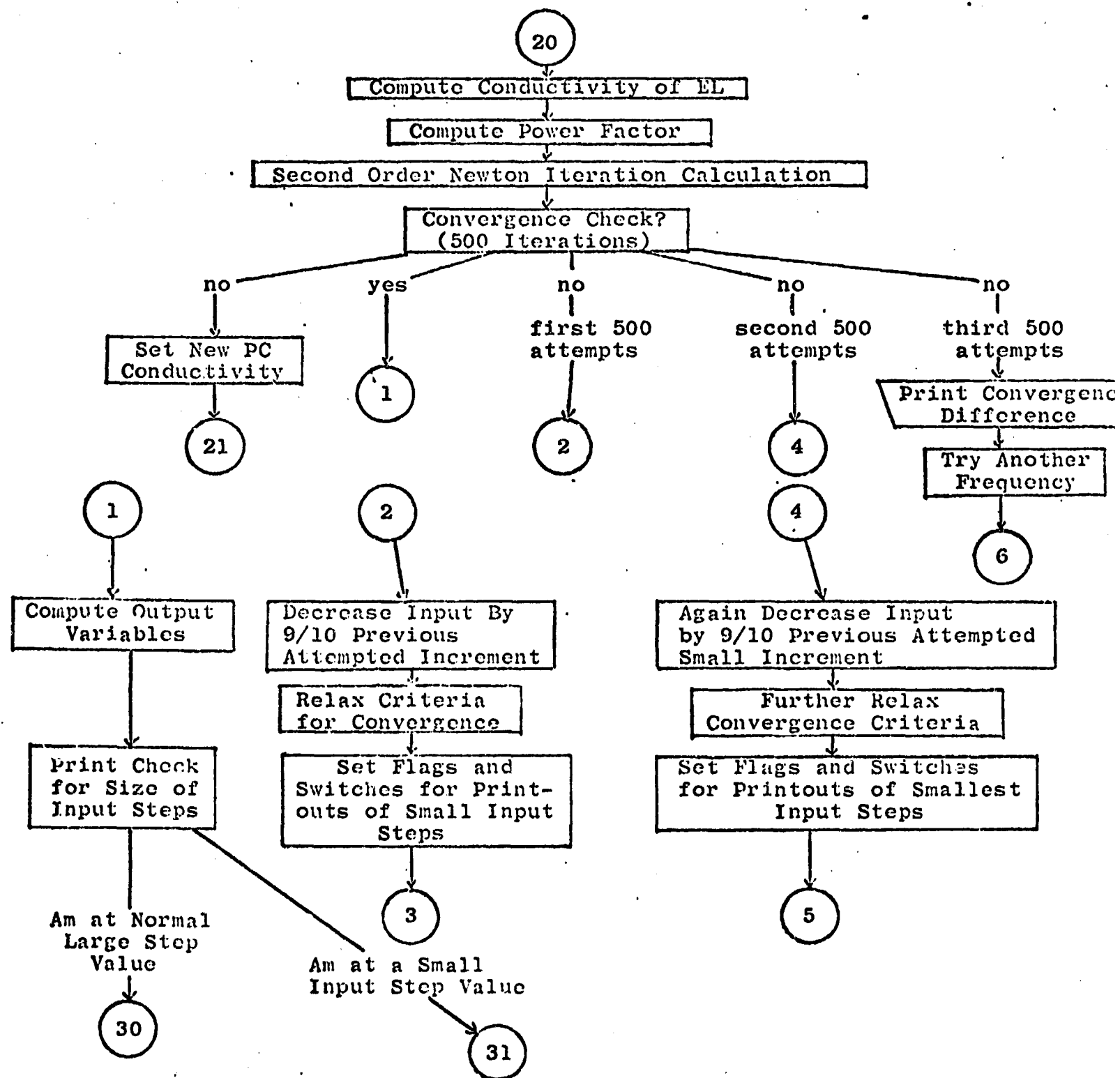
BLOCK DIAGRAM OF IR PROGRAM

FIGURE A4



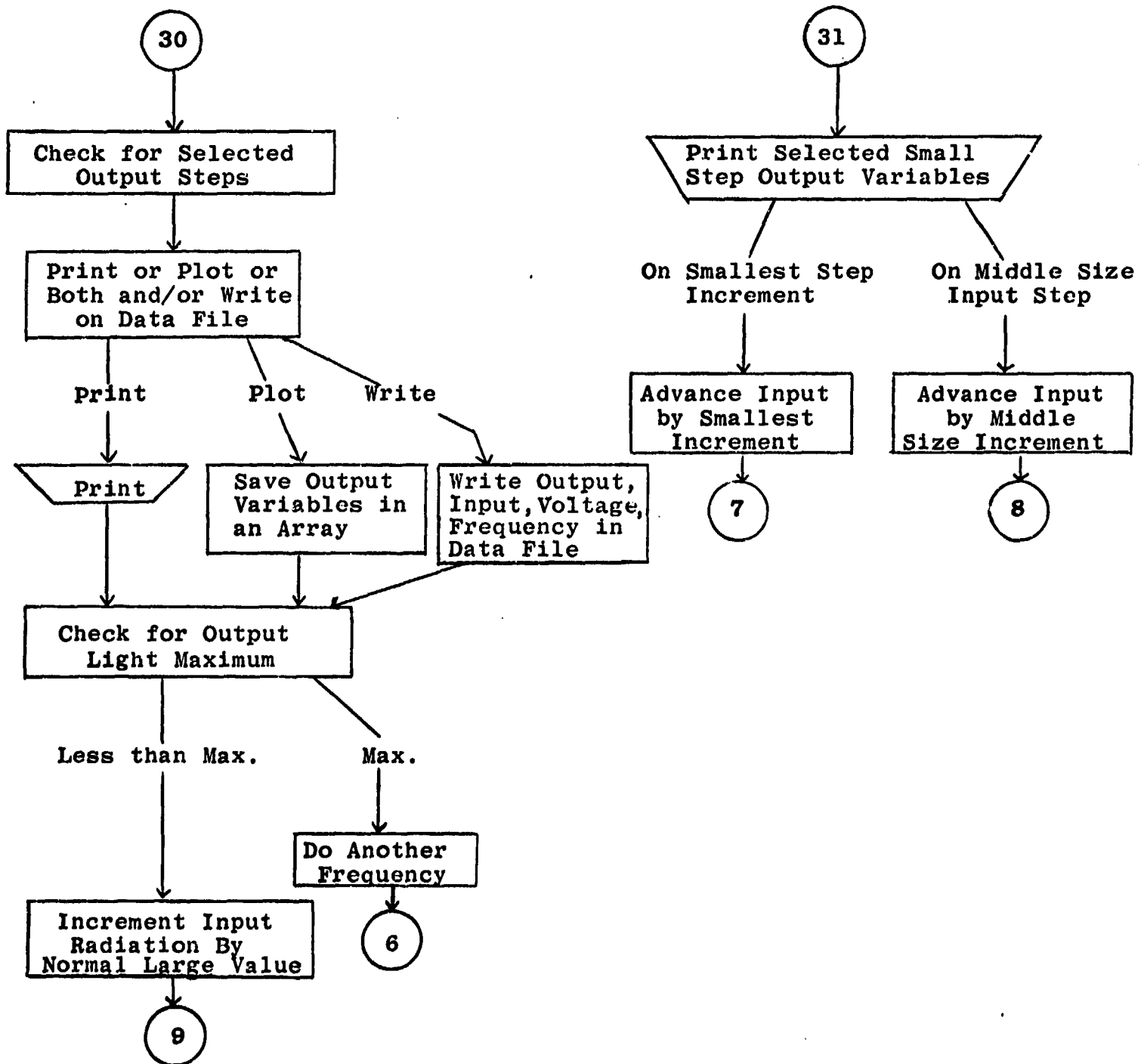
BLOCK DIAGRAM OF IR PROGRAM

FIGURE A4



BLOCK DIAGRAM OF IR PROGRAM

FIGURE A4



BLOCK DIAGRAM OF IR PROGRAM

FIGURE A4

## INPUT DATA FORMAT FOR IR

DATE:

## EQUATIONS:

$$B = DV(I) * FALF(I) \exp -\sqrt{\frac{AV(I)}{VE}}$$

$$Y2G(\text{Leakage}) = DD * FR(k)^{AALF} \exp^{(AA * V(J) - V1)}$$

$$G1(g) = U * (UD + T^S) * (V1^{R-1})$$

## DATA BLOCKS:

<u>NAME</u>	<u>DEVICE</u>	<u>DATA</u>
EL	1: C _____	(E15.6)
	AALF _____ DD _____ AA _____	(E15.6)
	(Optional: 30 character line for labeling)	
PC	2: R _____ S _____ U _____ UD _____	(E15.2)
	(Optional: 30 character line for labeling)	
KNOBS	3: V(I) _____	(F10.1)
	FR(I) _____	(F10.1)
BRITE	4: VEA(I) _____	(E16.2)
	DV(I) _____	(E16.2)
	AV(I) _____	(E16.2)
	ALF(I) _____	(E16.2)
	(Optional: 30 character line for labeling)	

Test Data:

FIGURE A5

APPENDIX B  
IMINT PROGRAM AND RUNGE SUBROUTINE

**B1. Introduction**

The IMINT Program treats essentially the same circuit as the IR Program with one important difference. The difference is that the conductance of the photoconductor is allowed to vary exponentially with time in response to step functions light input. A schematic diagram of the circuit treated is shown in Figure B1.

**B2. Circuit Analysis and Solution Procedure**

To solve this circuit we do not use any linear approximations. Instead, we write the equations for the total current through the combined circuit in a form:

$$I = C_{EL} \frac{d(V_{EL})}{dt} + V_{EL} \frac{1}{R_{EL}} \quad \text{Equation B1}$$

$$I = C_{PC} \frac{d(V_{PC})}{dt} + V_{PC} \frac{1}{R_{PC}} \quad \text{Equation B2}$$

The conductivity of the EL cell is written again as it was for the IR Program and is expressed below:

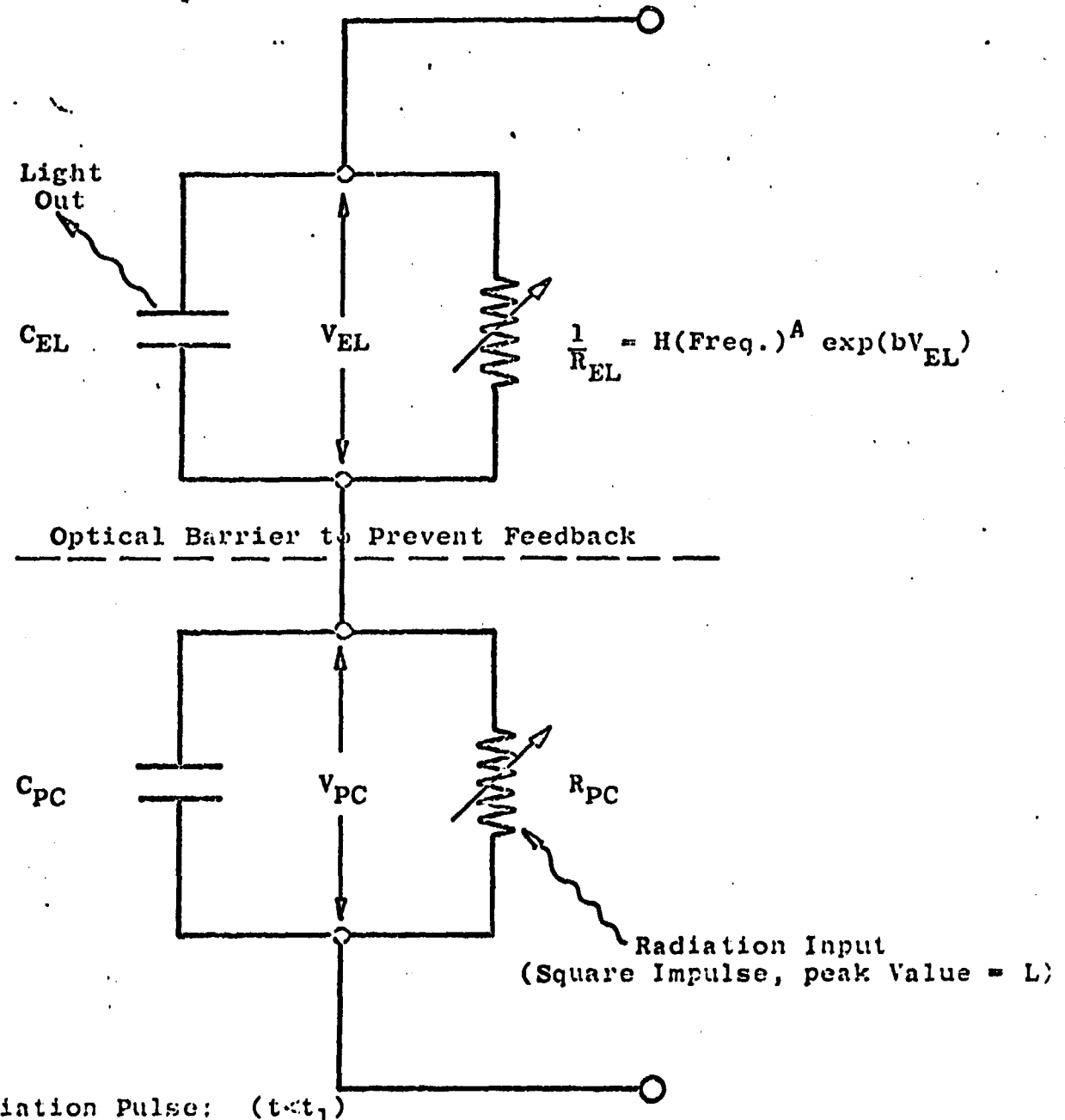
$$\frac{1}{R_{EL}} = H F^A \exp(K(V_{EL})) \quad \text{Equation B3}$$

where H is a dimensional constant, F is the frequency, and A and K are constants. The photoconductor conductivity is again expressed in the same form as before, but modified with an exponential time term.

In the equation below, the upper exponential term is for the duration of the light pulse. The lower time term is for the decay time of the photoconductor after the input radiation pulse has ceased.

$$\frac{1}{R_{PC}} = U(U_d + L^s) V_{PC}^{r-1} \left\{ \begin{array}{ll} \frac{1 - \exp(-\lambda_1(t-t_1))}{\exp(-\lambda_2(t-t_2))}, & \text{if } t_1 < t < t_2 \\ \exp(-\lambda_2(t-t_2)), & \text{if } t_2 < t \end{array} \right\}$$

Equation B4



$$\frac{1}{R_{PC}} = (U)(U_d)(V_{PC})$$

During Radiation Pulse:  $(t_1 < t < t_2)$

$$\frac{1}{R_{PC}} = U(U_d + L^s)(V_{PC})^{r-1} [1 - \exp(-\lambda_1(t - t_1))]$$

After Radiation Pulse:  $(t_2 < t)$

$$\frac{1}{R_{PC}} = U(U_d + L^s)(V_{PC})^{r-1} [\exp(-\lambda_2(t - t_2))]$$

Circuit Used in Simulation of EL/PC Image Converter Response to Transient Stimulation

FIGURE B1

In this equation,  $U$  is dimensional constant,  $U_d$  is a dark conductivity term,  $L$  is peak input radiation,  $s$  and  $r$  are constants,  $\lambda_1$  is a rise time constant,  $\lambda_2$  is a decay time constant,  $t_1$  is the beginning of the light pulse, and  $t_2$  is the end of the light pulse. The applied voltage is assumed to be of the form:

$$V_{app} = V_m \sin(\omega t - \delta_0) \quad \text{Equation B5}$$

Where  $\delta_0$  is chosen so that the beginning voltage on the EL for the simulation is zero. This gives us for the voltage on the photoconductor the following term:

$$V_{PC} = [V_m \sin(\omega t - \delta_0)] - V_{EL} \quad \text{Equation B6}$$

Putting Equation B6 into the combined Equation B1 and B2, we have Equation B7.

$$(C_{EL} + C_{PC}) \frac{d}{dt} V_{EL} = -V_{EL} [HF^A \exp(K(V_{EL}))] + C_{PC} [V_m \omega \cos(\omega t - \delta_0)] + [U(U_d + L^s)] [V_m \sin(\omega t - \delta_0) - V_{EL}]^r \left\{ \frac{1 - \exp(-\lambda_1(t - t_1))}{\exp(-\lambda_2(t - t_2))} \right\}$$

Equation B7

This equation is of the functional form:

$$\frac{dy}{dt} = f(y, t) \quad \text{Equation B8}$$

This equation is a first order equation which is easily integrable by several numerical techniques. We have used one of the simplest techniques which is the Runge-Kutta method. The present IMINT Program is not ideally suited for the simulation of thin film EL light output because it has no provision yet for the inclusion of multiple curve fits to the TFEL brightness versus voltage curve.

### B3. Description of IMINT Program and Runge Subroutine

IMINT is written in FORTRAN IV and is used on a time sharing computer system through a standard teletype terminal. Figure B2 contains a listing of IMINT. The time sharing system it has been

used on has excellent file editing capabilities if the file contains line numbers. The first field of numbers on a line are the line numbers. The second field of numbers is the FORTRAN statement number field. The "\*" are for comment lines. The program is liberally laced with comments as to the function of flags and switches and the purpose of a group of statements. A complete listing of the input parameters for the program along with the device number called for in the program are shown in Table B1. Table BII contains the input parameters which are entered at the keyboard at program execution time along with comments as to the nature of the parameters. The IMINT Program integrates Equation B4 in the section above by means of a subroutine called RUNGE. The program is basically a simple integration program except for two parts. The first of these parts is the determination of the phase difference between the applied voltage and the voltage on the EL. This phase difference ( $\delta_0$ ) is determined such that the voltage on the EL at the beginning of the simulated voltage cycle is passing through zero in the positive direction. The program finds this phase angle from an initial guess by the designer by means of an iteration technique and computing the rate of change of the convergence difference between two cycles run with different phase angles and computing a new phase angle based on this rate of change of convergence with respect to phase angle. Once the program has determined a  $\delta_0$  so that the voltage on the EL returns to zero in one period of the applied frequency, the program then integrates from the end of this one cycle (with no input radiation during this cycle) forward in time for as many cycles as the designer chooses.

The second part of the program differs from a simple integration routine because of the time varying nature of the radiation input. This time varying nature is handled by introducing the exponential rise of decay functions as shown in Equation B4 of the section above at the appropriate time in the integration.

Figure B3 is a block diagram of the IMINT Program. This is not a flow chart. It is meant to be used as a guide for finding one's way through the program in addition to providing a brief overview of the operation of the program. Table BIII and Table BIV are data sheets that have been useful to the computer operator when using the program and contain the format specifications used in the files.

The subroutine RUNGE is a simple form of the Runge-Kutta technique for integrating first order differential equations. The flags, switches, and variables in the subroutine are described in the comment statements at the beginning of the subroutine listing. A listing of RUNGE is contained in Figure B4.

As yet, we do not have a useful plotting subroutine to plot the output of the IMINT Program. At present, the output is the time, voltage on the EL, EL current, and derivative of the voltage on the EL. The data must then be plotted by hand. From the plot, one can find peak AC voltages applied to the EL as a function of time and use this in a simple calculation with EL brightness formulas that are appropriate for thick film or thin film EL to get the brightness output.

PAGE 1

IMINT PROGRAM

```
10      * IMAGE INTENSIFIER PROGRAM
20      * OFFICE OF NAVAL RESEARCH PROGRAM
30      *
40      *
50      DIMENSION Y(10),DY(10)
60      CALL DEFINE(1,6HIIIDAT )
70      READ(1,10) CEL,CPC,FREQ,A,H,AK
80      READ(1,10) VM,U,UD,S,PASMX,VEL
90      READ(1,26) T,GLAM1,GLAM2
100     READ(1,11) N
110     WRITE(9,12)
120     12 FORMAT('EL,ELP,PHSE,DPHSE')
130     READ(9,25) EL,ELP,PHSE,DPHSE
140     WRITE(9,13)
150     13 FORMAT('TF,DPRT,DT,VDED')
160     READ(9,25) TF,DPRT,DT,VDED
170     WRITE(9,14)
180     14 FORMAT('R,T1,T2')
190     READ(9,26) R,T1,T2
200     WRITE(9,16)
210     16 FORMAT('CYCMX')
220     READ(9,15) CYCMX
230     WRITE(9,17)
240     17 FORMAT('CONVCR')
250     READ(9,15) CONVCR
260     *
270     10 FORMAT(6E12.5)
280     11 FORMAT(14)
290     15 FORMAT(E12.5)
300     25 FORMAT(4E12.5)
310     26 FORMAT(3E12.5)
320     *
330     * INITIALIZATION OF FLAGS AND SWITCHES
340     *
350     * "MG" IS INPUT STATE INDICATOR. MG=1 IS BEFORE PULSE
360     * MG=2 IS DURING PULSE, MG=3 IS AFTER PULSE
370     MG=1
380     * "CYC" IS VOLTAGE CYCLE COUNTER
390     CYC=1.
400     L=1
410     IG=1
420     PI=3.14159
430     * "APPSW" IS 0 FOR FIRST INTEGRATION OF FIRST CYCLE
440     APPSW=0.
450     * "TPRT" IS TIME TO PRINT OUTPUT VARIABLES
460     TPRT=T
470     * "DTF" IS PERIOD OF DRIVING FREQ.
480     DTF=TF-T
490     M=1
500     * "NCON=1" IS SWITCH TO CONVERGENCE CHECK
510     * "NCON=2" IS SWITCH AROUND CONVERGENCE CHECK AFTER
520     * INTEGRATING SECOND TIME WITH PHSE=PHSE+DTFSE
530     * "NCON=3" IS SWITCH COMPLETELY AROUND CONVERGENCE
540     * CHECKS AND PHASE ANGLE CORRECTIONS
550     NCON=1
560     * "ISAVE" IS FLAG TO SAVE 'VEL', 'T', 'TPRT'
```

Figure B2  
Page 1 of IMINT Program

## IMINT PROGRAM

```

570      ISAVE=1
580      *
590      WRITE(9,31)
600      31 FORMAT(1X,'CEL',9X,'CFC',9X,'FREQ',8X,'VM')
610      WRITE(9,30) CEL,CFC,FREQ,VM
620      WRITE(9,32)
630      32 FORMAT(1X,'H',11X,'A',11X,'AK',10X,'VEL')
640      WRITE(9,30) H,A,AK,VEL
650      WRITE(9,33)
660      33 FORMAT(1X,'U',11X,'UD',10X,'S',11X,'R')
670      WRITE(9,30) U,UD,S,R
680      WRITE(9,34)
690      34 FORMAT(1X,'PHSE',8X,'DPHSE',7X,'TF',10X,'DT')
700      WRITE(9,30) PHSE,DPHSE,TF,DT
710      WRITE(9,35)
720      35 FORMAT(1X,'GLAM1',7X,'GLAM2',7X,'EL',10X,'ELP')
730      WRITE(9,30) GLAM1,GLAM2,EL,ELP
740      WRITE(9,36)
750      36 FORMAT(1X,'T1',10X,'T2')
760      WRITE(9,30) T1,T2
770      *
780      30 FORMAT(1P4E12.5)
790      OMEGA=2*PI*FREQ
800      DPHSE=DPHSE*PI/180.
810      PHSE=PHSE*PI/180.
820      U=OMEGA*OMEGA*VM
830      VEL7=(OMEGA/(2.*PI))*A
840      *
850      40 GO TO (45,46),ISAVE
860      45 A1=T
870      A2=VEL
880      A3=TPRT
890      ISAVE=2
900      GO TO 48
910      46 T=A1
920      VEL=A2
930      TPRT=A3
940      *
950      48 PPH=PHSE*180./PI
960      WRITE(9,840) PPH
970      840 FORMAT(/'PHASE ANGLE = ',F10.3)
980      WRITE(9,49)
990      49 FORMAT(/'X, 'TIME',6X,'VEL',6X,'CURR',6X,'VELD')
1000      * INTEGRATION REENTRY
1010      50 VEL1=VEL5*COS(OMEGA*T+PHSE)
1020      VEL4=VM* SIN(OMEGA*T+PHSE)-VEL
1030      GO TO (54,55,56),MG
1040      55 VEL6=(1.-EXP(-(T-T1)/GLAM1))*VEL3
1050      GO TO 58
1060      56 VEL6=(EXP(-(T-T2)/GLAM2))*VEL8
1070      GO TO 58
1080      54 VEL6=U*(UD+EL)*S
1090      58 CONTINUE
1100      VEL2=VEL1-VEL6*ADS(VEL4)*R
1110      VEL3=-VEL*VEL7*EXP(AK*VEL)
1120      *

```

Figure B2  
Page 2 of IMINT Program

## IMINT PROGRAM

```

1130 * BASIC DIFFERENTIAL EQUATION
1140 . VELD=(VEL1+VEL2+VEL3)/(CEL+CPC)
1150 *
1160 GO TO (60,100),M
1170 60 IF(T.LT.(TPRT-1.E-7)) GO TO 80
1180 *
1190 . CURR=(CEL*VELD)+(VEL)*(FREQ**A)*H*EXP(AK*VEL)
1200 WRITE(9,70) T,VEL,CURR,VELD
1210 *
1220 70 FORMAT(1P2E12.5,E9.2,E12.5)
1230 TPRT=TPRT+DPRT
1240 *
1250 80 CONTINUE
1260 GO TO (81,82,83),MG
1270 81 IF(T.LT.(T1-1.E-7)) GO TO 83
1280 EL=ELP
1290 MG=2
1300 VEL8=U*(UD+EL**S)
1310 GO TO 50
1320 82 IF(T.LT.(T2-1.E-7)) GO TO 83
1330 MG=3
1340 EL=0.
1350 VEL8=U*(UD+EL**S)
1360 GO TO 50
1370 83 CONTINUE
1380 *
1390 IF(T.GE.(TF-1.E-7)) GO TO 200
1400 M=2
1410 100 CONTINUE
1420 DY(1)=VELD
1430 Y(1)=VEL
1440 *
1450 CALL RUNGE(L,IG,Y,DY,DT,M,T,N)
1460 *
1470 VEL=Y(1)
1480 GO TO 50
1490 200 CONTINUE
1500 GO TO (210,240,300),NCON
1510 * TEST FOR CONVERGENCE
1520 210 VDE=VEL
1530 VDEAI=-VDE
1540 IF(ABS(ABS(VDEAI)-ABS(VDED))-CONVCR) 300,300,230
1550 *
1560 * DERIVE NEW PHASE ANGLE FOR SECOND CONVERGENCE ATTEMPT
1570 230 IF(APPSW.EQ.1.) GO TO 250
1580 APPSW=1.
1590 PASS=1.
1600 PSAVE=PHSE
1610 PHSE=PHSE+DPHSE
1620 NCUM=2
1630 GO TO 40
1640 240 DELVDE=VEL-VDE
1650 PVDE=DELVDE/DPHSE
1660 GO TO 270
1670 *
1680 * DERIVE NEW PHASE ANGLE BASED ON PREVIOUS TRIES

```

Figure B2  
Page 3 of IMINT Program

## IMINT PROGRAM

```
1690 250 IF(PASS.EQ.PASMX) GO TO 400
1700      PASS=PASS+1.
1710 270 CURN=VDEAI/PVDE
1720      PHSE=PSAVE+CURN
1730      PSAVE=PHSE
1740      NCUN=1
1750      GO TO 40
1760      *
1770 300 CONTINUE
1780      IF(CYC.EQ.CYCNX) GO TO 400
1790      IF(CYC.EQ.1.) NCUN=3
1800      CYC=CYC+1
1810      TF=TF+DTF
1820      ISAVE=1
1830      TPRT=T
1840      APPSW=0.
1850      GO TO 40
1860      *
1870 400 STOP
1880      END
```

Figure B2  
Page 4 of IMINT Program

TABLE BI

Input Parameters for IMINT Program from Data File

File Name: IIDAT      Device Number: 1

Parameter Name	Comments
CEL	Capacitance/Cell of EL [in farads].
CPC	Shunt Capacitance around PC cell [in farads].
FREQ	Applied power supply frequency to the device [in Hz].
A	Exponent of frequency dependence of EL leakage conductivity according to: $G_{EL} \propto (Freq.)^A$ .
H	Dimensional constant of leakage conductivity of EL [EL leakage in mhos].
AK	Exponential coefficient of voltage dependence of leakage conductivity of EL according to: $G_{EL} \propto \text{Exp}(AK * \text{Volt.})$ , Note: Volt. is absolute value of peak applied voltage.
VM	Maximum peak applied voltage to the device.
U	Dimensional constant of PC conductivity [PC conductivity in mhos].
UD	Dark conductivity term ( $U_d$ ) of PC conductivity.
S	Exponent of steady state dependence of PC conductivity upon input radiation.
PASMX	Upper limit on number of searches for convergence of first voltage cycle.
VEL	Voltage across EL cell at time = T.
T	Time at which simulation begins [in seconds].
GLAM1	PC conductivity rise time constant used in form: $G_{pC} \propto 1 - \text{Exp}(-\frac{T-T1}{GLAM1})$ . (Times in seconds)

TABLE BI

Input Parameters for IMINT Program from Data File (Cont.)

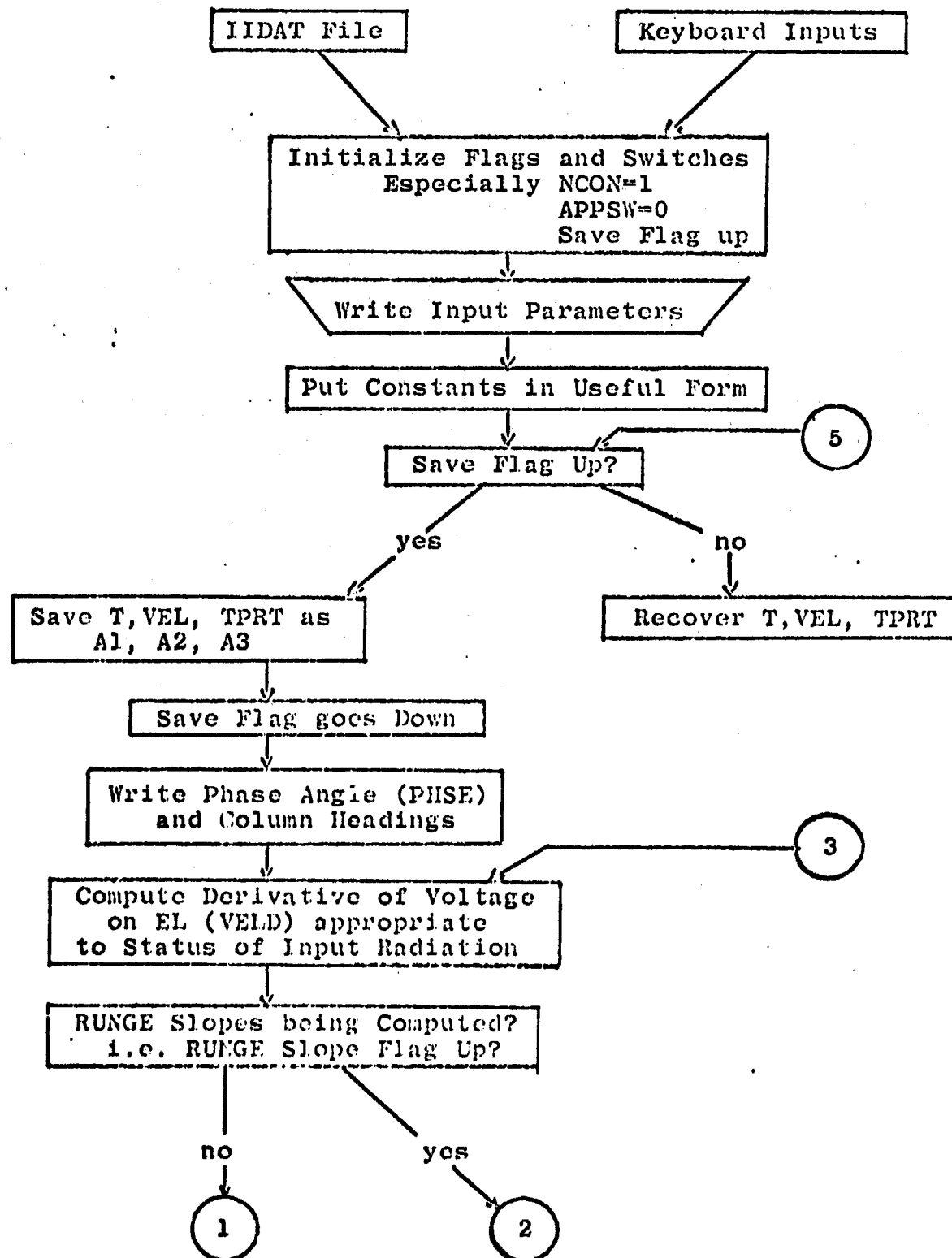
File Name: IIDAT Device Number: 1

Parameter Name	Comments
GLAM2	PC conductivity decay time constant used in form: $G_{PC} \propto \text{Exp}(-\frac{T-T_2}{GLAM2})$ . [Times in seconds]
N	Number of simultaneous first order differential equations to be integrated by RUNGE subroutine. In IMINT, N = 1.

TABLE BII

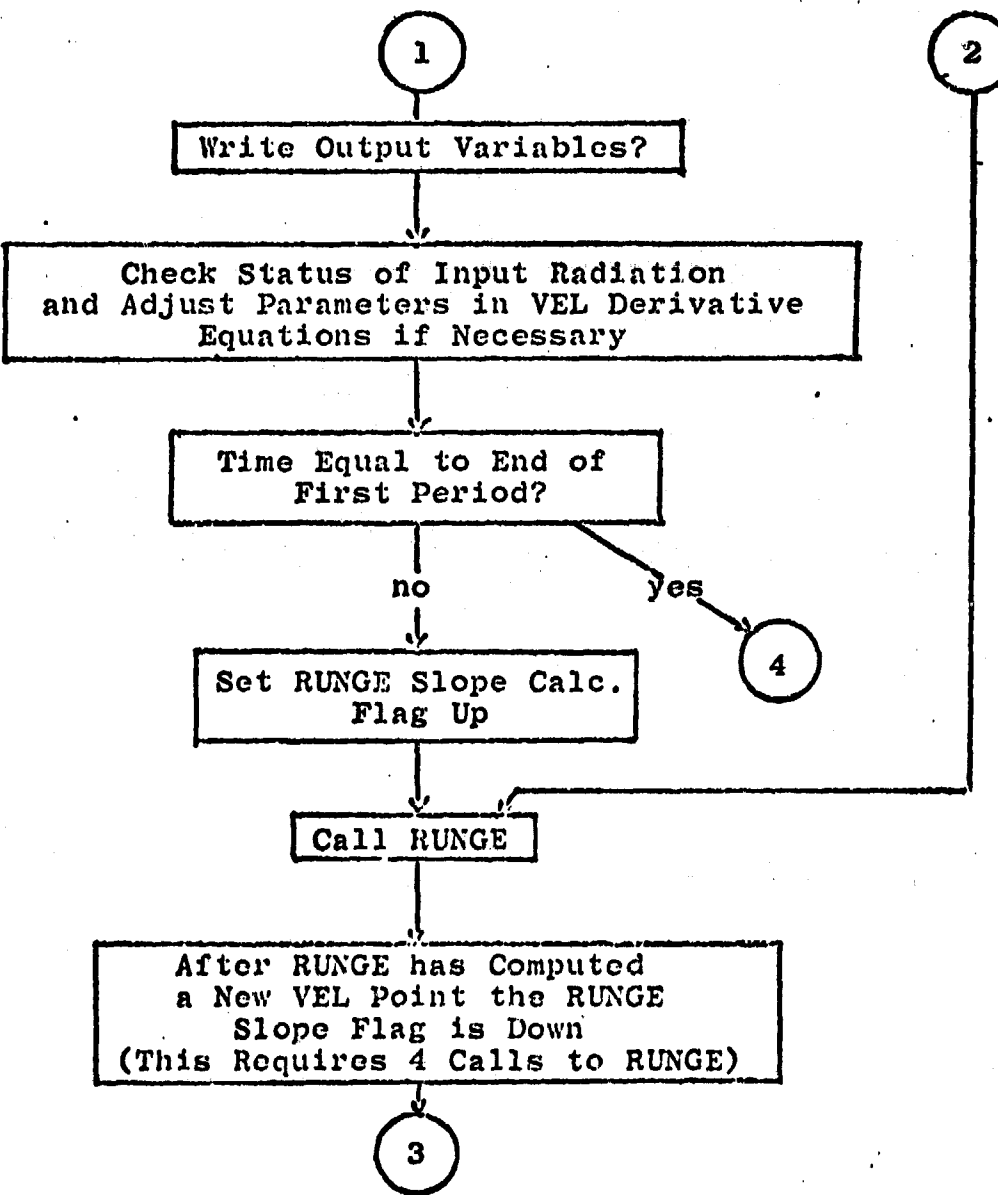
Input Parameters for IMINT Program Entered at  
Program Execution Time

<u>Parameter Name</u>	<u>Comments</u>
EL	Input radiation before input pulse [in units consistent with PC conductivity equation].
ELP	Peak value of square pulse input radiation [same units as EL above].
PHSE	Initial guess at voltage phase angle for first steady-state cycle [in degrees].
DPHSE	Increment for adjusting PHSE after integration of first steady-state cycle [in degrees].
TF	Time at which voltage on EL repeats its value at T. (TF-T) is period of the driving frequency [in seconds].
DPRT	Time increment between printouts [in seconds].
DT	Time increment used per integration step [in seconds].
VDED	Desired value of voltage on EL after integration of first steady-state voltage cycle (usually equal to VEL).
R	Exponent of input radiation dependence of PC conductivity: $G_{pC} \propto (L)^R$ (Note R = r-1 in equations).
T1	Start time of input radiation pulse [in seconds].
T2	Stop time of input radiation pulse [in seconds].
CCMX	Maximum number of EL voltage cycles computed.
CONVCR	Difference allowed between EL voltage computed at end of first voltage cycle and the desired voltage value (VDED) [in volts].



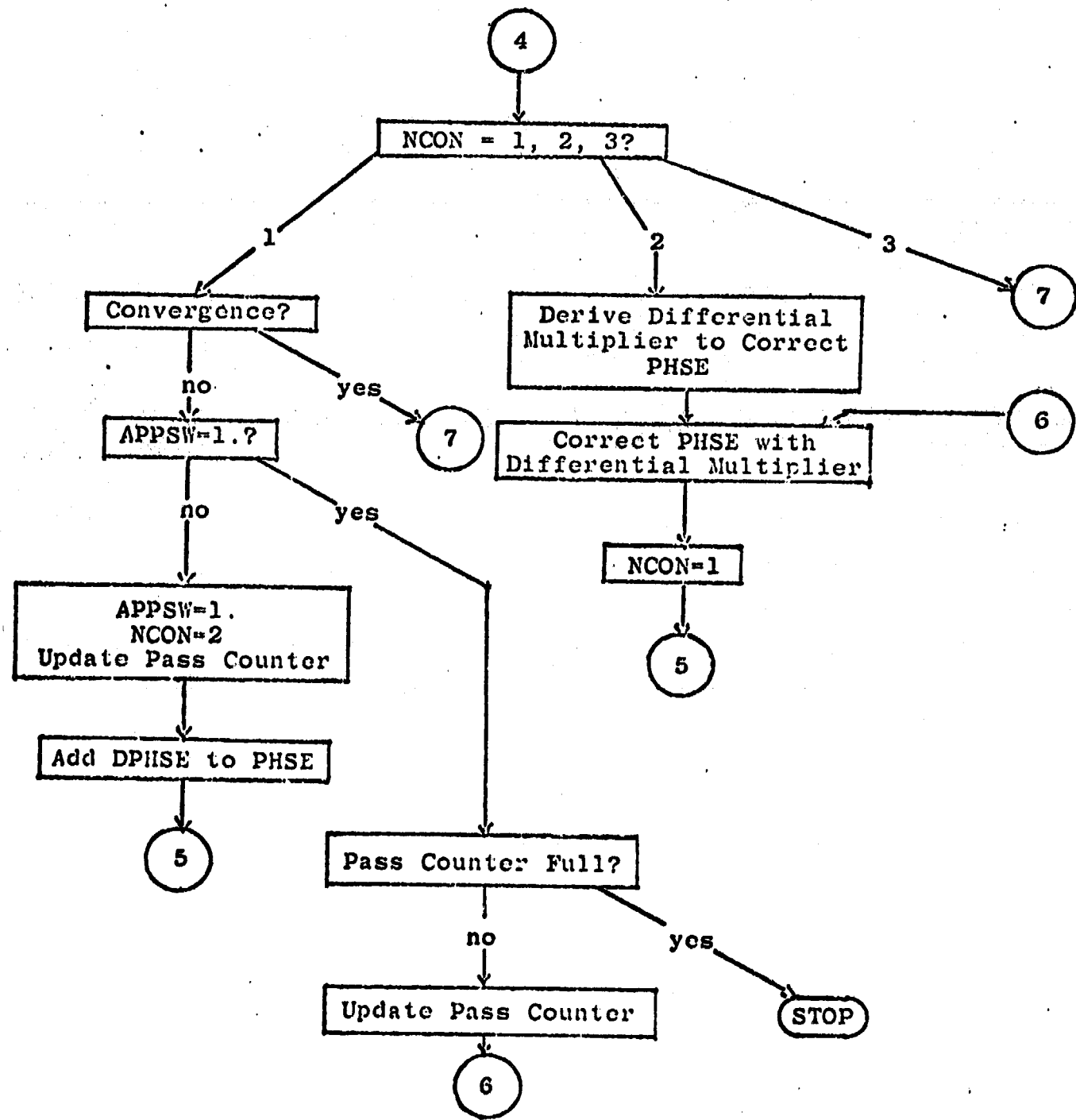
BLOCK DIAGRAM OF IMINT PROGRAM

FIGURE B3



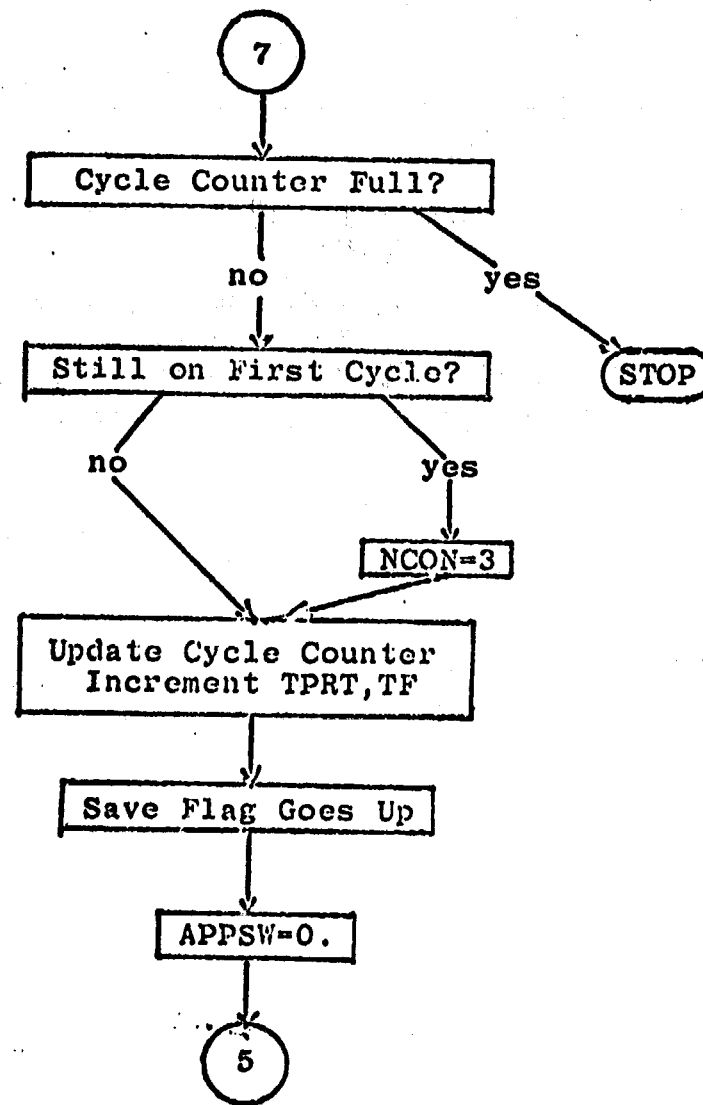
BLOCK DIAGRAM OF IMINT PROGRAM

FIGURE B3



BLOCK DIAGRAM OF IMINT PROGRAM

FIGURE B3



BLOCK DIAGRAM OF IMINT PROGRAM

FIGURE B3

## IIDAT DATA FILE INPUTS FORMAT FOR IMINT

DATE:

CEL	CPL	FREQ	EL Leakage Constants		
			A	H	AK
_____	_____	_____	_____	_____	_____

(6E12.5)

VM	PC Constants			PASMX	VEL
	U	UD	S		
_____	_____	_____	_____	_____	_____

(6E12.5)

T	GLAM1	GLAM2
_____	_____	_____

(3E12.5)

N

\_\_\_\_\_ (14)

COMMENTS:

TEST DATA:

TTY Inputs for IMINT

DATE:

EL

ELP

PHSE

DPHSE

(4E12.5)

TF

DPRT

DT

VDED

(4E12.5)

R

T1

T2

(3E12.5)

CCMX

(E12.5)

CONVCR

(E12.5)

COMMENTS:

TEST DATA:

## RUNGE SUBROUTINE

```

10      SUBROUTINE RUNGECL, IG, Y, DY, DT, M, T, N
20      * N=NUMBER OF DIFFERENTIAL EQUATIONS (MAX. OF 10)
30      * IG=1 INDICATES IF CALL IS FOR FIRST RUNGE SLOPE
40      * CALC. IN THE SUBROUTINE
50      * T=INDEPENDENT VARIABLE
60      * DT=INTEGRATION INCREMENT OF IND. VARIABLE
70      * Y=DEPENDENT VARIABLE
80      * DY=DERIVATIVE OF Y
90      * L=2 IS SWITCH AROUND "IG" CHECK AT STATEMENT 100 (ON
100     * FIRST CALL TO RUNGE SLOPES)
110     * M=2 INDICATES TO MAIN PROGRAM THAT RUNGE SLOPES ARE
120     * BEING COMPUTED
130     DIMENSION DY(10), Y(10), F(80)
140     90 GO TO (100, 110), L
150     100 GO TO (101, 110), IG
160     101 J=1
170     L=2
180     DO 106 K=1,N
190     K3=N+K
200     106 F(K3)=Y(K)
210     GO TO 90
220     110 DO 140 K=1,N
230     K1=K
240     K2=K+5*N
250     K3=K2+N
260     K4=K+N
270     GO TO (111, 112, 113, 114), J
280     111 F(K1)=DY(K)*DT
290     Y(K)=F(K4)+.5*F(K1)
300     GO TO 140
310     112 F(K2)=DY(K)*DT
320     GO TO 124
330     113 F(K3)=DY(K)*DT
340     GO TO 134
350     114 Y(K)=F(K4)+(F(K1)+2.*(F(K2)+F(K3))+DY(K)*DT)/6.
360     GO TO 140
370     124 Y(K)=.5*F(K2)
380     Y(K)=Y(K)+F(K4)
390     GO TO 140
400     134 Y(K)=F(K4)+F(K3)
410     140 CONTINUE
420     GO TO (170, 180, 170, 180), J
430     170 T=T+.5*DT
440     180 J=J+1
450     IF (J-4) 404, 404, 299
460     299 IG=1
470     M=1
480     GO TO 406
490     404 IG=2
500     405 L=1
510     406 RETURN
520     END

```

Figure B4  
RUNGE Subroutine

## APPENDIX C

### UTILITY PROGRAMS

#### C1. Introduction

Several smaller programs were developed to aid in the analysis of proposed devices. The first group of programs are used as aids in extracting useful parameters of the light-emitting materials and the photoconductive materials. This group includes the GFIT, ELFIT, ELDG, and PLDATA programs and the SLPILOT subroutine.

The GFIT program fits a non-voltage dependent equation to resistance vs. input radiation measurements of photoconductor cells. The ELFIT program fits the electroluminescent brightness vs. frequency and voltage measurements to an equation over three consecutive ranges of applied voltage. The ELDG program creates pairs of brightness vs. voltage data from an equation. The data is put in a file for plotting with the PLDATA program. The PLDATA program takes data from a file, modifies it for use in the SLPILOT subroutine, and calls the subroutine. The SLPILOT subroutine generates a four-cycle semi-logarithmic plot of a maximum of five curves of fifty points each.

The second group of utility programs simulate unusual ways of driving image conversion panels and the stacking or cascading of image conversion panels. The AM and FM programs use data files generated by the IR program to simulate the time averaged light output from image conversion panels driven by very simple amplitude or frequency modulated voltage waveforms. The MASSA program condenses the data files generated by the IR program for use in the AM or FM programs. The CASCAD program uses data files of input

PAGE 1

RUNGE SUBROUTINE

```
10      SUBROUTINE RUNGE(L, IG, Y, DY, DT, M, T, N)
20      * N=NUMBER OF DIFFERENTIAL EQUATIONS (MAX. OF 10)
30      * IG=1 INDICATES IF CALL IS FOR FIRST RUNGE SLOPE
40      * CALC. IN THE SUBROUTINE
50      * T=INDEPENDENT VARIABLE
60      * DT=INTEGRATION INCREMENT OF IND. VARIABLE
70      * Y=DEPENDENT VARIABLE
80      * DY=DERIVATIVE OF Y
90      * L=2 IS SWITCH AROUND "IG" CHECK AT STATEMENT 100 (ON
100     * FIRST CALL TO RUNGE SLOPES)
110     * M=2 INDICATES TO MAIN PROGRAM THAT RUNGE SLOPES ARE
120     * BEING COMPUTED
130     DIMENSION DY(10), Y(10), F(60)
140     90 G0 T0 (100,110),L
150     100 G0 T0(101,110),IG
160     101 J=1
170     L=2
180     D0 106 K=1,N
190     K3=N+K
200     106 F(K3)=Y(K)
210     G0 T0 90
220     110 D0 140 K=1,N
230     K1=K
240     K2=K+5*N
250     K3=K2+N
260     K4=K+N
270     G0 T0(111,112,113,114),J
280     111 F(K1)=DY(K)*DT
290     Y(K)=F(K4)+.5*F(K1)
300     G0 T0 140
310     112 F(K2)=DY(K)*DT
320     G0 T0 124
330     113 F(K3)=DY(K)*DT
340     G0 T0 134
350     114 Y(K)=F(K4)+(F(K1)+2.*(F(K2)+F(K3))+DY(K)*DT)/6.
360     G0 T0 140
370     124 Y(K)=.5*F(K2)
380     Y(K)=Y(K)+F(K4)
390     G0 T0 140
400     134 Y(K)=F(K4)+F(K3)
410     140 CONTINUE
420     G0 T0(170,180,170,180),J
430     170 T=T+.5*DT
440     180 J=J+1
450     IF(J-4)404,404,299
460     299 IG=1
470     M=1
480     G0 T0 406
490     404 IG=2
500     405 L=1
510     406 RETURN
520     END
```

Figure B4  
RUNGE Subroutine

vs. output of simulated image conversion panels to compute the light output of a cascaded pair of panels. The MASSA2 program is used after the MASSA program to condense IR2 data output for use in CASCAD. In addition, the AM or FM programs can be used to effectively sort IR output data before use in CASCAD.

#### C2. GFIT Program

This program fits an equation of the form:

$$g \approx \text{conductivity} = u(u_d + T^S)$$

where  $u$  and  $u_d$  are constants,  $T$  is input radiation, and  $S$  is a constant, to resistance vs. input radiation data obtained by measuring individual PC cells under stimulation. The fit is obtained by assuming that for  $T \geq 10^{-3}$ ,  $g \approx u \cdot u_d T^S$ . The natural logarithm of both sides is taken and the resulting equation is fitted by means of the least-squares method to the test data. This determines  $S$  and  $U$ . After this fit, the simple average of the dark current data is used for the product  $u \cdot u_d$  and  $u_d$  is computed.

The program uses data from a stored data file containing the input radiation and resulting cell resistances. The file is called for at program execution time. A zero input radiation value signifies the end of the data file and reads in the average (computed manually) dark resistance of the cells.

Table C1 summarizes the necessary data inputs and formats for the program. Figure C1 is a listing of the GFIT program.

PAGE 1

GFIT PRJGRM

```
20 * CONDUCTIVITY EQUATION FIT
40 * G=U*(UD+I)**S
60 DIMENSION T(75),G(75),TL(75),GL(75)
80 DATA S1,S2,S3,S4/ 4*0. /
100 DO 20 I=1,75
120 READ(1,2) T(I),G(I)
140 G(I)=1./G(I)
160 2 FORMAT(2E16.4)
180 IE=I-1
200 IF(T(I).LE.0.) GO TO 30
220 20 CONTINUE
240 30 DO 40 J=1,IE
260 GL(J)=ALOG(G(J))
280 TL(J)=ALOG(T(J))
300 40 CONTINUE
320 DO 50 K=1,IE
340 S1=S1+GL(K)*TL(K)
360 S2=S2+TL(K)**2
380 S3=S3+GL(K)
400 S4=S4+TL(K)
420 50 CONTINUE
440 FN=IE
460 S=(((S3+S4)/FN)-S1)/(((S4**2)/FN)-S2)
480 BL=(S3-S*S4)/FN
500 4 FORMAT(1P3E10.2)
520 U=EXP(BL)
540 UD=G(IE+1)/U
560 WRITE(9,3)
580 3 FORMAT(2X,'LIGHT IN',2X,'G MEAS.',2X,'G CALC.')
600 II=IE+1
620 DO 60 L=1,II
640 GG=U*(UD+T(L)**S)
660 WRITE(9,4) T(L), G(L), GG
680 60 CONTINUE
700 WRITE(9,5) U, UD, S
720 5 FORMAT(/'U=',1PE10.2/, 'UD=',1PE10.2/, 'S=',1PE10.2/)
740 STOP
760 END
```

FIGURE C1

INPUT DATA FORMAT FOR GFIT

EQUATIONS:  $G = U*(UD + T**S)$

DATA BLOCK:

<u>Device</u>	<u>Data Format</u>
	Energy Input
1	_____, _____, _____, ' ' ' 0.,
	Cell Resistance(Ω) (E16.4)
	Average Dark Resistance

(Maximum of 75 lines of data)

### C3. ELFIT Program

This program fits an equation of the form:

$$B = \text{Brightness} = D \cdot F^\alpha \cdot \exp\left(-\sqrt{\frac{A}{V}}\right),$$

where D,  $\alpha$ , and A are constants; V is the applied r.m.s. voltage; and F is the applied frequency, to the brightness vs. voltage and frequency data obtained from sample EL material. The natural logarithm of both sides of the equation is taken and the resulting equation is fitted by the method of least-squares to the measured values. The program accepts up to 10 frequencies and 30 voltage-brightness number pairs per frequency. The data is stored in a data file and called for at program execution time.

In practice, it is best to first plot the measurements as  $\ln B$  vs.  $\sqrt{\frac{A}{V}}$  and determine the Voltage ranges over which the resulting curves are approximately straight lines. Usually, for thick film EL, the curves are straight lines for all practical voltages. TFEL curves are not and in the IR program, we make provisions for dividing up the brightness vs. voltage dependence of the TFEL into 3 voltage ranges. The ELFIT program is then used on the measurements falling into each separate range. The IR program then uses the  $\alpha$ , A, and D parameters only when the EL voltage is in their range of validity.

Table CII lists the data format for the stored data file used by ELFIT. Figure C2 is a listing of the ELFIT program.

## ELFIT PROGRAM

```

10 * EL EQUATION FIT
20 * B=D*(F**ALPH)/EXP((A/V)**.5)
30 DIMENSION CF(10),JJ(10),V(10,30)
40 +,B(10,30),F(10)
50 DATA FN,S1,S2,S3,S4,S5,S6,S7,S8/ 9*0. /
60 D0 10 I=1,10
70 READ(1,2) F(I)
80 2 FORMAT(E12.3)
90 IF(F(I)-0.) 30, 30, 40
100 40 CONTINUE
110 FI=I
120 II=I
130 D0 20 J=1,30
140 READ(1,5) V(I,J), B(I,J)
150 5 FORMAT(2E12.3)
160 IF(V(I,J)-0.) 10, 10, 22
170 22 CONTINUE
180 CF(I)=J
190 JJ(I)=J
200 20 CONTINUE
210 10 CONTINUE
220 30 CONTINUE
230 *
240 D0 50 K=1,II
250 50 FN=FN+CF(K)
260 *
270 *
280 D0 60 L=1,II
290 *
300 IF(L-1) 55, 55, 23
310 55 S1=S1+ALOG(B(L,MM))
320 S3=S3+(V(L,MM)**-.5)
330 S7=S7+(V(L,MM)**-.5)*ALOG(B(L,MM))
340 S8=S8+(1./V(L,MM))
350 G0 T0 70
360 23 CONTINUE
370 *
380 IF(II-1) 55, 55, 23
390 55 S1=S1+ALOG(B(L,MM))
400 S3=S3+(V(L,MM)**-.5)
410 S7=S7+(V(L,MM)**-.5)*ALOG(B(L,MM))
420 S8=S8+(1./V(L,MM))
430 G0 T0 70
440 23 CONTINUE
450 *
460 S1=S1+ALOG(B(L,MM))
470 S2=S2+ALOG(F(L))
480 S3=S3+(V(L,MM)**-.5)
490 S4=S4+(ALOG(F(L))**2)
500 S5=S5+ALOG(B(L,MM))*ALOG(F(L))
510 S6=S6+(V(L,MM)**-.5)*ALOG(F(L))
520 S7=S7+(V(L,MM)**-.5)*ALOG(B(L,MM))
530 S8=S8+(1./V(L,MM))
540 70 CONTINUE
550 60 CONTINUE
560 *
570 *
580 *
590 IF(II-1) 44, 44, 45
600 *
610 45 CONTINUE
620 DET=FN*(-S4*S8+S6*S6)-S2*(-S2*S8+S3*S6)-S3*(S2*S6-S3*S4)

```

FIGURE C2

## ELFIT PROGRAM

```

630      DLUG=(S1*(-S4*S8+S6*S6)-S2*(-S5*S8+S7*S6)-S3*(S5*S6-S7
640      +      *S4)) / DET
650      ALPH=(FN*(-S5*S8+S7*S6)-S1*(-S2*S8+S3*S6)-S3*(S2*S7
660      +      -S3*S5)) / DET
670      SORA=(FN*(S4*S7-S6*S5)-S2*(S2*S7-S3*S5)+S1*(S2*S6-
680      +      S3*S4)) / DET
690      GO TO 31
700      *
710      44 CONTINUE
720      DET=-FN*S8+S3*S3
730      DLUG=(-S1*S8+S3*S7) / DET
740      SORA=(FN*S7-S3*S1) / DET
750      ALPH=0.
760      *
770      *
780      31 A=SORA*SORA
790      D=EXP(DLUG)
800      *
810      WRITE(9,99)
820      99 FORMAT(// 'RESULTS', 7(1-1))
830      DO 80 LL=1,II
840      WRITE(9,6) F(LL)
850      6 FORMAT(// 'FREQ.', 1PE10.2/, 'VOLT.', 5X, 'BRIGHTNESS',
860      +      2X, 'CALC. BR.', 1/)
870      JJJJ=JJ(LL)
880      DO 90 M=1,JJJJ
890      1F(II-1) 71, 71, 72
900      71 BR=D/EXP((A/V(LL,M))**.5)
910      GO TO 73
920      72 CONTINUE
930      D=D*((F(LL))**ALPH)/EXP((A/V(LL,M))**.5)
940      73 CONTINUE
950      WRITE(9,7) V(LL,M), B(LL,M), BR
960      7 FORMAT(1P3E10.2)
970      90 CONTINUE
980      80 CONTINUE
990      WRITE(9,8) D, A, ALPH
1000     8 FORMAT(// 'D=', 1PE10.2/, 'A=', 1PE10.2/, 'ALF=', E10.2//)
1010     STOP
1020     END

```

FIGURE C2

INPUT DATA FORMAT FOR ELFIT

EQUATION:  $B = D * (F^{**}ALPH) / \text{EXP}((A/V)^{**.5})$

DATA BLOCK:

<u>Device</u>	<u>Data Format</u>	
1	Frequency	_____ (E12.3)
	Voltage	_____ , Brightness _____ (E12.3)
		_____ , _____
		_____ , _____
		_____ , _____
		_____ , _____
		0. (0. voltage - ready for new frequency)
		0. (0. frequency terminates data input)

Maximum: 10 Frequencies  
30 Volt, Brightness/frequency

#### C4. SLPLOT Subroutine

This subroutine generates a four-cycle, base ten, semi-logarithmic plot of up to five curves. The subroutine uses an X-array (linear scale), a Y-array (log scale) and a variable named DEC which determines the lowest ordinate on the plot. The lowest ordinate is  $10^{-DEC}$ .

The program automatically determines the end points of the linear scale and picks a convenient scale factor for reading values from the plot.

For plotting brightness data of EL lamps, the PLDATA program discussed in the next section is used as a calling program. Table CIII summarizes the calling arguments of the subroutine. Figure C3 is a listing of the SLPLOT subroutine.

## SUBROUTINE SLPLOT

```

20      SUBROUTINE SLPLOT (X, Y, DEC)
40      DIMENSION MCT(5), PLUT(5), LINE(62), SCALE(7), X(5,50), Y(5,50)
60      INTEGER BLANK, DOT, XPLUT, PLUS, PLUT
80      * ARRAY COMPRESSION
100     DO 200 I=1,5
120     MC=0
140     DO 201 J=1,50
160 207 IF(J-(50-MC)) 208,206,206
180 208 IF(X(I,J)-0.) 202,202,201
200 202 MC=MC+1
220     JJ=J
240 203 X(I,JJ)=X(I,JJ+1)
260     Y(I,JJ)=Y(I,JJ+1)
280     JJ=JJ+1
300     IF((50-MC)-(JJ-1)) 205,207,207
320 205 GO TO 203
340 201 CONTINUE
360 206 MCT(I)=50-MC
380 200 CONTINUE
400      *
420      * DEP. VARIABLE RANGE
440     XMIN=X(1,1)
460     XMAX=X(1,1)
480     DO 10 I=1,5
500     MAXJ=MCT(I)
520     DO 20 J=1,MAXJ
540     IF(X(I,J)-0.) 20,20,11
560 11 IF(X(I,J)-XMIN) 30,30,31
580 30 XMIN=X(I,J)
600 31 IF(X(I,J)-XMAX) 20,20,32
620 32 XMAX=X(I,J)
640 20 CONTINUE
660 10 CONTINUE
680      *
700      * SCALE DEP. VARIABLE
720     IX=0
740     XRANGE=XMAX-XMIN
760     XRSAV=XRANGE
780 12 IF(XRANGE-60.) 13,14,14
800 13 XRANGE=10.*XRANGE
820     IX=IX+1
840     GO TO 12
860 14 IF(XRANGE-600.) 15,15,16
880 16 XRANGE=XRANGE/10.
900     IX=IX-1
920     GO TO 14
940 15 CONTINUE
960     XDIV=XRANGE/60.
980     IF(XDIV-1.) 61,61,63
1000 61 DIV=1.
1020     GO TO 69
1040 63 IF(XDIV-2.) 62,62,64
1060 62 XDIV=2.*((10.***(-IX)))
1080     DIV=2.
1100     GO TO 69
1120 64 IF(XDIV-5.) 65,65,66

```

FIGURE C3

## SUBROUTINE SLPLUT

```

1140 65 XDIV=5.* (10.**(-IX))
1160  DIV=5.
1180  GO TO 69
1200 66 CONTINUE
1220 70 XDIV=10.* (10.**(-IX))
1240  DIV=10.
1260 69 CONTINUE
1280 *
1300 * LOWEST SCALE VALUE
1320  XS=XMIN
1340  IXM=0
1360 80 IF(XS-1.) 72,75,73
1380 72 XS=XS*10.
1400  IXM=IXM+1
1420  GO TO 80
1440 73 IF(XS-10.) 75,75,74
1460 74 XS=XS/10.
1480  IXM=IXM-1
1500  GO TO 73
1520 75 XS=XS*10.
1540  IXS=XS/5.
1560  XS=1XS
1580  XS=XS*5.
1600  XS=XS*(10.**(-IXM-1))
1620 1FC (XMIN-XS).GE.(10.*XDIV) > XS=XS+(10.*XDIV)
1640 *
1660 * CHOOSE PLOT SYMBOLS
1680  BLANK=1H
1700  DOT=1H*
1720  XPLOT=1HX
1740  PLUS=1H+
1760  PLOT(1)=1H1
1780  PLOT(2)=1H2
1800  PLOT(3)=1H3
1820  PLOT(4)=1H4
1840  PLOT(5)=1H5
1860 *
1880 * SCALE THE POINTS
1900  DO 300 I=1,5
1920  MAXJ=ACT(I)
1940  DO 301 J=1,MAXJ
1960  XC(I,J)=(XC(I,J)-XS)/ XDIV
1980  IF(YC(I,J).LE.0.) YC(I,J)=1.E-10
2000  YC(I,J)=CALC610(YC(I,J))*18.-(18.*DEC)+1.
2020 301 CONTINUE
2040 300 CONTINUE
2060 *
2080 * PRINT BORDER
2100  SCALE(1)=XS
2120  DO 120 I=2,7,1
2140 120 SCALE(I)=SCALE(I-1)+(10.*XDIV)
2160  WRITE(9,400)
2180 400 FORMAT(//)
2200  WRITE(9,121) SCALE
2220 121 FORMAT(7(1PE8.2,2X))
2240  WRITE(9,122)

```

FIGURE C3

## SUBROUTINE SLPL0T

```

2260 122 FORMAT(7('I',9X))
2280      D0 123 I=1,61
2300 123 LINE(I)=PLUS
2320      D0 124 I=1,61,10
2340 124 LINE(I)=XPL0T
2360      WRITE(9,125)(LINE(IDUM),IDUM=1,61)
2380 125 FORMAT(61A1)
2400      * BLANK THE LINE
2420      D0 126 I=1,61
2440 126 LINE(I)=BLANK
2460      *
2480      * PLOT THE POINTS
2500      IDEC=DEC+4.
2520      IDOT=0
2540      IXPL0T=0
2560      LINE(62)=0.
2580      D0 310 N=1,71
2600      LINE(I)=PLUS
2620      IDOT=IDOT+1
2640      IF(IDOT.NE.6) G0 TO 315
2660      IDOT=0
2680      LINE(I)=DOT
2700      IXPL0T=IXPL0T+1
2720      IF(IXPL0T.NE.3) G0 TO 315
2740      IXPL0T=0
2760      LINE(I)=XPL0T
2780      LINE(61)=XPL0T
2800      IDEC=IDECK-1
2820      LINE(62)=IDECK
2840 315 IY=73-N
2860      D0 311 I=1,5
2880      MAXJ=MCT(I)
2900      D0 312 J=1,MAXJ
2920      IY=Y(I,J)*1.001
2940      IX=X(I,J)
2960      IF(IY-73) 316,317,317
2980 317 Y(I,J)=0.
3000      IY=0
3020 316 IF(IY-IPY) 312,313,313
3040 313 LINE(IX+1)=PLOT(I)
3060      Y(I,J)=0.
3080 312 CONTINUE
3100 311 CONTINUE
3120      IC=61
3140      D0 314 IDUM=1,61
3160      IF (LINE(IC).NE.BLANK) G0 TO 384
3180 314 IC=IC-1
3200 384 IC=IC+1
3220      WRITE(9,380) (LINE(NDUM),NDUM=1,IC)
3240 380 FORMAT(61A1,'1.0E',I2)
3260      D0 382 II=1,61
3280 382 LINE(II)=BLANK
3300 310 CONTINUE
3320      D0 383 I=1,61
3340 383 LINE(I)=PLUS
3360      D0 385 I=1,61,10

```

FIGURE C3

PAGE 4

SUBROUTINE SLPLOT

```
3380 385 LINE(I)=XPL0T
3400      WRITE(9,125)(LINE(IDUM),IDUM=1,61)
3420      WRITE(9,122)
3440      WRITE(9,121) SCALE
3460      WRITE(9,400)
3480      RETURN
3500      END
```

FIGURE C3

DATA BLOCK FOR SLPLOT SUBROUTINE

(X, Y, DEC)

Dimensions of Arrays:

X(5,50)

Y(5,50)

X direction is linear scale

Y direction is  $\log_{10}$  scale

Maximum of 5 curves plotted

DEC: Bottom ordinate of the Plot is  $10^{DEC}$

#### C5. PLDATA Program

PLDATA converts raw measurements of brightness of EL vs. voltage at a fixed frequency into a data block for plotting by the SLPLOT subroutine. The program lets you choose at execution time whether to plot vs. voltage or the inverse square root of the voltage. This second form allows the operator to determine ranges of applied voltage over which the ELFIT program can provide accurate results.

Table CIV summarizes the format of the data file used with the program. Figure C4 is a listing of the PLDATA program. It must be loaded with the SLPLOT subroutine.

PAGE 1

PLDATA PROGRAM

```
20 * PLOT DATA WITH SLPLOT
40 DIMENSION X(5,50),Y(5,50)
60 DATA X/250*0.,Y/250*0./
80 DO 10 I=1,5
100 DO 20 J=1,50
120 READ(1,1) X(I,J),Y(I,J)
140 IF(X(I,J).LE.0.) GO TO 21
160 20 CONTINUE
180 21 CONTINUE
200 10 CONTINUE
220 READ(1,2) DEC
240 1 FORMAT(2E16.3)
260 2 FORMAT(16.2)
280 WRITE(9,3)
300 3 FORMAT(///'STYLE OF PLOT'/
320 + '1= X-VALUES AS READ'/
340 + '2= X=1/SORT(X)'/
360 +
380 READ(9,4) IS
400 4 FORMAT(1I1)
420 GO TO (30,40),IS
440 40 DO 50 I=1,5
460 DO 60 J=1,50
480 IF(X(I,J).NE.0.) X(I,J)=1./SORT(X(I,J))
500 60 CONTINUE
520 50 CONTINUE
540 GO TO 100
560 30 CONTINUE
580 100 CALL SLPLOT(X,Y,DEC)
600 IF(IEOF(1).GT.102) 102,102,103
620 102 READ(1,101)
640 101 FORMAT('
660 WRITE(9,101)
680 WRITE(9,200)
700 200 FORMAT(///)
720 103 STOP
740 END
```

FIGURE C4

**INPUT DATA FORMAT FOR PLDATA (Uses SLPLOT Subroutine)**

**DATA FORMAT:**

<u>Device</u>	<u>Linear Scale</u>	<u>Log Scale</u>
1	X _____ ,	Y _____ (2 E16.3)
	_____ ,	_____
	'	'
	'	'
	'	'
	0.	(terminates a curve)
	0.	
	0.	
	0.	
	0.	
DEC	DEC	(After five zero. X inputs, ready for DEC) (E16.2) (Lowest ordinate plotted = 10 <sup>DEC</sup> )
		(Optional 30 Character Line for Data Identification)

**Beware of Blank Records in File!!**

**TABLE CIV**

#### C6. ELDG Program

This program generates a set of EL brightness vs. voltage and frequency values computed from the equation:

$$\text{Brightness} = D \cdot F^\alpha \exp(-\sqrt{\frac{A}{V}})$$

where D,  $\alpha$ , and A are constants, F is the applied frequency, and V is the applied voltage. This program is useful in checking the results of the ELFIT program. The resultant data file is ready for use by the PLDATA program.

The program asks for the D,  $\alpha$  and A values along with their ranges of validity at execution time. All data is entered at the keyboard. The program will accept five voltage ranges but the IR program can only use three ranges.

Table CV lists the formats for the input data. Figure C5 is a listing of the ELDG program.

## ELDG PROGRAM

```

20 * EL DATA GENERATOR FOR PLDATA
40 DIMENSION F(10),A(5),VL(5),VU(5),DV(5),AV(5)
60 DO 10 I=1,5
80 WRITE(9,1)
100 1 FORMAT('VOLTAGE RANGE; VL,VU')
120 READ(9,2) VL(I),VU(I)
140 2 FORMAT(2E10.2)
160 IF(VL(I)-0.) 30, 30, 20
180 20 II=I
200 WRITE(9,3)
220 3 FORMAT('DV , AV , ALPHA')
240 READ(9,4) DV(I),AV(I),A(I)
260 4 FORMAT(3E10.2)
280 10 CONTINUE
300 30 CONTINUE
310 ZERO=0.
320 *
340 WRITE(9,5)
360 5 FORMAT('FREQUENCIES')
380 DO 40 J=1,10
400 READ(9,6) F(J)
420 6 FORMAT(E10.2)
440 IF(F(J)-0.) 50, 50, 60
460 60 JJ=J
480 40 CONTINUE
500 50 CONTINUE
510 WRITE(9,7)
511 7 FORMAT('EXPONENT OF SMALLEST ORDINATE (F10.1)')
512 READ(9,8) DEC
513 8 FORMAT(F10.1)
520 *
530 DO 80 L=1,JJ
540 DO 70 K=1,II
560 C=1.
580 V=VL(K)
600 INTVS=VL(K)/5.
620 VS=INTVS
640 VM5=VS*5.
660 90 CONTINUE
680 IF(V-VU(K)) 21,22,22
690 22 V=VU(K)
700 C=200.
720 21 CONTINUE
740 ELUG=SQRT(AV(K)/V)
760 FLUG=A(K)*ALUG(F(L))
780 DVFLUG=ALUG(DV(K))
800 BLOG=DVFLUG+FLUG-ELUG
820 B=EXP(BLOG)
840 WRITE(1,9) V,B
860 9 FORMAT(2E16.3)
880 IF(C.EQ.1.) V=VM5+5.
900 IF(C.GT.1.) V=V+5.
920 C=C+1.
940 IF(C.GE.200.) GO TO 70
960 GO TO 90
980 70 CONTINUE

```

PAGE 2

ELDG PROGRAM

```
1188      WRITE(1,9) ZERO,ZERO
1190  80 CONTINUE
1192      IF(JJ.EQ.5) GO TO 99
1193      DO 98 KK=JJ,4,1
1194      WRITE(1,9) ZERO,ZERO
1195  98 CONTINUE
1196  99 WRITE(1,11) DEC
1197  11 FORMAT(E16.2)
1200      STOP
1220      END
```

FIGURE C5

**INPUT DATA FORMATS FOR ELDG**

**EQUATION:  $B = (F(L) ** A(K)) * DV(K) / SQRT(AV(K)/V)$**

**DATA BLOCK:**

<u>Device</u>	<u>Formats</u>
TTY (as asked for)	VL _____, VU _____ (E10.2)
	DV _____, AV _____, ALPHA _____ (E10.2)
	VL _____, VU _____
	DV _____, AV _____, ALPHA _____
	0. (0 Voltage terminates parameter inputs)
<u>Frequencies</u>	(E10.2)
	_____
	_____
	0. (0 frequency terminates data input)
Exponent of Smallest Ordinate	(E16.2)
	Maximum of 5 voltage ranges
	Maximum of 10 frequencies
	VL < Voltage Range < VU

**TABLE CV**

### C7. FM, AM and MASSA Programs

The MASSA program condenses the data file created by the IR program into a more compact form for use with the AM and FM programs. Figure C6 lists the MASSA program. It calls for the input data file at program execution time.

The FM program uses the brightness vs. radiation input data generated by the IR program and condensed by the MASSA program to approximate the operation of an image conversion panel driven by several applied frequencies in rotation. The simulation is that a panel is driven at a constant voltage and one frequency ( $F_1$ ) for a short time ( $t_1$ ), then driven at another frequency ( $F_2$ ) for a short time ( $t_2$ ), and so on up to  $F_n$  for time  $t_n$  and then driven again at  $F_1$ , etc. If the sum  $\sum_{i=1}^n t_i$  is less than the time for the eye to see flicker in the brightness of the panel, the viewer perceives a simple average brightness of the panel. The FM program sorts through the response curves generated by the IR program and weights the output brightnesses for a selected frequency by the fraction  $t_j / \sum_{i=1}^n t_i$  for that frequency. The program will accept up to 20 desired frequencies but seldom is it worthwhile to construct a data base large enough for use with that many frequencies.

Figure C7 is a listing of the FM program. Table CVI is a summary of the data file format for the FM program. The FM program may also be used to effectively sort and condense data for use in the CASCAD program. The FM program must be loaded with the PLOT subroutine.

The AM program works in an identical manner to the FM program only it computes a weighted average of different voltages applied for short time periods at one frequency. Figure C8 is a listing

of the program. Table CVII describes the formats of the data file. This program may also be used to sort data for CASCAD. The AM program must be loaded with the PLOT subroutine.

## MASSA PROGRAM

```
20 * MASSAGE LIGHT AMP DATA
30 IFLAG=1
32 READ(1,4) LP
34 WRITE(2,4) LP
36 4 FORMAT(I2)
40 10 READ(1,1) B,T,V,F
60 1 FORMAT(4E12.4)
80 12 I=0
100 BS=B
120 TS=T
140 VS=V
160 FS=F
180 WRITE(2,2) V,F
200 2 FORMAT(2E12.4)
210 *
220 20 READ(1,1) B,T,V,F
240 IF(IEOF(1)) 30,30,100
260 30 IF(F-FS) 40,50,40
280 40 IF(I-19) 60,70,70
300 60 D0 80 J=1,18,1
320 WRITE(2,3) BS
340 3 FORMAT(E12.4)
360 80 CONTINUE
370 GO TO (70,110), IFLAG
380 70 GO TO 12
400 *
420 50 WRITE(2,3) BS
440 I=I+1
460 BS=B
480 TS=T
500 VS=V
520 FS=F
540 GO TO 20
560 *
580 100 IFLAG=2
590 GO TO 40
595 110 STOP EOF
600 END
```

FIGURE C6

PAGE 1

FM PROGRAM

```
20 * FM DRIVEN LIGHT AMP
40 *
60 DIMENSION FD(20),FRA(20),B0(19,5),VS(5),XX(19,5)
80 COMMON XX,B0,LP
100 DATA VS/5*0.0/
120 DO 23 I=1,19
140 DO 24 J=1,5
160 XX(I,J)=0.
180 B0(I,J)=0.
200 24 CONTINUE
220 23 CONTINUE
240 WRITE(9,40)
260 4 FORMAT(/'CREATE DATA FILE? 0=NO, 1=YES'/)
280 READ(9,5) ISWIT
300 5 FORMAT(11)
320 ISWIT=ISWIT+1
340 WRITE(9,99)
360 99 FORMAT(/'WANT PLOT? 0=NO, 1=YES'/)
380 READ(9,5) ISWIT2
400 ISWIT2=ISWIT2+1
420 WRITE(9,2)
440 2 FORMAT(/'FREQ. ,FRACTIONS'/'TERMINATE WITH 0.'/)
460 IGOUD=1
480 DO 10 I=1,20
500 READ(9,1) FD(I),FRA(I)
520 1 FORMAT(2E12.4)
540 1F(FD(I)) 11,12,11
560 11 IC=I
580 10 CONTINUE
600 12 CONTINUE
620 FS=FD(1)
640 *
660 READ(1,7) LP
680 7 FORMAT(12)
700 1F(ISWIT.EQ.2) WRITE(2,7) LP
720 20 READ(1,1) V,F
740 DO 30 I=1,IC
760 1F(ABS(FD(I)-F)-1.0) 21,21,30
780 21 IGOUD=2
800 1SAVE=I
820 GO TO 82
840 30 CONTINUE
860 IGOUD=1
880 22 CONTINUE
900 GO TO (40,60), IGOUD
920 40 DO 50 J=1,19
940 READ(1,3)
960 3 FORMAT(E12.4)
980 50 CONTINUE
1000 1F(IEUF(1)) 20,20,80
1020 *
1040 60 DO 69 K=1,5
1060 1F(ABS(V-VS(K))-1.0) 66,66,69
1080 69 CONTINUE
1100 DO 68 K=1,5
1120 1F(VS(K)) 68,67,68
```

FIGURE C7

PAGE 2

FM PROGRAM

```
1140 68 CONTINUE
1160 1GO0JD=1
1180 GO TO 22
1200 67 VS(K)=V
1220 66 CONTINUE
1240 DO 70 I=1,19
1260 READ(1,3) B
1280 B0(I,K)=B0(I,K)+(FRAC(1SAVE)*B)
1300 70 CONTINUE
1320 FS=F
1340 IF(CIEOF(1)) 20,20,80
1360 80 CONTINUE
1380 GO TO(91,92),ISWIT
1400 92 CONTINUE
1420 DO 93 K=1,5
1440 DO 94 J=1,19
1460 IF(B0(J,K)) 93,93,95
1480 95 WRITE(2,6) B0(J,K)
1500 6 FORMAT(E12.4)
1520 94 CONTINUE
1540 93 CONTINUE
1560 91 GO TO (97,96),ISWIT2
1580 96 CALL 1 GPL
1600 97 CONTINUE
1620 STOP
1640 END
```

FIGURE C7

INPUT DATA FORMATS FOR FM

Device:

TTY  
(as asked for)

Data Format:

Frequency \_\_\_\_\_, Fraction \_\_\_\_\_ (E12.4)  
\_\_\_\_\_, \_\_\_\_\_  
\_\_\_\_\_, \_\_\_\_\_  
0. (maximum of 20)

1

Voltage \_\_\_\_\_, Frequency \_\_\_\_\_ (E12.4)  
Brightness \_\_\_\_\_ (E12.4)  
\_\_\_\_\_

19 values

Voltage \_\_\_\_\_, Frequency \_\_\_\_\_  
Brightness \_\_\_\_\_  
\_\_\_\_\_

etc.

PAGE 1

AM PROGRAM

```
20 * AM DRIVEN LIGHT AMP
40 *
60 DIMENSION VD(20),FRA(20),B0(19,5),FS(5),XX(19,5)
80 COMMON XX,B0,LP
100 DATA FS/5*0.0/
120 DO 23 I=1,19
140 DO 24 J=1,5
160 XX(I,J)=0.
180 B0(I,J)=0.
200 24 CONTINUE
220 23 CONTINUE
240 WRITE(9,4)
260 4 FORMAT('CREATE DATA FILE? 0=NO, 1=YES')
280 READ(9,5) ISWIT
300 ISWIT=ISWIT+1
320 5 FORMAT(I1)
340 WRITE(9,99)
360 99 FORMAT('WANT PLOT? 0=NO, 1=YES')
380 READ(9,5) ISWIT2
400 ISWIT2=ISWIT2+1
420 WRITE(9,2)
440 2 FORMAT('VOLTAGES,FRACTIONS//TERMINATE WITH 0.')
460 1600D=1
480 K=0
500 DO 10 I=1,20
520 READ(9,1) VD(I),FRA(I)
540 1 FORMAT(2E12.4)
560 IF(VD(I)) 11,12,11
580 11 IC=I
600 10 CONTINUE
620 12 CONTINUE
640 VS=VD(1)
660 *
680 READ(1,7) LP
700 7 FORMAT(I2)
720 IF(ISWIT.EQ.2) WRITE(2,7) LP
740 20 READ(1,1) V,F
760 DO 30 I=1,IC
780 IF(ABS(VD(I)-V)-1.0) 21,21,30
800 21 1600D=2
820 ISAVE=I
840 GO TO 22
860 30 CONTINUE
880 1600D=1
900 22 CONTINUE
920 GO TO (40,60), 1600D
940 40 DO 50 J=1,19
960 READ(1,3)
980 3 FORMAT(E12.4)
1000 50 CONTINUE
1020 IF(IEOF(1)) 20,20,80
1040 *
1060 60 DO 69 K=1,5
1080 IF(ABS(F-FS(K))-1.0) 66,66,69
1100 69 CONTINUE
1120 DO 68 K=1,5
```

FIGURE C8

## AM PROGRAM

```
1140 IF(FS(K)) 68,67,68
1160 68 CONTINUE
1180 I600D=1
1200 GO TO 22
1220 67 FS(K)=F
1240 66 CONTINUE
1260 DO 70 I=1,19
1280 READ(1,3) B
1300 B0(I,K)=B0(I,K)+(FRAC(1SAVE)*B)
1320 70 CONTINUE
1340 VS=V
1360 IF(CIEOF(1)) 20,20,80
1380 80 CONTINUE
1400 GO TO (91,92),ISWIT
1420 92 CONTINUE
1440 DO 93 K=1,5
1460 DO 94 J=1,19
1480 IF(CB0(J,K)) 93, 93, 95
1500 95 WRITE(2,6) B0(J,K)
1520 6 FORMAT(E12.4)
1540 94 CONTINUE
1560 93 CONTINUE
1580 91 GO TO (97,96), ISWIT2
1600 96 CALL LOCPL
1620 97 CONTINUE
1640 STOP
1660 END
```

FIGURE C8

INPUT DATA FORMATS FOR AM

Device:

TTY  
(as asked for)

Data Format:

Voltage \_\_\_\_\_, Fraction \_\_\_\_\_ (E12.4)  
\_\_\_\_\_, \_\_\_\_\_  
\_\_\_\_\_, \_\_\_\_\_  
\_\_\_\_\_. 0. (maximum of 20)

1

Voltage \_\_\_\_\_, Frequency \_\_\_\_\_ (E12.4)  
Brightness \_\_\_\_\_ (E12.4)

19 values

Voltage \_\_\_\_\_, Frequency \_\_\_\_\_  
Brightness \_\_\_\_\_

etc.

### C8. CASCAD Program and MASSA 2 Program

The MASSA 2 program converts the data files generated by IR and MASSA into a form compatible with the CASCAD program. The IR program can generate up to 25 output brightness curves for different voltage and frequency combinations. The CASCAD program will only plot data for 5 possible output combinations of the second stage panel. The operator should edit his data files to make sure that the files used in device 2 contain no more than 5 curves. The AM or FM program can be used to sort the files generated by IR and MASSA. For instance, if the operator using AM selects 100% of one voltage to be used, the output data file will contain brightness curves at only that operating voltage and all frequencies that were available.

The CASCAD program takes a set of 19 output brightnesses from the first image panel and uses these brightnesses with linear interpolations from all sets of output brightnesses for the second state image panel to generate an approximate simulation for a two-stage image converter. The program permutes all curves of the second stage panel on each curve of the first stage panel.

Either or both of the simulated image conversion panels may have been AM or FM simulated panels. At this stage in the simulations, operator discretion is mandatory or one may drown in output curves.

Figure C9 is a listing of the MASSA 2 program. Figure C10 is a listing of the CASCAD program. Table C<sub>VII</sub> is a summary of input data formats for CASCAD.

PAGE 1

MASSA2 PROGRAM

```
20 * MASSA2
40 * PREPARES MASSAGED DATA FOR CASCAD
60 DIMENSION B(19)
80 READ(1,1) LP
100 WRITE(2,1) LP
120 1 FORMAT(I2)
140 2 FORMAT(E12.4)
160 3 FORMAT(2E12.4)
180 30 READ(1,3)V,F
200 DO 10 I=1,19
220 READ(1,2) B(I)
240 10 CONTINUE
260 DO 20 I=1,19
280 WRITE(2,2) B(I)
300 20 CONTINUE
320 IF(IEOF(1)) 30,30,40
340 40 STOP EOF
360 END
```

FIGURE C9

PAGE 1

CASCADE PROGRAM

```
20 * CASCAD
40 * COMPUTES OUTPUT OF CASCADED LIGHT AMPS
60 DIMENSION B1(19),B2(19),T(19),BU(19,5),XX(19,5)
80 COMMON XX,BU,LP
100 DATA 1(1),T(2),T(3)/1.E-6,2.E-6,5.E-6/
120 DATA 1(19)/1./,J/0/
140 DO 12 I=1,19
160 DO 13 J=1,5
180 XX(I,J)=0.
200 13 CONTINUE
220 12 CONTINUE
240 DO 10 I=4,16,3
260 T(I)=T(I-3)*10.
280 T(I+1)=T(I-2)*10.
300 T(I+2)=T(I-1)*10.
320 10 CONTINUE
340 *
360 WRITE(9,1)
380 1 FORMAT('CREATE DATA FILE? 0=NO, 1=YES')/
400 READ(9,2) ISWIT
420 2 FORMAT(1I)
440 ISWIT=ISWIT+1
460 WRITE (9,3)
480 3 FORMAT('BEGINNING INPUT RADIATION')/
500 READ(1,6) LP
520 WRITE(9,7) LP
540 READ(2,6) LP
560 WRITE(9,7) LP
580 IF(ISWIT.EQ.2) WRITE(3,6) LP
600 6 FORMAT(12)
620 7 FORMAT(10X,'1.E ' I2)
640 4 FORMAT(E12.4)
660 TB=10.**LP
680 *
700 DO 20 I=1,19
720 T(I)=T(I)*TB/1.E-6)
740 20 CONTINUE
760 *
780 30 IF(TLEOF(1).EQ.1) GO TO 101
800 DO 31 I=1,19
820 READ(1,5) B1(I)
840 31 CONTINUE
860 5 FORMAT(E12.4)
880 35 CONTINUE
900 DO 32 I=1,19
920 READ(2,5) B2(I)
940 32 CONTINUE
960 J=J+1
980 N=2
1000 40 DO 50 I=1,19
1020 DO 60 K=N,19,1
1040 IF(B1(I)-1(K)).GT.70,70,80
1060 80 IF(K-19) 60,90,90
1080 60 CONTINUE
1100 90 B1(I,J)=B2(K)
1120 GO TO 50
```

FIGURE C10

PAGE 2

CASCADE PROGRAM

```
1140 70 N=K
1160  BU(I,J)=B2(K-1)+((B2(K)-B2(K-1))*(B1(I)-T(K-1))
1180  + / (T(K)-T(K-1) ) )
1200  IF(BU(I,J).LE.0.) BU(I,J)=1.E-10
1220  50 CONTINUE
1240  IF(IEOF(2).EQ.1) GJ 10 100
1260  GJ 10 35
1280  *
1300  *
1320 100 GJ 10 (103,102),ISWIT
1340 102 WRITE(3,4) ((BU(L,M),L=1,19),M=1,J=1)
1360 103 CALL LOGPL
1380  D9 25 I=1,J=1
1400  D9 26 K=1,19
1420  BU(K,I)=0.
1440 26 CONTINUE
1460 25 CONTINUE
1480  J=0
1500  REWIND 2
1520  GJ 10 30
1540 101 STOP
1560  END
```

FIGURE C10

INPUT DATA FORMAT FOR CASCAD

Device:

1  
(First Stage)

Data Format:

LP \_\_\_\_\_ (I2) (Beginning input Radiation =  
10<sup>LP</sup>)

Output Brightness \_\_\_\_\_ (E12.4)

19 values

Brightnesses are in groups of 19

2  
(Second Stage)

LP \_\_\_\_\_ (I2 )

Output Brightness \_\_\_\_\_

19 values

(Same format as for device 1)

(Maximum of 5 groups of Brightnesses)

TABLE CVIII